Organic-Inorganic Ion-Exchange in Cellulosic Fiber Matrices

Richard D. Champion

A dissertation
submitted in partial fulfillment of the
requirements for the degree of

Doctor of Philosophy

University of Washington
2012

Reading Committee:
G. Graham Allan, Chair
James H. Wiley
Joe P. Mahoney

Program Authorized to Offer Degree:

Chemical Engineering

University of Washington

Abstract

Organic-Inorganic Ion-Exchange in

Cellulosic Fiber Matrices

Richard D. Champion

Chair of the Supervisory Committee:

Professor G. Graham Allan

Department of Environmental and Forest Resources

Adjunct Professor of Chemical Engineering

Previous work on the topic of ion-exchange with cellulosic fiber matrices has been limited as well as confined to the interactions of metal cations, from metal salts. The findings of this earlier work were that often the adsorption of metal cations followed the Donnan theory. Also, it was found that the adsorption process, for well-mixed systems was very rapid, often within 2 minutes, and adhered to the Intraparticle Diffusion Model.

The research detailed in this dissertation expands upon this earlier research by investigating both the organic-inorganic and organic-organic ion-exchange in cellulosic fiber matrices. It was found that with smaller organic cations, the ion-exchange behavior followed the Donnan model, but larger molecules did not; likely due to Van der Waals forces. Also, it was found that the kinetics of adsoption of larger organic

cations was far slower, taking several hours, and, as opposed to metal cations, adhered to the Convective mass-transfer model. This work was untilized in commercial product development, from which a patent was published.

TABLE OF CONTENTS

List of Figures

Figure Number Page

List of Tables

Chapter 1: Introduction

In this section the fundamentals of wood and wood pulps are discussed. This begins with an overview the physical structure of wood fibers. Following that is basic information about the fiber chemistry. Then there is a quick review of the basics of wood pulping and relevant post-pulping treatments of wood fibers. This precedes a more scientific and in-depth discussion of cellulosic fiber surface chemistry and acid/base characteristics. The Donnan equilibrium is explained and how this principle has been applied cellulosic fiber matrices. This is followed by a discussion of non-ideal Donnan competitive adsorption, which has been used to study cellulosic fiber matices, given the ideal Donnan model cannot be applied to them. Finally, the chapter is concluded with a discussion of the aims and importance of this research.

1.1 – Structure of Wood

Wood is generally classified into two major categories, i.e., softwood and hardwood.[1] Examples of softwoods include southern pine, spruce, redwood and jack pine, whereas examples of hardwoods include aspen, oak, and birch etc. The hardwoods and softwoods are composed of different cell types. In softwood trees, the wood substance is composed of tracheids and ray cells only. By contrast, hardwood trees contain many more different types of cells (e.g. libriform, vessels, fiber tracheids and rays) due to the cells having greater specialization in their function. A key difference

between the structure of hardwoods and softwoods is that hardwoods have relatively large pores (up to hundreds of microns in diameter), while softwoods do not. Softwoods and hardwoods also differ in fiber length with the fibers of softwoods being generally longer. The average length of a softwood fiber is between 2 and 4 mm, while the fibers of hardwoods are approximately 1 mm in length. For both types of wood the average fiber width is approximately 0.02-0.04 mm.[2]

The individual cells, or wood fibers, are separated by the middle lamella (ML), which glues the cells together and is primarily composed of lignin. The fiber contains the primary wall and a three-layered secondary wall.[3] In the primary wall, the cellulose fibrils are oriented in a crossing mesh due to this being the first layer of the cell deposited in the development of a cell. The primary wall consists of cellulose, hemicellulose and extractives completely embedded in lignin. In the first secondary wall (S1), the cellulose fibrils are arranged in a several lamellae of countering helical configurations. The inner secondary wall, S2, forms the main body of the fiber with a thickness of 2 to 8 microns wherein the cellulose fibrils align almost completely parallel to the length of the cell and to one another. A third secondary wall (S3) is present in the cells of some different species. Inside the secondary walls is a tertiary wall (T), which is the last fibrillar layer, surrounds the lumen (L) which is a void space in the middle of the fiber that provides wood with buoyancy and bulk. Below is a diagram (Figure 1.1) of the ultrastructure of wood, which has just been discussed.

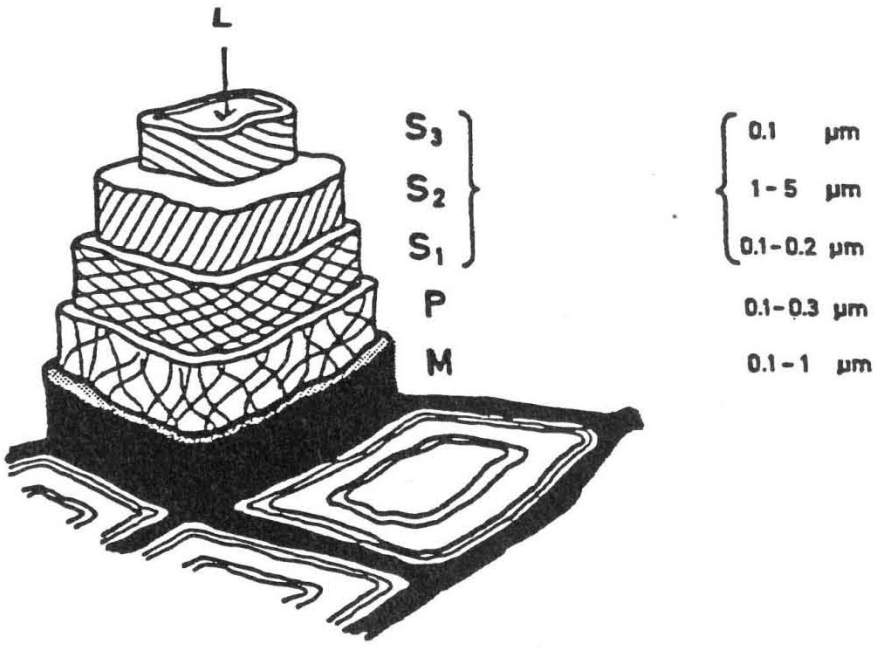

Figure 1.1. Ultrastructure of a wood fiber.[2]

This schematic illustrates the wood fiber wall.[4] Cellulose in a fiber wall is composed of elementary cellulose fibrils that are only about 35 Angstroms in diameter and aggregate together to form microfibrils. The fibrils exist as sheets of parallel fibrils with different layers orientated relative to the fiber's longitudinal axis, as mentioned in the previous paragraph. The crystalline cellulose fibrils can be seen as providing a skeleton structure of the fiber, which is surrounded by hemicellulose. The hemicellulose, therefore, serves as a matrix. The lignin serves as an encrusting agent that holds everything together.

1.2 – Chemical Composition of Wood

The main chemical composition of wood fibers includes cellulose, hemicellulose, and lignin. Cellulose is a white solid material that makes up the backbone of the wood fiber. It is a polysaccharide carbohydrate composed of glycopyranose units, connected via 1,4 β–bonds, as seen in Figure 1.2. The degree of polymerization of the cellulose is a chemical property that determines the pulp strength. For untreated wood fiber, the degree of polymerization of cellulose is usually more than 10,000 which translates into an approximate length of 5 microns, though shortening occurs during the pulping and bleaching of the wood. Cellulose constitutes about 40% of the dry fiber weight, as seen in Table 1.1.[5] In its natural state, cellulose is a neutral and linear polymer with highly crystalline regions. A minute number of induced carboxylic acid groups are typically introduced during the pulping and bleaching of the wood.

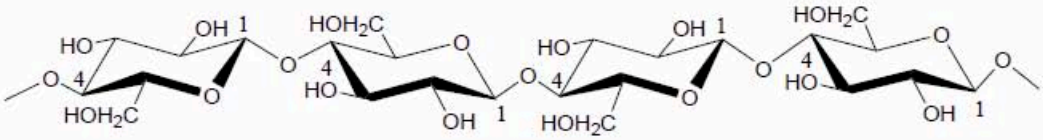

Figure 1.2. Structure of Cellulose.

Unlike cellulose, hemicellulose, which constitutes about 30% of the dry fiber weight, has a degree of polymerization of about 100-200, and is not ordered in nature.[6] Hemicelluloses are readily hydrolyzed in an acid environment (carboxylic acid groups'

pK_a ~ 3-5) and are alkali soluble. Unlike cellulose, which is linear, pendant groups are often attached to the primary polymer chains of hemicellulose. These pendant groups, which are sugar groups as well, can be chemically active in that, in the case of hemicellulose, they are acid groups, such as glucuronic or galacturonic acids. Sjostrom reported that these groups are predominantly carboxylic acids and it is commonly accepted that they may serve as binding sites between fibers or other chemicals.[7] The qualities of these groups have been examined with various methods, such as conductometric,[8] potentiometric titrations,[9,10] and zeta potential measurements.[11]

The chemical structures of hemicellulose polymer chains differ markedly between softwoods and hardwoods, though hemicelluloses from both groups contain a large number of acidic pendant groups. In hardwoods, the hemicelluloses are primarily glucuroxylans. Glucuroxylans are carbohydrate polymer chains with xylose sugar units composing the backbone of the polymer. Xylose, when cyclized (as found in wood), is D-xylopyranose, a monosaccharide six-membered, 5-carbon ring with 4 hydroxy groups (see Figure 1.3).

Xylans are polymer chains of xylopyranose subunits linked by β(1→4)-bonds. In hardwoods, the principle glucuroxylan, with 4-0-methyl-α-D-glucopyranosyluronic acid linked via an α(1→4) bond, is displayed in Figure 1.4. Typical concentrations of these 4-*0*-methyl-α-D-glucopyranosyluronic acids in hardwoods is 0.1 mole per mole of xylopyranose in the backbone of the hemicellulose polymer chain, thus meaning one of these pendant groups per ten polymer subunits. In softwoods, the primary hemicelluloses are arabinoglucuronoxylans and galactoglucomannans, respectively. The

polymer backbones of galactoglucomannans are composed of β(1→4) -D-glucopyranose and D-mannopyranose subunits, which are cyclized forms of the monosaccharides glucose and mannose, respectively. Glucose and mannose have the exact same chemical composition with a six-membered, 5-carbon ring with 4 hydroxyl and 1 hydroxymethyl side groups, though with differing stereochemistry (Figure 1.5). Galactoglucomannans, as seen in Figure 1.5, have a D-galactopyranose units linked to D-mannopyranose units via an α(1→6) bond. It is evident that galactoglucomannans do not have any acid groups.

The other primary group of hemicelluloses found in softwoods is arabinoglucuronoxylans, on the other hand, do. Arabinoglucuronoxylans are nearly the exact same polymers as glucuronoxylans, but in addition to possessing 4-O-methyl-α-D-glucopyranosyluronic acid pendant groups arabinoglucuronoxylans also have L-arabinofuranose pendant groups as well. Arabinofuranose is the cyclized monosaccharide of arabinose (Figure 1.6), which has the same chemical structure as xylose monosaccharides though with different stereochemistry, but arabinofuranose, unlike the aforementioned xylopyranose, exists in the five-membered furan-based ring structure. The L-arabinofuranose pendant groups are linked to the xylopyranose subunits making up the polymer backbone via α(1→3) bonds. Understandably, the arabinoglucuronoxylans, owing their similar structure, contain acidic groups. In total, over the range of tree species, the typical glucuronic acid content is typically 5-15 millimoles/100g.

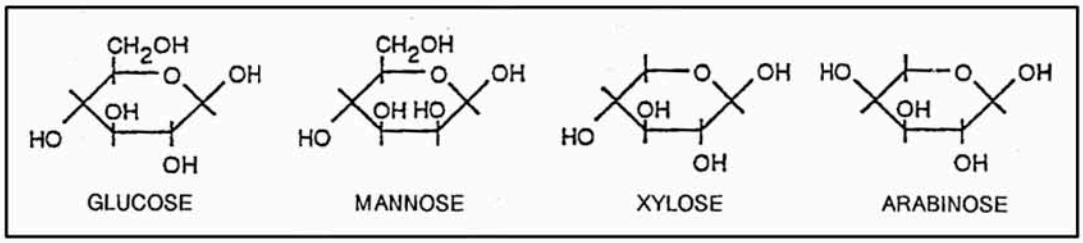

Figure 1.3. Glucose, mannose, xylose and arabinose unit.

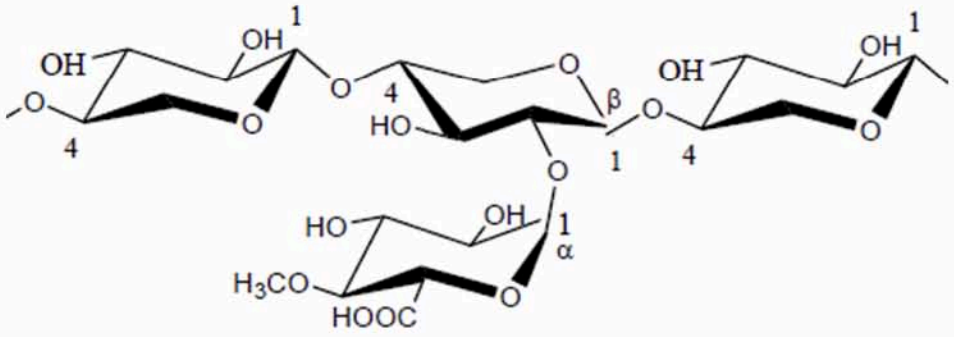

Figure 1.4. The chemical structure of glucuronoxylan.

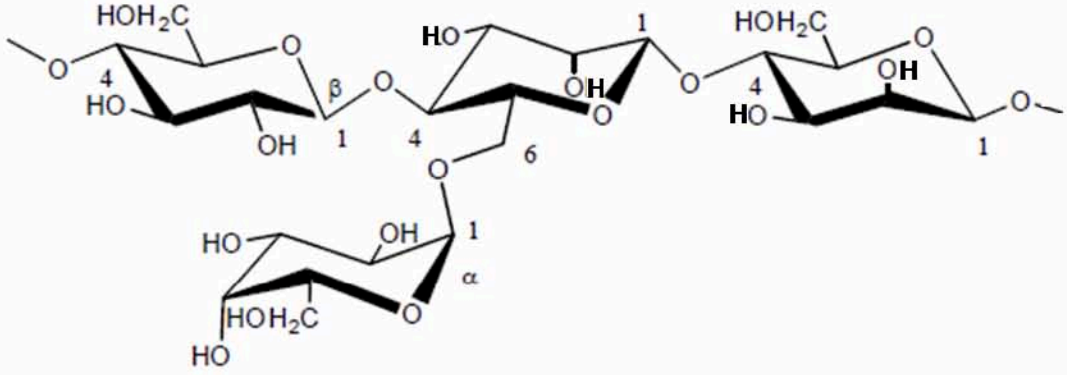

Figure 1.5. The chemical structure of galactoglucomannan.

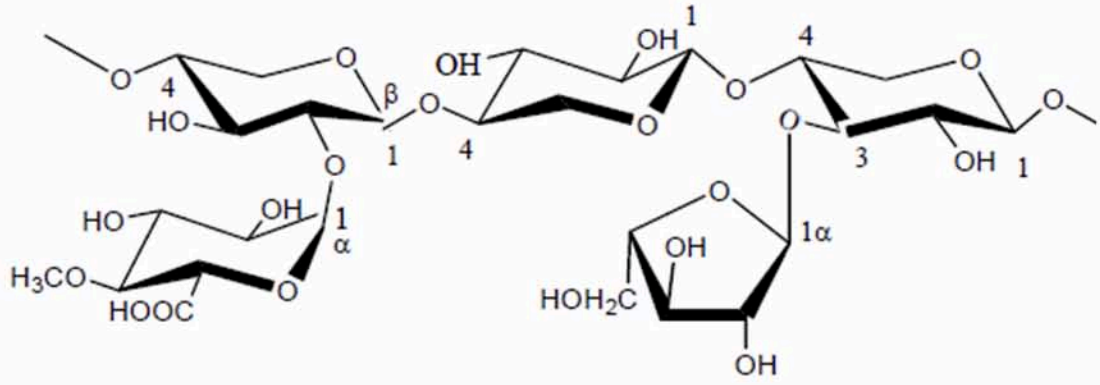

Figure 1.6. The chemical structure of arabinoglucuronoxylan.

Lignin is the third major component of wood listed herein. Lignin is an amorphous, highly polymerized substance with a three-dimensional structure comprised primarily of subunits: coniferyl alcohol, sinapyl alcohol and p-hydroxy-cinnamic alcohol. The lignin of softwood is dominated by prevalence of coniferyl alcohol subunits, often > 90%, whereas the lignin of hardwoods possesses a sinapyl alcohol content nearly equal to that of coniferyl alcohol. Lignin's main function is to hold the cellulose fibers together in the wood. In addition to lignin and carbohydrates, there are other chemical substances, collectively called extractives, which impart color, odor, taste, and decay resistance to the wood. It is clear that lignin does not have any charged moieties before pulping.

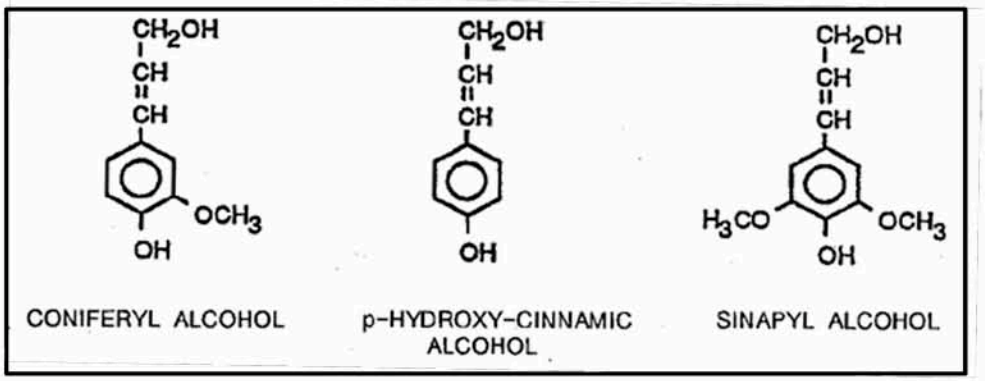

Figure 1.7. Primary subunits found in lignin.

Table 1.1 contains the typical chemical compositions found in the wood of spruce (Picea abies) and pine (Pinus sylvestris) trees, softwoods, as well as birch (Betula berrucosa) trees, a hardwood.

Main Components	Spruce	Pine	Birch
Cellulose	41	39	40
Glucomannan	18	17	3
Xylan	8	8	30
Other carbohydrates	4	5	4
Total carbohydrates	69	67	74
Lignin	27	27	20
Extractive substances	2	4	3
Total	100	100	100

Table 1.1. Wood composition of spruce (Picea abies), pine (Pinus sylvestris) and birch (Betula berrucosa).[5]

1.3 – Wood Pulping and Bleaching

There are two principally different processes to separate the cellulose fibers; the mechanical and chemical processes. By mechanical defibrillation, the fiber retains its chemical composition and, consequently, the yield is almost 100%. The primary drawback of this process is the decreased fiber strength resulting from the treatment and the inherent light sensitivity of the fibers produced. In the chemical process, the cellulose fibers are liberated from the lignin by increasing the lignin solubility under special chemical conditions. This should theoretically decrease the pulp yield to approximately 75% by removal of lignin. However, since the cooking chemicals used are partly non-specific, parts of the cellulose and the hemicellulose polymers are also dissolved. Therefore, a typical yield for the chemical pulping processes is about 50%. The two most common cooking procedures utilize a combination of hydroxide and hydrogen sulphide ions (the sulfate or kraft process) and sulphite ions (the sulphite process), respectively. The choice of defibrillation method is made to obtain suitable fiber properties for the final paper product.[12]

Due to the consolidated fiber structure it is not possible to completely remove all lignin during the cooking step, without causing a considerable deterioration of the pulp yield and properties. To remove the residual lignin, for increased brightness of the final paper product, a bleaching process is therefore applied. Traditionally, chlorine gas has been used for this purpose, due to its lignin selectivity and efficiency already at a low process temperature. During the last two decades, however, its use has been banned due

to negative environmental effects of the bleach plant discharges. New bleaching techniques have been developed; the elementary chlorine free (ECF) and the total chlorine free (TCF) bleaching processes. In these new sequences, oxygen-based chemicals e.g. oxygen, ozone and hydrogen peroxide, have come into use as the active delignification agents. The advantage of these chemicals is that they potentially allow for a "total" closure of the bleach plant since a recovery cycle can be applied. With such a closed cycle, the discharges can be significantly reduced and the water consumption decreased. A major drawback, however, is that the concentrations of metal ions in the water phase increase compared to mills with an open water system. These metal ions, commonly referred to as non-process elements, enter the pulp mill with the wood chips, the water supply and the pulping chemicals, and have in general a negative effect on the plant performance.[13] The increased concentrations of these metals have lead to more frequent scaling problems and filtration failures, equipment corrosion, and have also been shown to reduce the bleaching efficiency.[14,15]

Chemical pulping of wood is known to introduce more charged groups into wood materials. The formerly favored sulphite pulping process was known to sulphonate the lignin subunits leading to typical acidic content far greater than Kraft pulps, though with similar carboxylic acid content. This is due to the introduction of far more $-SO_3H$, or sulphonate, groups brought about during the pulping process. Sulphite pulping now, though, only accounts for less than 10% of wood pulps. Kraft pulping, or sulfate pulping, is the dominate means of chemical wood pulping. During Kraft pulping, a very small amount of carboxylic acid groups are introduced due to the oxidation of

phenyl propane units in the lignin; though during delignification a breakdown of the lignin polymers occurs leading to much of the oxidized lignin to be removed in the black liquor.

Some typical post-pulping chemistry analyses are shown in Table 1.2,[5] as opposed to the pre-pulping wood chemistry shown in Table 1.1. As is readily evident, almost all of the cellulose is preserved, almost all of the extractives and lignin are removed, and typically a <50% of hemicellulose is retained.

Components	Spruce Sulfite	Pine Kraft	Birch Sulfite	Birch Kraft
Cellulose	**41**	**35**	**40**	**34**
Glucomannan	**5**	**4**	**1**	**1**
Xylan	**4**	**5**	**5**	**16**
Other carbohydrates	-	-	-	-
Total carbohydrates	**50**	**44**	**46**	**51**
Lignin	**2**	**3**	**2**	**2**
Extractive substances	**0.5**	**0.5**	**1**	**0.5**
Total	**52**	**47**	**49**	**53**

Table 1.2. Typical post-pulping chemical analysis of three different species of trees and two different types of pulping processes.[5]

1.4 – Fiber Surface Chemistry

The fiber surface, before pulping, is coated with a layer of hydrated and negatively charged hydrophilic polymers, which originate either from hemicellulose or soluble lignin fragments. It is suggested that wood pulp fibers are rough, porous, complicated surfaces exhibiting behavior characteristics of both a hydrogel and a micro-porous solid.[16]

The wood fibers are negatively charged during the whole pH range of paper manufacturing. The ionizable groups on the cellulose fibers can be carboxyl groups, hydroxyl groups, and/or sulfonic acid and phenolic groups. For carboxyl groups, there are three sources: (A) the uronic acid residues in the form of 4-O-methyl-a-D-glucopyranosyluronic acid, which account for most of the carboxylic acid groups; (B) the pectic substances localized in the middle lamella; and (C) the fatty acids and resin acids in the extractives.[2] The carboxyl group of hemicellulose is the largest source of surface charge for kraft fibers, and a typical range of carboxyl content in wood fiber is from 5 to 15 meq per 100 grams pulp.[17]

During the preceding century an enormous amount of thermodynamic data for the behavior of chemical compounds at surfaces have been reported for a whole range of different chemical systems and, due to the aid provided by computer calculations, the complexity of these systems under study has significantly increased during the last few decades. Surface complexation models based on thermodynamic concepts have been proposed, with different expressions for describing the electric double layer at the surface.[18] Without going into great detail, the electric double layer model states that

when a charged surface is immersed in a solution containing ions, an electrical double layer is formed. This is shown in Figure 1.8 for the situation close to a negatively charged surface. As seen in Figure 1.8, positive ions are attracted to the negatively charged surface while similarly charged negative ions are repelled. This layer closest to the surface, where ions are bound and do not move freely, is known as the Stern layer. The second layer, known as either the Guoy or diffuse layer, is outside the Stern layer and where the ions can move about freely extents to where the electrical potential reaches zero. The plane separating them is referred to as the Helmholtz plane and the distance of the Helmholtz plane for the charged surface is affected by several parameters. Mathematically, the Stern layer is observed where the electric potential approaches zero linearly.[19] The overall thickness of the double layer, 1/κ, is defined as:

$$\frac{1}{\kappa} = \sqrt{\frac{\varepsilon_r \varepsilon_0 RT}{F^2 \sum_i C_i {Z_i}^2}} \qquad (1)$$

Where, in Equation (1), F, ε_0, R, and T are Faraday's constant, the permittivity of vacuum, the gas constant and temperature. Also, C_i and Z_i are the respective concentrations and the valence state of each ion in the solution surrounding a charged surface, whereas ε_r is the dielectric constant of the solvent. Thus, the thickness of an electrical double layer decreases with increasing ionic strength, $\frac{1}{2}\sum_i C_i {Z_i}^2$, and increases with increasing dielectric constant of the solvent.

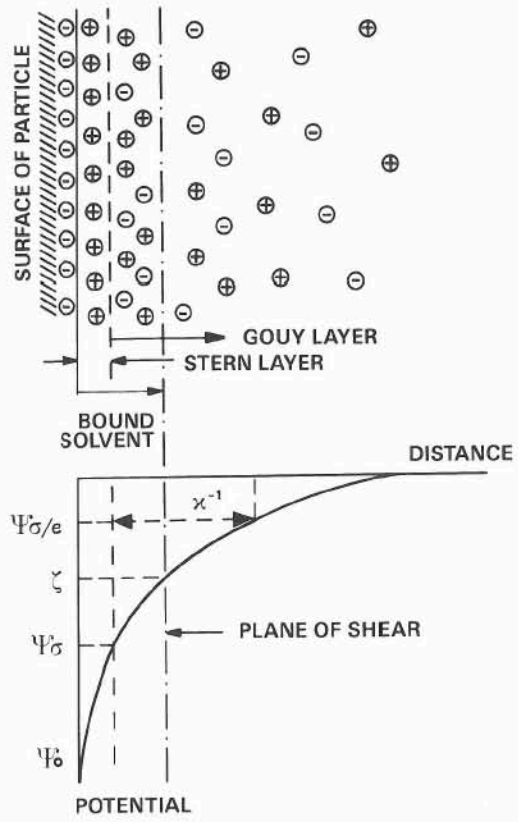

Figure 1.8. The electrical double layer.

Some of the other commonly used models for describing these properties of the surface are the Diffuse Layer Model (DLM),[20,21] the Constant Capacitance Model (CCM),[22] the Extended Constant Capacitance Model (ECCM)[23] and the Triple Layer Model (TLM).[24,25] in which the number of planes/layers between which the ions are distributed, varies. In both the DLM and CCM models only one plane/layer of the specifically adsorbed ions is present. In the DLM model, the counter ions are distributed in a diffuse layer and the surface charge-potential relationship is given by the Guoy-Chapman theory of the electric double layer. In the CCM model, the ions coordinate

directly at the surface, i.e. the ions form inner sphere complexes. In this case, the surface potential is related to the charge utilizing a constant capacitance value. In the ECCM and TLM models, two and three different layers, respectively, are used. Like in the Constant Capacitance Model, the strongly coordinating ions are found at the surface plane. However, in addition ligands of weaker surface affinity can be positioned at the β-plane, where they form outer sphere complexes. The surface charge-potential relationship of both these layers is described by using constant capacitance values. In the TLM model a third layer, a diffuse layer (compared to the DLM), is located outside the β-plane.

In recent work regarding the behavior of ions near wood fiber surfaces, the CCM model has been employed to account for the electrostatic build-up of charge due, in part, to the simplicity of this model and since it accommodates higher ionic strengths. This approach has been applied with success to describe the acid/base properties of unbleached kraft fibers.[9] Details regarding that work is described later in the text.

In the Constant Capacitance Model briefly described above, it is assumed that the ions studies form specific bonds to the sites on the surface, i.e. the fiber. In recent works it has been proposed that,[26,27] in contrast, the interactions between metal ions and fiber sites are not specific. The model used to describe such non-specific interactions was based on the ion exchange theory developed by Donnan and Harris for describing the distribution of ions between two membrane-separated solutions.[28] This theory and how it has been adapted for the interactions of ions with wood fibers is discussed later in the text.

1.5 – Wood Fiber Acid/Base Characterization

For a long time researchers have been looking at ways of measuring the acid/base properties of wood fibers. Since, as it has been stated previously, most of the acidic moieties are carboxylic acid groups from the hemicelluloses, much of the testing of wood fibers has been focused on these acid groups. These methods include exchanging calcium or zinc acetate at the acid site and then titrating with ethylenediaminetetraacetic acid to find the number of calcium or zinc cations adsorbed;[29,30] titrating with methylene blue;[31] and crystal violet.[32] Currently, the standard method of finding the carboxylic acid content in kraft wood pulp is placing the pulp in a sodium bicarbonate-sodium chloride solution and titrating this with hydrochloric acid to find the number of protons consumed by the by the pulp after eliminating those negated by the sodium bicarbonate.[33]

The work by Lars-Olof Öhman's group in Sweden has built upon the work by Forsling[34] and Pettersson[35] studies of acid/base behavior of wood pulp suspensions, as well as the work by Lövgren[36] and Laine[8] on metal oxide/water interfaces to discover the total acidic content in kraft pulp beyond those of the carboxylic acid group of the hemicelluloses.[38] Öhman's group began with a simplified expression of the equilibrium reactions describing the acid/base properties of wood fibers can be expressed as:

$$mH^+ + \equiv L^- \leftrightarrow \equiv LH \quad (2)$$

where we only consider a single type of monoprotic weak acid, $\equiv LH$, and its conguate base, $\equiv L^-$, that exists on the fibers, i.e. carboxylic acid groups from glucuronic acids in hemicelluloses. There exists a dissociation constant, β_L, for this weak acid, wherein:

$$\beta_L = \frac{[\equiv LH]}{[\equiv L^-][H^+]} \quad (3)$$

A dissociation constant exists due to a build-up of electrostatic charge on the material, i.e. the electrostatic energy needed to remove a proton from the fiber increases with the amount of negative charge on the fiber. This implies that the apparent equilibrium constant must be corrected for the corresponding coulombic energy to obtain the intrinsic equilibrium constant:

$$\beta_{L(int)} = \beta_L \cdot e^{\frac{\Psi F}{RT}} \quad (4)$$

where Ψ is the potential, in volts, at the fiber in comparison to the bulk solution. As discussed earlier, electric double layer at the surface is not applicable to wood fiber systems. The model used in the of Schindler and Gamsjäger,[22] the Constant Capacitance Model, has been successfully used for describing complexation at fiber surfaces as well as at mineral surfaces.[9,36,39] According to this model, the potential (Ψ) at the fiber is defined as the ratio between the charge, σ (in C/m^2) and the specific capacitance, κ (in $C \cdot V^{-1}m^{-2}$):

$$\Psi = \frac{\sigma}{\kappa} \quad (5)$$

The capacitance is specific for the material studied and also for the ionic medium and the temperature employed in the experiment. Consequently, κ has to be experimentally

determined for each fiber material under study and for the actual chemical conditions used. The charge can be calculated from the equation:

$$\sigma = \frac{T_\sigma F}{s \cdot a} \tag{6}$$

In this equation, s is the specific area of the fiber (m^2/g), a is the concentration of the solid phase (g/dm^3) and T_σ is the charge of the fiber, expressed as $mole/dm^3$ of the suspension. By combining equations 4 and 5, the following relationship for the potential at the fiber is obtained):

$$\Psi = \frac{T_\sigma F}{s \cdot a \cdot \kappa} \tag{7}$$

T_σ can be calculated as the sum of all charged fiber species by using the law of mass action:

$$T_\sigma = \sum \beta_{L(int)} e^{\frac{-\Psi F}{RT}} hl \tag{8}$$

Here, in equation (8), h and l are used to represent the free concentration of each component, respectively. The total concentrations can be denoted as $[H^+]_{TOT}$ and $[\equiv L^-]$ and the law of action gives the following equations:

$$[H^+]_{TOT} = h - K_w h^{-1} + \sum \beta_{L(int)} e^{\frac{-\Psi F}{RT}} hl \tag{9}$$

$$[\equiv L^-] = l + \sum \beta_{L(int)} e^{\frac{-\Psi F}{RT}} hl \tag{10}$$

In the experiments by Öhman's group, $[H^+]_{TOT}$ is known and h is measured by the potentiometric cell, and the mathematical task is thus to evaluate the relevant value of $[\equiv L^-]$, which is model independent, as well as κ and the dissociation constant β_L.

Using a potentiometric titration set-up to measure the electromotive force (EMF) of pulp suspension vs. pH, Öhman's group were able to approximate these values. Below in Figure 1.9, the EMF was plotted vs. pH, or $-\log[H^+]$, for a softwood Kraft pulp aqueous suspensions at varying ionic contents, 10-600 mM NaCl. The advantage of this method, unlike the standard TAPPI method for determining carboxylic acid group content,[33] is that it accounts for acid groups other than carboxylic acid groups. Though, since this is a Kraft pulp there is not the introduction of sulphonate groups, as there are from sulfite pulping, and does not have significant lignin content, due to the chemical pulping, there should be almost exclusively carboxylic acid groups present from remaining hemicellulose polymers. Thus, the estimated 3.1 millimoles per 100g of pulp, based on an oven-dried basis is reasonable.

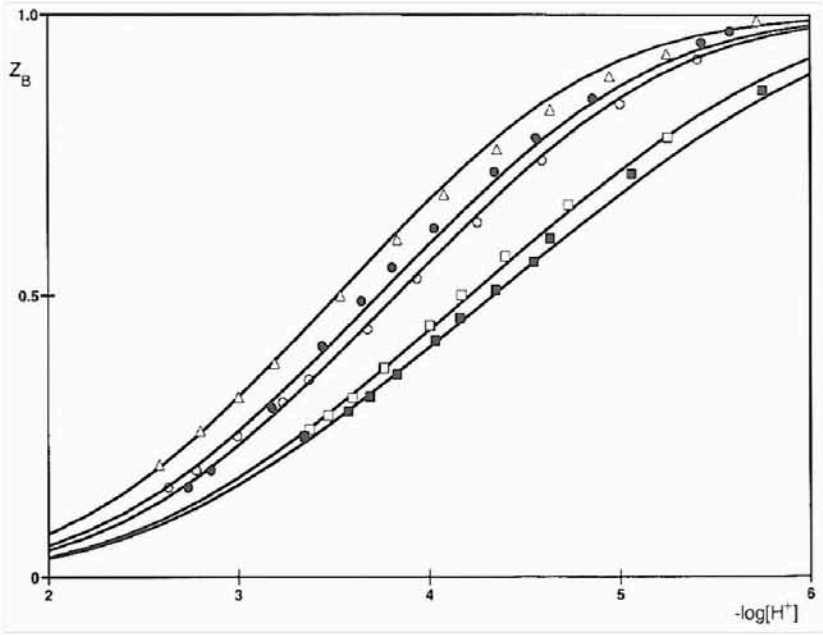

Figure 1.9. Experimental data from acid/base titrations of fully bleached softwood pulp.[40]

Later work by Öhman's group compared their potentiometric method to another method developed by Katz, Beatson, and Scallan[35] that employed conductometric titrations.[41] The conductance of a solution is the sum of the conductances of all ions present with a neutral salt added to minimize the differences in ion concentration between the fiber and solution. This method is used to calculate the total ionic content of wood fibers. An example of data from a typical conductometric titration is shown below in Figure 1.10.

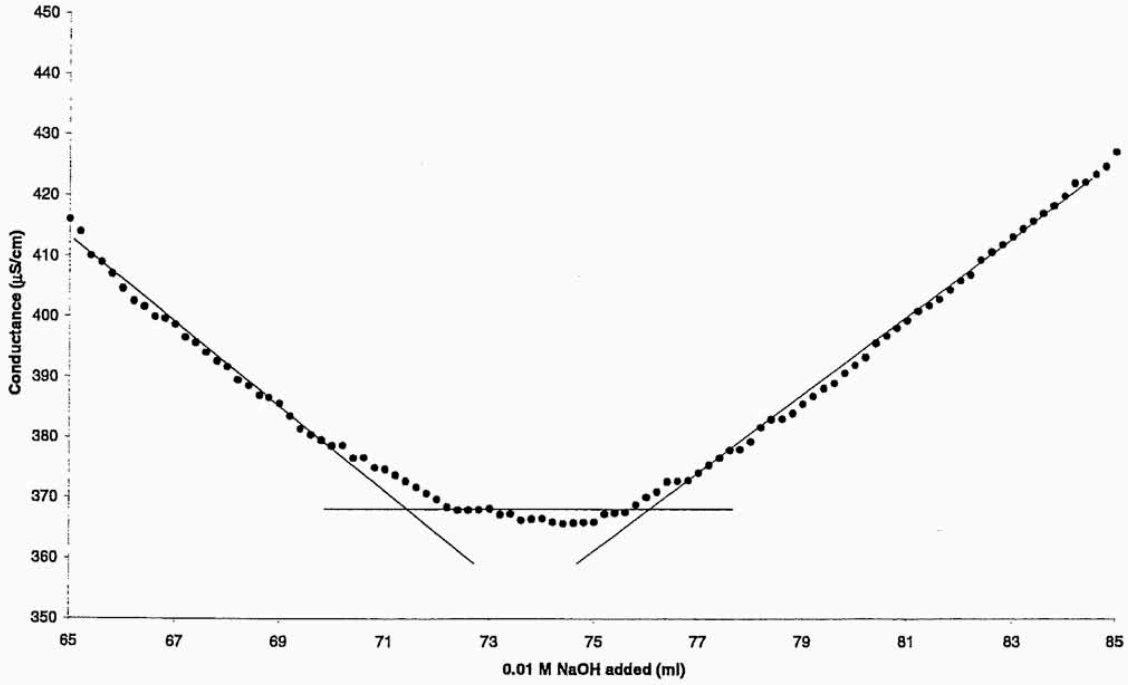

Figure 1.10. Experimental data from a conductometric titration of kraft wood pulp plotted as conductance vs. volume of NaOH added.[41]

Herein, the negative slope at the beginning of the titration is associated with the neutralization of the sodium hydroxide by the stronger carboxylic acids present in the pulp. The plateau is associated with the weaker acids, phenolic, ester or lactone groups,[38,39] which slowly dissociate. The final segment of the plot is associated with the added conductance by the ever-increasing hydroxide content of the titrant. Thus, the first intercept is associated with the carboxyl content, while the second corresponds to the total acid content.

Potentiometric titration studies, similar to those described previously, but extended to a pH range above 6 exhibits the existence of these weak acid groups as shown in Figure 1.11.

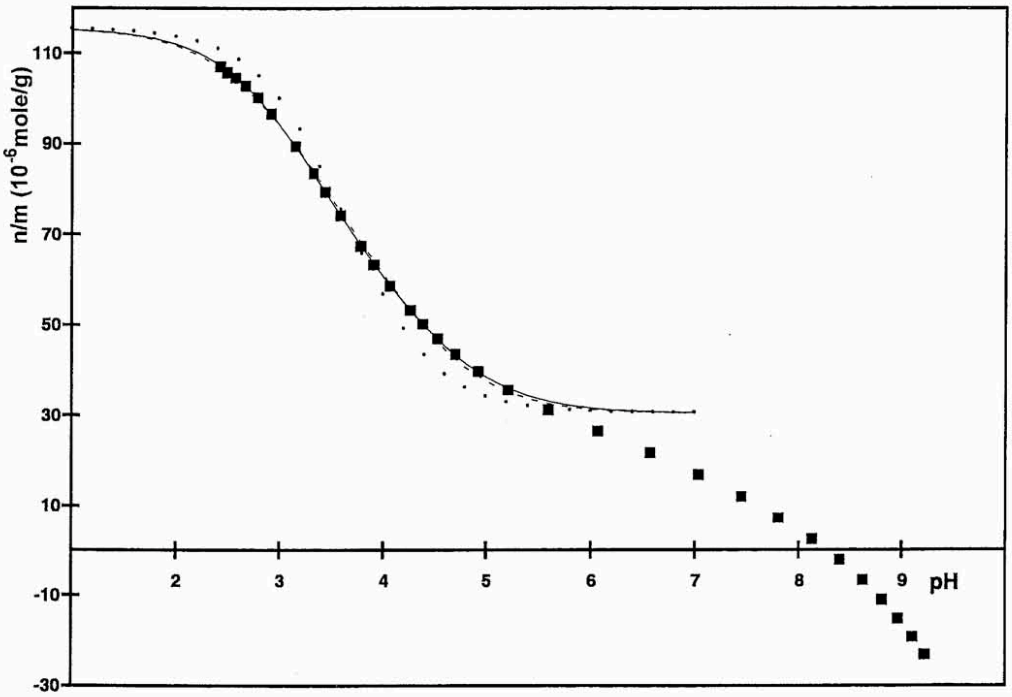

Figure 1.11. A potentiometric plot of a softwood kraft pulp at pH range of 1-9.[41]

1.6 – Donnan Equilibrium

The Donnan Theory or the Gibbs–Donnan Effect was first used to describe the distribution of ions between two solutions separated by a membrane, and where at least one ion is unable to cross that membrane.[28] The theory was further refined by Procter and Wilson[43] who showed that the model also could be applied to other equilibrium systems in the absence of a physical membrane, but where at least one ion was physically bound to only one part of the aqueous solution. Farrar and Neal[44] were the first to describe aspects of the cellulose chemistry by means of this theory. Towers and Scallan[26] have created the most prominent work on the subject of metal ions and cellulosic wood pulp. Towers and Scallan studies the distribution of Na^{+}, Mg^{2+}, Ca^{2+} and Mn^{2+} ions in a pulp suspension and observed an enrichment of these cations in the fiber phase.

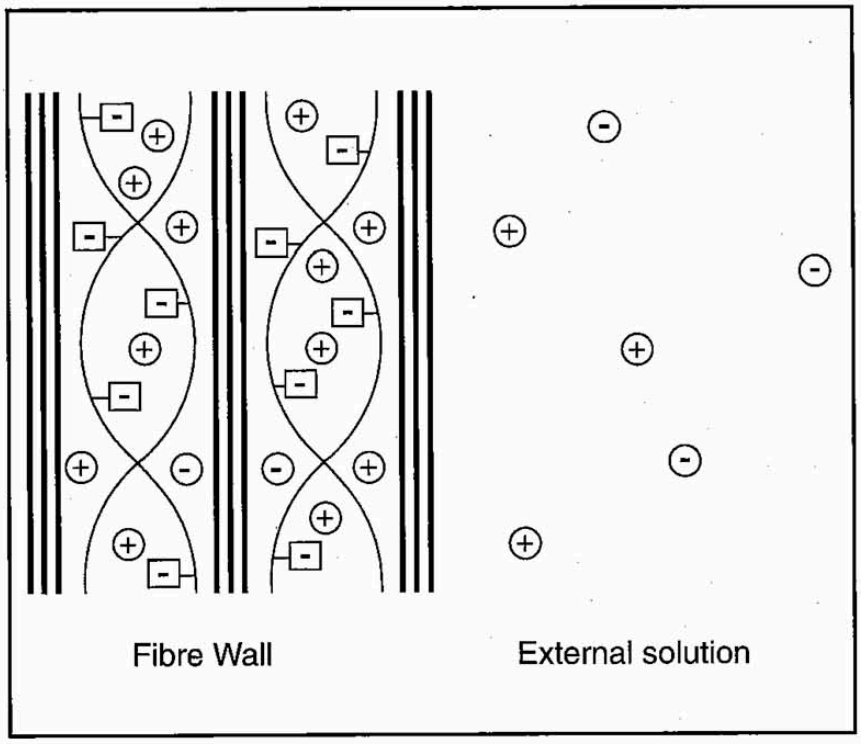

Figure 1.12. Towers and Scallan[26] depiction of Donnan equilibrium in ionic pulp suspensions.

When the Donnan theory is applied to a cellulosic material (Figure 1.12), the total aqueous volume of the suspension is divided into two sub-volumes, the suspension liquid (s) and the fiber volume (f). The latter volume is commonly referred to as the Donnan volume and is given by the mass of the fiber employed in the experiment and the specific Donnan volume of the material. Towers and Scallan[26] suggested that his specific Donnan volume could be approximated by the Water Retentions Value (WRV) of the studied material. It is assumed that the acidic groups on the fiber have access to the Donnan volume only, while all other ions can move freely between the two

volumes. It is also assumed that the anionic charges which these acidic groups give rise to, are connected to a cation (M^{z+}) enrichment and an anion (A^{z-}) depletion in the fiber volume. The anions in the wood pulp - metal cation Donnan equilibrium experiments are the counter ions of the metal cations, typically conjugate bases of strong acids. In Tower and Scallan's work,[26] the counter anions are monovalent chlorine anions, Cl^-. According to the Donnan theory, the relationship between the ion concentrations (expressed in mole/dm^3) in the two compartments can be expressed as:

$$\lambda = \left(\frac{[M^{z+}]_{(f)}}{[M^{z+}]_{(s)}}\right)^{\frac{1}{z}} = \left(\frac{[A^{z+}]_{(f)}}{[A^{z+}]_{(s)}}\right)^{\frac{1}{z}} \tag{11}$$

where λ is the distribution coefficient between the two water phases. In Tower and Scallan's system,[26] there are only protons, mono-, and divalent cations and monovalent anions (they used all metal chlorides in their experiments) and thus, under these conditions, the equations become:

$$\lambda = \frac{[H^+]_{(f)}}{[H^+]_{(s)}} = \frac{\sum[M^+]_{(f)}}{\sum[M^+]_{(s)}} = \sqrt{\frac{\sum[M^{2+}]_{(f)}}{\sum[M^{2+}]_{(s)}}} = \frac{\sum[A^-]_{(s)}}{\sum[A^-]_{(f)}} \tag{12}$$

In both of the water volumes, the demand of electric neutrality must be met, i.e. the total positive charge must equal the total negative charge. This can be expressed as:

$$\sum[A^-]_{(s)} = [H^+]_{(s)} + \sum[M^+]_{(s)} + 2 \cdot \sum[M^{2+}]_{(s)} \tag{13}$$

$$[\equiv L^-]_{(f)} + \sum[A^-]_{(f)} = [H^+]_{(f)} + \sum[M^+]_{(f)} + 2 \cdot \sum[M^{2+}]_{(f)} \tag{14}$$

where $\equiv L^-_{(f)}$ represents the anionic ligands in cellulosic material, principally glucuronic acids from hemicellulose. Equation 13 is the sum of all the exterior anions, $\sum[A^-]_{(s)}$, which equals to all of the exterior cations. Equation 14 is the sum of all of the fiber

volume anions, $[\equiv L^-]_{(f)} + \sum[A^-]_{(f)}$, which is equal to the combined charge of all of the fiber volume's cations. By combining equations 12, 13, and 14, the following equation was obtained:

$$(\lambda^2 - 1) \cdot [H^+]_s + (\lambda^2 - 1) \cdot \sum[M^+]_{(s)} + 2 \cdot (\lambda^3 - 1) \cdot \sum[M^{2+}]_{(s)} - \lambda \cdot [\equiv L^-]_{(f)} = 0$$

$$\lambda \cdot [\equiv L^-]_{(f)} = 0 \quad (15)$$

By combined Equations 12 and 15, and using the mass balance equations the following final equation is obtained:

$$(\lambda^2 - 1) \cdot [H^+]_s + (\lambda^2 - 1) \cdot \frac{\sum[M^+]_{TOT} \cdot V_{TOT}}{V_{TOT} + D \cdot m_f \cdot (\lambda - 1)} + 2 \cdot (\lambda^3 - 1) \cdot \frac{\sum[M^{2+}]_{TOT} \cdot V_{TOT}}{V_{TOT} + D \cdot m_f \cdot (\lambda^2 - 1)} = \lambda \cdot \frac{[\equiv L^-] \cdot V_{TOT}}{D \cdot m_f} = 0$$

$$= \lambda \cdot \frac{[\equiv L^-] \cdot V_{TOT}}{D \cdot m_f} = 0 \quad (16)$$

In this equation 16, $\sum[M^{z+}]_{TOT}$ denotes the total concentration of z-charged cations (in mole•dm^{-3}), V_{TOT} is the total volume (in dm^3) and m_f is the mass of the fiber used (in kilograms) in the experiment. D denotes the specific Donnan volume per unit weight and, in the work by Towers and Scallan,[26] is given the value of 1.4 dm3/kg for all calculations.

Since Equation 16 has multiple solutions for λ, it is necessary to determine the solution of chemical interest. Since only weak acidic groups are present in the fiber, the pulp will be fully protonated and thus uncharged at low pH. As a consequence, equal ionic concentrations will result in the two phases and, according to equation 2, λ will attain a value of one. To model the acid/base properties of the fiber, Towers and

Scallan[26] used an idealized monoprotic acid with a pK_a of 4, the average properties of a carboxylic acid group in wood pulps, and did not correct that model for any electrostatic effects on the fiber. Metal content in the free solution and of the fibers (with and without metal doping) was determined by atomic absorption spectroscopy. Towers and Scallan found that their model achieved relatively good agreement with the experimental data, though the r^2 values for actual monovalent metal cation concentrations were less than 0.9 from the predicted values. Examples of the work of Towers and Scallan are shown in Figure 1.13.[26] As shown in Figure 1.13, the external solution and fiber volumes reach an equilibrium concentration at elevated pH while being roughly equal at lower pH. At higher pH, the fiber will gradually become increasingly negatively charged and, as a consequence, λ will gradually exceed the value of one. The solution of interest is therefore the lowest possible value, equal to or exceeding ($\lambda \geq 1$). For solving the equation, with given total concentrations, a specific Donnan volume, and a given fiber acid/base model, several numerical methods have been used.

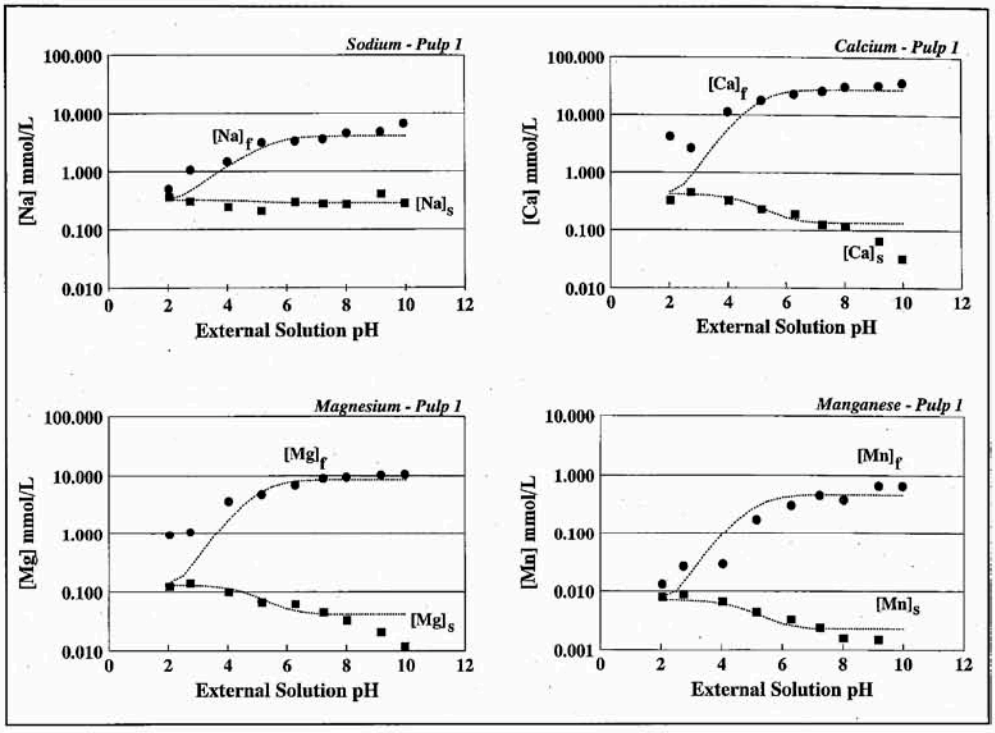

Figure 1.13. Towers and Scallan[26] representation of the Donnan equilibrium for Na, Ca, Mg, and Mn. The solid line represents the predicted value, while the data points display the experimental data.

The chemistry of these metal ions and their interactions with the wood fibers may, therefore, interest, particularly in situations where modifying the fibers or working in systems where cationic materials are present. A key feature is to have a working model for the metal ion-fiber interaction as a function of the chemical environment, i.e. pH and electrolyte concentration (ionic strength) of the solution.

Sodium ions are the metal ions of the highest concentration in the pulp/paper mill, due to their use as counter ions in most of the chemicals added. Consequently, this

ion contributes to the total metal ion concentration in the fiber line. Following the fiber line, the ionic strength varies between the different steps of refinement. The ionic strength generally decreases from about 4 M during cooking, down to approximately 5 mM after the last washer. In the bleach plant, an open chlorine dioxide stage in a filter – based plant can result in an ionic strength of below 10 mM, where as an alkaline hydrogen peroxide-stage using presses can result in an ionic strength of 60 mM. In the paper mill, different degrees of closure and different degrees of carryover from the pulp mill result in a variation in the ionic strength from approximately 5 mM to more than 50 mM.[46]

Räsänen and Stenius[27] further developed this model by using the acid/base model evaluated by Laine *et al.*[9] The study was made with the same metal ions as those examined by Towers and Scallan and by using the Debye-Hückel limiting law, they extrapolated the acid/base model from 100 mM Na^+ to the actual ionic strength (3-15 mM Na^+) of the experiments. In a later study by Tervola and Räsänen[47] developed a model for cationic transfer during kraft pulp washing. In their report, they combined the Donnan equilibrium model with the concept of advection-dispersion to accurately predict the ion concentration within the fiber volume and in the external solution while also forecasting the kinetics of mass transfer. One key conclusion they came to is that, by varying the external ion concentration, the kinetics were found to be such that an ion needs to be in the external solution during the washing phase in an industrial setting for it to be removed. In another case study, the Donnan ion exchange theory has also been found useful in predicting problems in scaling of calcium compounds and

decomposition of hydrogen peroxide due to manganese catalysis, in two Swedish TCF mills with "closed" bleach plants.

In works by Kongdee and Bechtold[48] and Chia *et al.*[49] the mass transfer characteristics of Fe^{2+} and Fe^{3+} ions were studied. In the report by Kongdee and Bechtold studied the competition for Fe^{3+} ions between cellulosic fibers and free-floating D-gluconate ligands. Their findings indicate that the affinity of cellulose over the ligands was significantly pH dependant. In the paper by Chia *et al.*[49] found that the Fe^{2+} ion distribution closely followed the Donnan equilibrium, but would precipitate within the fibers at higher pH values. Additionally, the researchers found that temperature positively affected iron sorption within the fibers. Fe(II) precipitation was similarly found by Susilo *et al.*[50] where they studied its adsorption as well as those of manganese and copper. The authors of the work found that low concentration of manganese and copper followed the Donnan expected equilibrium closely. Duang, Hoang, and Nguyen[51] have studied the adsorption of calcium and sodium cations onto unbleached kraft fibers and found that the distribution of the cations closely followed the Donnan Equilibrium. The primary deviation they found was that uptake of the cations increased when the pH was greater than 8. This could be explained in the previous section as some of the weaker acids become deprotonated at higher pH's. This conclusion is supported by the earlier work by Bygrave and Englezos[52] which found that there existed a non-ideal Donnan equilibrium at higher pH values.

1.7 – **Non-ideal Donnan Competitive Adsorption**

The non-ideal Donnan competitive adsorption model was first coined by Li and Englezos[53] and was intended to describe lignocellulosic materials, but the term and also be applied to wood fibers that have gone through pulping and bleaching. The Donnan model has been found to be insufficient in circumstances where the ionic strength of the solution is high or where there are significant amount of multiple cationic materials. In these circumstances, there is a finite adsorption of cations onto a negatively charged surface due to a finite number of anionic sites on that surface and the cations are competing with each other for adsorption onto those sites. Independent studies by Yantasee and Rorrer[54] and Rudie *et al.*[55] have reached similar conclusions as to how to properly model these types of ion-exchanges in cellulosic fibers. Firstly, the researchers considered the equilibrium processes occurring when there is cationic adsorption onto a fixed anionic site:

$$yM^{z+} + zL^{x-} \rightleftharpoons M_yL_z \tag{17}$$

The equilibrium equation state in (17) represents the adsorption of a z-charged metal (M) cation onto a y-charged anionic ligand (L). Thus, as there is equilibrium process occurring, there exists a formation constant defined as:

$$K_M = \frac{[M_y L_z]}{[M^{z+}]^y [L^{y-}]^z} \tag{18}$$

Thus, K_M is the equilibrium constant for metal M adsorbing onto anionic ligand L. If an example were to be given for metals known to adsorb onto cellulosic fibers, calcium and sodium, where the cellulosic fibers anionic groups are defined as carboxylic acid

groups (based on the information previously stated at < 8 pH), equations 18 and 19 would be thus:

$$Na^{+} + L^{-} \rightleftharpoons NaL \tag{19}$$

$$K_{Na} = \frac{[NaL]}{[Na^{+}][L^{-}]} \tag{20}$$

$$Ca^{2+} + 2L^{-} \rightleftharpoons CaL_2 \tag{21}$$

$$K_M = \frac{[CaL_2]}{[Ca^{2+}][L^{-}]^2} \tag{22}$$

Now if there is a circumstance where both, for instance, calcium and sodium cations are present significant amounts in solution then there exists a competitive co-equilibrium constant which is found by combining equations 22 and the square of 20:

$$K_{Na}^{Ca} = \frac{[CaL_2][Na^{+}]^2[L^{-}]^2}{[NaL]^2[Ca^{2+}][L^{-}]^2} = \frac{[CaL_2][Na^{+}]^2}{[NaL]^2[Ca^{2+}]} = \frac{K_{Ca}}{K_{Na}^2} \tag{23}$$

The constant K_{Na}^{Ca} is defined as the selectivity coefficient. Experimentally this selective coefficient is readily obtained by first doing a log of each side of an equation wherein there exists exponents, which is the case as with calcium and sodium where the metal cations possess different charges:

$$log\frac{[CaL_2]}{[Ca^{2+}]} = \frac{1}{2}log\frac{[NaL]}{[Na^{+}]} + logK_{Na}^{Ca} \tag{24}$$

but where the cations have equal charge, the equation would be thus:

$$log\frac{[ML_2]}{[M^{2+}]} = log\frac{[N_2L]}{[N^{2+}]} + logK_N^M \tag{25}$$

wherein M and N represent +2 charged metal cations. Both equations 24 and 25 are readily found via a log-plot of $\frac{[M_yL]}{[M^{z+}]^y}$ and $\frac{[N_yL]}{[N^{z+}]^y}$. The ligand concentration can be readily

found via one of the carboxylic acid content methods previously discussed. To find $[M_yL]$ and $[N_yL]$ one must estimate the fiber volume, which for kraft fibers has been speculated as being 1.4 dm^3/kg, though this can be found by finding the metal adsorption at low pH values as that concentration will equal that in the external solution. The slope of this log-plot should be that of the ratio of valences of the cations interaction, while the intercept is the log value of the selectivity coefficient. Based on this work, the researchers were able to gauge the respective affinities of several metal cations as well as they hydronium ion in relation to each other. In Figure 1.14 the competitive ion-exchange between hydronium vs. calcium (1) and sodium vs. calcium (2) are displayed.

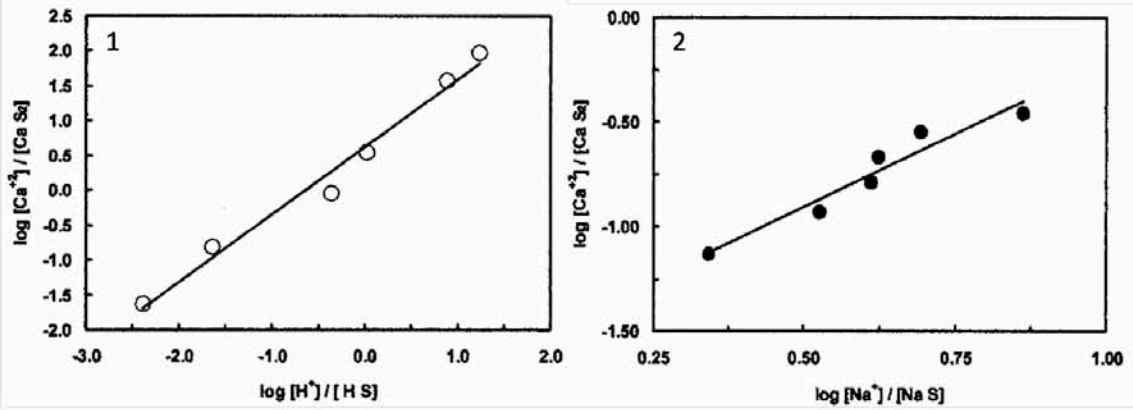

Figure 1.14. (1) log-plot of $\frac{[H^+]}{[HS]}$ vs. $\frac{[Ca^{2+}]}{[CaS]}$ and (2) $\frac{[Na^+]}{[NaS]}$ vs. $\frac{[Ca^{2+}]}{[CaS]}$.

This competitive adsorption has been observed by other scientists, but they did not identify a cogent scientific argument for the phenomena. The group of researchers

Duong, Nguyen, and Hoang[51] has previously been mentioned for their studies of on calcium and sodium adsorption onto unbleached kraft pulps, but also did a competitive study of these metal cations wherein they observed that calcium had a great adsorption affinity, but did not devise a model to describe this behavior. The other works on competitive adsorption was undertaken with modified cellulosic pulp wherein the number of carboxylate groups was greatly increased, thus differing from work on unmodified pulp materials. Saito and Isogai[56] observed the relative adsorption affinities for 12 different metal cations onto 2,2,6,6-tetramethylpiperidine-1-oxy oxidized pulps. Sundman et al. observed the Ca^{2+} and Cu^{2+} adsorption in relation to NaCl content and pH wherein the researchers found deviations from the Donnan theory, but failed to come up with an adequate model to describe the behavior of the multi-component adsorption.

1.8 - **Aims and Importance of Research**

The primary objective of this research is to develop an understanding of both organic-inorganic and organic-organic ion-exchange with cellulosic fibers. The objectives of this research focus on addressing several issues previously not studied in the field.

1. Understanding the adsorption behavior of organic cations with cellulosic fibers and whether they follow the standard Donnan model.

2. Discovering the selectivity coefficients of organic-inorganic ion-exchange phenomena when cellulosic fibers are the ion-exchange material.
3. Discovering the selectivity coefficients of organic-organic ion-exchange phenomena when cellulosic fibers are the ion-exchange material using both small, large and macromolecules and if the organic-organic ion exchange follows the Donnan theory.
4. Developing an understanding of the kinetics of organic adsorption onto cellulosic fibers.
5. Expand the existing literature's number of studied metal salts and their adsorption onto cellulosic fibers.

In this chapter an overview of wood, its chemistry, structure and pulping has been given. Also, a discussion of wood pulps surface charge and acid-base properties has been discussed, including a number of methods for characterizing each. Furthermore, the Donnan equilibrium expression for ionic-exchange on a charge volume was derived along with work that's been done for applying it to the adsorption of cations onto cellulosic fibers. Additionally, the newer adaptation of this Donnan equilibrium expression was derived for situations where the ionic strength is high and/or there are significant amounts of multiple cations.

Chapter 2, discusses research involving both organic-inorganic and organic-organic ion-exchange with cellulosic fibers. The organic cations studied are ammonium compounds, varying in size size from ammonium to polybrene – a cationic macromolecule with ammonium function groups, and PolyDADMAC, a macromolecule

with N-substituted pyrrolidine groups. It has been shown previously that many metal cations exhibit ion-exchange phenomena that adheres Donnan theory, thus it is of interest to discover whether organic cations, whether in combination with metal cation or with other organic cations, similarly exhibit ion-exchange behavior adhering to the Donnan theory. If a Donnan equilibrium exists, then comparative affinities for the cellulosic material, or more specifically its carboxylic acid groups, can be determined, as explained earlier in the chapter.

Chapter 3 details the research on the kinetic behavior of the adsorption of organic cations. In the chapter, a detailed overview of the two leading theories of regarding adsorption onto, or within, cellulosic fibers is given; those being Intraparticle Diffusion and Convective Mass Transfer Models. Earlier work by Wassana Yantasee showed that the adsorption of metal cations as moderate or better mixing exhibited adsorption kinetics following the Intraparticle Diffusion Model. It is the purpose of this work to investigate whether or not organic molecules, particularly larger ones, follow this model.

In chapter 4, there is a discussion of research involving organic-inorganic ion-exchange with cellulosic fibers for a commercial purpose. The organic cations of interest are quaternary ammonium salts, also known as quat salts. Many quat salts are used as disinfectants in commercial and industrial cleaning products. Previous work has shown that a majority of said quat salts in an aqueous solution with cellulosic fiber meshes or “wipes” adsorb onto the fibers and, therefore, are not capable fo being delivered to a wiped surface. It is the goal of this work to explore whether this issue can

be addressed by using competitive adsorption of other cations to occupy the cellulosic fiber anionic groups and, therefore, allow for more of the quat salts to remain in the solution. Chapter 4 details the success of that work. Subsequent to this chapter, in chapter 5 is a reprint of the patent based on this work.

In Chapter 6, conclusions of the research conducted on organic-inorganic and organic-organic ion-exhange are made. There is a discussion of what understanding of this topic has been gained by this work and what research is left to be conducted. Also, future projects building off this work are discussed.

Notes to Chapter 1

(1) Clark, J. d'A. *Pulp technology and treatment for paper*, 2nd edition, **1985**, Miller Freeman Publications, San Francisco.

(2) Fengel, D.; Wegenger, G. *Wood; Chemistry, Ultrastructure, and Reactions*, 1st edition, **1984**, Walter de Gruyter Publications, Berlin.

(3) Biermann, C.J. *Handbook of Pulping and Papermaking*, 2nd Edition, **1996**.

(4) Kerr, A.J.; Goring, D.A.I. *Cellulose Chem. Tech.*, **1975**, *9*, 563.

(5) Eklund, D.; Lindström, T. *Paper Chemistry; An Introduction*, 1st Edition, **1991**.

(6) Smook, G.A. *Handbook for Pulp and Paper Technologists*, **1992**, Angus Wilde, Vancouver, B.C.

(7) Sjöström, E. *Nord. Pulp Pap. Res. J.*, **1989**, *4*, 90.

(8) Katz, S.; Beatson, R.P.; Scallan, A.M. *Svensk Papperstidn*, **1984**, *6*, 48.

(9) Laine, J.; Lövgren, L.; Stenius, P.; Sjöberg, S. *Colloids and Surfaces*, **1994**, *88*, 277.

(10) Wennerstrm, M. "*Komplexbildning mellan metalljoner och vedpolymerer*", **1996**, Licentiate Thesis, Royal Institute of Technology, Sweden.

(11) Strazdins, E. *Tappi J.*, **1974**, *57*, 76.

(12) Sjöström, E. *Wood Chemistry, Fundamentals, and Applications 2nd Ed*, **1992**, Academic Press INC, New York.

(13) Gleadown, P.; Hastings, J.; Barynin, J.; Schroderus, S.; Warnqvist, B. *Pulp Pater Can.* **1997**, *98*, 27.

(14) Brooks, T.R.; Edwards, L.L.; Nepote, J.C.; Caldwell, M.R. *Tappi J.*, **1994**, *77*, 83.

(15) Ulmgren, P. *Nord. Pulp Pap. Res. J.*, **1997,** *12*, 32.

(16) Pelton, R. *Nord. Pulp Pap. Res. J.*, **1993**, *8*, 113.

(17) Scott, W. E. *Principles of wet end chemistry*, TAPPI Press, Atlanta, GA, (1996).

(18) (a) Helmholtz, H. *Pogg. Ann.* **1853**, *LXXXIX*, 211; (b) Gouy, G. *Comt. Rend.* **1909,** *149*, 654; (c) Gouy, G. *J. Phys.* **1910**, *4*, 457; (d) Chapman, D.L. *Phil. Mag.* **1913**, *6*, 475; (e) Stern, O. *Z. Electrochem*, **1924**, *30*, 508.

(19) Hiemenz, P.C. *Principles of Colloid and Surface Chemistry*, **1977**, Marcel Dekker, Newy York.

(20) Stumm, W.; Huang, C.P.; Jenkins, S.R. *Croat. Chem. Acta*, **1970**, *42*, 223.

(21) Huang, C.P.; Stumm, W. *J. Colloid Interface Sci.*, **1973**, *22*, 231.

(22) Schindler, P.W.; Gamsjöger, H. *Kolloid Z. u. Z. Polymere*, **1972**, *250*, 759.

(23) Nilsson, N.; Persson, P.; Lövgern, L.; Sjöberg, S. *Geochim. Cosmochim. Acta* **1996**, *60*, 4385.

(24) Yates, D.E.; Levine, S.; Healy, T.W. *J. Chem. Soc. Faraday Trans.1*, **1974**, *70*, 1807.

(25) Davis, J.A.; James, R.O.; Leckie, J.O. *J. Colloid Interfae Sci*. **1978**, *63*, 480.

(26) Towers, M..; Scallan, A.M.; *J.Pulp Paper Sci*, **1996**, *22*, 332.

(27) Räsänen, E.; and Stenius, P. *"The sorption of* Na^{+}, Ca^{2+}, Mg^{2+} *and* Mn^{2+} *on cellulose fibres: Prediction and analysis of sorption equilibrium with electrostatic models"*, 9th ISWPC, **1997**, 94.

(28) Donnan, F.G.; Harris, A.B. *J. Chem. Soc.* **1911**, *99*, 1554.

(29) Doering, H. *Das Paper*, **1956**, *10*, 140.

(30) Wilson, K. *Svensk Papperstidn*, **1948**, *51*, 45.

(31) Wilson, W.K.; and Mandel, J. *Tappi*, **1961**, *44*, 131.

(32) Rebek, M.; Klaus, K.; Baumgartner, H. *Das Paper.*, **1956,** *10*, 91.

(33) TAPPI method – *"Carboxyl Content of Pulp"* T 237 cm-08.

(34) Forsling, W.; Hietanen, S.; Sillén, L.-G. *Acta Chem. Scand.* **1952**, *6*, 901.

(35) Pettersson, L. *"Equilibrium and structure studies of aqueous three component polyanion complexes fromed in the systems* $H^{+} - MoO_4^{2-} - HPO_4^{2-}, H^{+} - MoO_4^{2-} - HAsO_4^{2-}$ *and* $H^{+} - MoO_4^{2-} - (D-)mannitol$" **1974**, PhD Dissertation, Umeå University, Sweden.

(36) Lövgren, L. *"Complexationproperties of a bog-water and of the surface of goethite (α-FeOOH"* **1990**, PhD Dissertation, Umeå University, Sweden.

(38) Öhman, L.-O.; Forsling, W. *Acta Chem. Scand.* **1981**, *A35*, 795.

(39) Laiti, E. "*Interactionsbetween phosphonate/phosphate ligands and hydrous alumina surfaces*" **1996**, PhD Thesis, Umeå University, Sweden.

(40) Samuelsson, O.; Törnell, B. *Svensk Papperstidn.* **1961**, *64*, 198.

(41) Philipp, B.; Rehder, W.; Lang, H. *Das Papie.* **1965**, *19*, 1.

(42) Lindgren, J.; Öhman, L.-O. *Nord. Pulp Pap. Res. J.* **2000**, *15*, 18.

(43) Lindgren, J.; Öhman, L.-O.; Gunnars, S.; Wågberg, L. "*Experimental Studies of Acid/Base Properties and Metal Ion Affinities of Wood Fibers*" **2000**, *III*, PhD Thesis, Umeå University, Sweden.

(44) Proctor, H.R.; Wilson, J.A. *J. Chem. Soc.* **1916**, *109*, 307.

(45) Farrar, J.; Neale, S.M. *J. Colloid Interface Sci.* **1952**, *7*, 186.

(46) Lidén, J.; Johansson, B.; Jönsson, A. Lorin, T. *6th Int. Conf. New Available Tech.* **1999**, 189.

(47) Tervola, P.; Räsänen, E. *Chem. Eng. Sci.* **2005**, *60*, 6899.

(48) Kongee, A.; Bechtold, T. *Carbohyd. Polym.* **2004**, *56*, 47

(49) Chia, C.H.; Duong, T.D.; Nguyen, K.L.; Zakaria, S. *J. Colloid Interf. Sci.* **2007**, *307*, 29.

(50) Susilo, R.; Chandraghatgi, R.; Englezos, P. *Pulp Pap-Canada*, **2005**, *106*, 47.

(51) (a) Duong, T.D.; Nguyen, K.L.; Hoang, M. *J. Colloid Interf. Sci.* **2006**, *303*, 69. (b) Duong, T.D.; Nguyen, K.L.; Hoang, M. *J. Colloid Interf. Sci.* **2006**, *301*, 446. (c) Duong, T.D.; Nguyen, K.L.; Hoang, M. *J. Colloid Interf. Sci.* **2004**, *276*, 6. (d) Duong, T.D.; Nguyen, K.L.; Hoang, M. *J. Colloid Interf. Sci.* **2005**, *287*, 438.

(52) Bygrave, G.; Englezos, P. *Nord. Pulp and Pap. Res. J.* **1998**, *13*, 220.

(53) Susilo, R.; Chandraghatgi, R.; Li, X.-S.; Englezos, P. *Can. J. Chem. Eng.* **2005**, *83*, 537.

(54) Yantasee, W.; Rorrer, G.L. *J. Wood Chem. Technol.* **2002**, *22*, 157.

(55) Rudie, A.W.; Ball, A.; Patel, N. *J. Wood Chem. Technol.* **2006**, *26*, 259.

(56) Saito, T.; Isogai, A. *Carbohyd. Polym.* **2005**, *61*, 183.

Chapter 2: Organic-Inorganic and Organic-Organic Ion-Exchange in Cellulosic Fiber Matrices

In this section I will briefly discuss the fundamentals

2.1 – Introduction

The equilibrium ion exchange between two different cations, A and B, with different charges, a and b, on a wood pulp functional group (S) as a cation exchanger can be expressed as follows:

$$bA^{+a} + aB \cdot S_b \overset{K^{A/B}}{\longleftrightarrow} bA \cdot S_a + aB^{+b} \tag{2.1}$$

The competition for the available binding site is represented by equilibrium constant:

$$K^{A/B} = \frac{[A{\cdot}S_a]^b[B^{+b}]^a}{[B{\cdot}S_b]^a[A^{+a}]^b} \tag{2.2}$$

Experimental data do not normally yield the exact stoichiometry as described by equation (2.1). Therefore, equation (2.1) is rewritten as:

$$A^{+a} + nB \cdot S_b \overset{K^{A/B}}{\longleftrightarrow} A \cdot S_a + nB^{+b} \tag{2.3}$$

Now $K^{A/B}$ becomes:

$$K^{A/B} = \frac{[A{\cdot}S_a][B^{+b}]^n}{[B{\cdot}S_b]^n[A^{+a}]} \tag{2.4}$$

Taking the largarithm of equation (3.4) yields:

$$\log\frac{[A\cdot S_a]}{[A^{+a}]} = n\cdot log\,\frac{[B\cdot S_b]}{[B^{+b}]} + logK^{A/B} \qquad (2.5)$$

A plot of $\log\frac{[A\cdot S_a]}{[A^{+a}]}$ vs. $log\,\frac{[B\cdot S_b]}{[B^{+b}]}$ is linear, where equilibrium constant $K^{A/B}$ and n are estimated from the intercept and slope, respectively.

The dissociation constant of a weak acid (HA) is related to the degree of ionization by Henderson-Hasselbalch equation, given by:

$$pK = pH + log[(1-\alpha)/\alpha] \qquad (2.6)$$

where α represents the degree of ionization of the acid as defined by:

$$\alpha = \frac{[A^-]}{[HA]} \qquad (2.7)$$

In the case of a gel polyelectrolytes and wood pulps, Katchalsky[1] modified equation (2.6) using the Donnan equilibrium to yield the apparent dissociation constant of wood pulp functional groups, K_{app}, as:

$$pK_{app} = pH + log[(1-\alpha)/\alpha] \qquad (2.8)$$

where α now represents the degree of ionization of the functional group, as defined by:

$$\alpha = \frac{[-COO^-]}{[-COOH]} = \frac{[-COO\cdot M]}{[-COOH]} \qquad (2.9)$$

Herrington and Midmore[2] proposed that the intrinsic dissociation constant, pK_{io}, of various types of cellulose fibers can be determined from a plot of pK_{app} vs. α, where pK_{io} is obtained by extrapolating pK_{app} to $\alpha = 0$. However, this plot was not appropriate for wood pulp since data were seldom obtained below $\alpha = 0.3$. Later, Herrington and Petzold[3] extended this model to wood pulp suspensions by showing that a plot of pK_{app} vs. $anti - log\ \alpha$ was a straight line with a value for pK_{io} at $anti - log\ (\alpha) = 1$. The Herrington and Petzold equation is:

$$pK_{app} = pK_{io} - m + m\ anti - log\ (\alpha) \qquad (2.10)$$

where m represents the slope of pK_{app} vs. $anti - log\ (\alpha)$.

The multi-component ion exchange equilibrium model was developed under five assumptions: (1) cationic ions bind with wood pulp by an ion-exchange process; (2) only the carboxylic group serves as the cationic ion binding site; (3) the pulp slurry is at equilibrium; (4) the temperature is constant; (5) there are no effects of ionic strength, aqueous electrolyte speciation, or precipitation on cationic ion partitioning. The batch equilibrium model has four components, which include equilibrium mass-action expressions for cationic ion partitioning between wood pulp and solution, a total site balance, material balances for adsorbed cationic ions and the probe ions, and a charge balance.

The cationic concentrations on the pulp and in the liquid are both expressed on a common aqueous phase basis so that the mass-action expressions are dimensionless. Consquently,

$$[A_i \cdot S_a] = q_i \frac{m_p}{V} \qquad [B_i \cdot S_b] = q_i \frac{m_p}{V} \qquad [H \cdot S] = q_H \frac{m_p}{V} \quad (2.11)$$

Rearranging, H^+, A_i^{+a}, and B_i^{+b} adsorbed on the wood pulp are given by

2.2 - Experimental

2.2.1 – Materials and Sample Preparation

Thiophene-Quinoxaline copolymers were synthesized in our laboratory and the laboratories of Professor W.C. Chen of National Taiwan University in Taipei[7] follow the previously published synthetic methods for **PTHQx**.[1b] Also the theoretical electronic structures and properties of the related poly[(thiophene-2,5-diyl-*alt*-(quinoxaline-5,8-diyl)] (**PTQx**) was studied.[7] **PTQx** was found to have a theoretical LUMO level of 2.73 eV, a HOMO energy level of 4.91 eV, and, therefore, a theoretical band-gap of 2.18 eV. Anhydrous toluene, octyltrichlorosilane (OTS-8), and octadecyltriethoxysilane (OTS-18) used in the deposition of self-assembled monolayers (SAMs) on the gate dielectric surface and solvents used for the thiophene-quinoxaline copolymers (trifluoroacetic acid, chloroform, and 1,2,4-trichlorobenzene) were purchased from Aldrich and used as received.

All **PTHQx** thin films for fabrication of OFETs were spin-coated from 0.15% (w/v) solutions in trifluoroacetic acid, filtered through a 0.2 μm pore filter, at a spin rate of 1200 rpm for 30 s. **PTDDQx** and **P2TDDQx** thin films for fabrication of OFETs were spin-coated from 0.2% (w/v) solutions in trifluoroacetic acid (TFA), chloroform, and heated 1,2,4-tricholorobenzene (TCB), filtered through a 0.2 μm pore filter, at a spin rate of 1000 rpm for 30 s and 1500 rpm for 45 s for TCB solutions. The spin-coated thin films were dried at 60 ^{o}C in vacuum for 10-12 h.

2.2.2 – Optical Absorption and Photoluminescence Spectroscopy

Optical absorption spectra were obtained by using a Perkin-Elmer Lambda 900 UV/vis/near-IR spectrophotometer. The PL emission spectra were obtained with a Photon Technology International (PTI) model QM-2001-4 spectrofluorimeter. Thin films (20-30 nm thick) for optical absorption spectroscopy and photoluminescence were spin-coated on glass slides from a 0.35% (w/v) solution; TFA for **PTHQx** and chloroform for **PTDDQx** and **P2TDDQx** at 1000 rpm for 30 s. The copolymer thin films for optical measurements were homogeneous and they showed good optical transparency. Solution optical absorption spectroscopy and photoluminescence was done with 10^{-5} M solutions of TFA for **PTHQx** and chloroform for **PTDDQx** and **P2TDDQx**.

2.2.3 – Copolymer Electrochemistry and Thermal Analysis

CV experiments were carried out on an EG&G Princeton Applied Research Potentiostat/Galvanostat (Model 273A). Data were collected and analyzed by using Model 270 Electrochemical Analysis System Software. A three-electrode cell was used in all experiments. Platinum-wire electrodes were used as both the counter and working electrodes and a Ag/Ag^+ electrode (Ag in a 0.1 M $AgNO_3$ solution, Bioanalytical System) was used as the reference electrode. The Ag/Ag^+ reference electrode was calibrated at the beginning of the experiments by recording a cyclic voltammogram of ferrocene; this was used as an internal standard. The potential values obtained in reference to the Ag/Ag^+ electrode were then converted to the SCE scale. The SCE energy level relative to vacuum of 4.4 eV was used to estimate the EA and IP values.[8] The platinum-wire working electrodes were coated with the thiophene-quinoxaline copolymers from 0.3% (w/v) solutions in TFA. Thin film electrochemistry was performed in an electrolyte solution of 0.1 M tetra-n-butylammonium hexafluorophosphate, $TBAPF_6$, in acetonitrile was used for all experiments. All solutions were purged with high-purity N_2 for 30–45 mins before each experiment and a blanket of N_2 was used during the experiment. Typical scan rates of 20–40 mV/s were used.

TGA measurements were carried out on a TA Instruments model Q50 TGA in nitrogen at heating rates of 20 °C min^{-1}.

2.2.4 - Surface Modification of SiO_2 Dielectric

The method for depositing a self-assembled monolayer (SAM) on the SiO_2 gate dielectric is similar to that reported by Lee et al.[9] The flasks and SiO_2/Si OFET substrates were dried in an oven at 120°C for 20 minutes. The substrates were immersed in anhydrous toluene under argon at room temperature. Octyltrichlorosilane (OTS-8) was added (10 mM) and left to form a self-assembled monolayer for 1 h under argon. The SAM-treated substrates were removed from the OTS-8 solution, rinsed with anhydrous toluene and baked at 120 °C for 20 min in an oven. The substrates were sonicated in anhydrous toluene for 1 min and then rinsed further with anhydrous toluene. The OTS-8 SAM-modified OFET substrates were dried in vacuum for 1 h before use.

Another method was used for depositing SAMs of octadecyltriethoxysilane (OTS-18). Here I placed FET SiO_2/Si substrates in a chamber with a small amount of OTS-18 and left it to from a SAM of OTS-18 while under vacuum and heated to 70°C. After 2 days, the FET substrates were removed from the chamber and rinsed and sonicated in anhydrous toluene. The OTS-18 SAM-modified OFET substrates were dried in vacuum for 1 h before use.

2.2.5 – Thin Film Morphology

The thin film morphologies of the thiophene-quinoxaline copolymers were investigated by atomic force microscopy (AFM) in standard tapping mode on a Digital

Instruments (Santa Barbara, CA) operated with NanoScope IIIa controller and on a Veeco Dimension 3100 Scanning Probe Microscope (SPM) system is operated by a NanoScope Iva Controller, integrated with the Dimension Hybrid XYZ Closed-Loop Scanner, and equipped with the Motorized Precision Sample Stage. Thiophene-quinoxaline copolymer thin films (10-30 nm thick) for AFM imaging were spin-coated from trifluoroacetic acid or TCB solutions onto OFET substrates with a 300-nm SiO_2 surface with or without an SAM deposited upon it. The film thickness was measured by using an Alpha-Step 500 profilometer (KLA Tencor, Mountain View, CA) with an accuracy of 1 nm.

2.2.6 – Fabrication and Characterization of Thin Film Transistors

Bottom-contact geometry was used to fabricate the thin film field-effect transistors as shown in Figure 2.1. Heavily n-doped Si with a conductivity of 10^3 S/cm was used as a gate electrode with 300 nm thick SiO_2 layer as the gate dielectric. Using photolithography and a vacuum sputtering system (2 x 10^{-6} Torr), two 90-nm thick gold electrodes (source and drain) with a 10-nm thick adhesive layer of TiW alloy were fabricated onto the SiO_2 layer. A channel length (L) of 25 μm and a channel width (W) of 500 μm were used. The gate electrode launching pad was placed on top of the Si gate electrode after the SiO_2 gate dielectric had been mechanically etched away. On the top of this device structure, thin films (10-30 nm) of thiophene-quinoxaline copolymers were spin-coated from TFA, chloroform, and TCB solutions and dried overnight (10-12 h) at 60°C in a vacuum oven. Electrical characteristics of the devices were measured

using a Keithley 4200 semiconductor parameter analyzer (Keithley Instruments, Inc., Cleveland, OH). All the measurements were done under ambient laboratory conditions.

2.3 – Results and Discussion

2.3.1 – Optical Absorption and Photoluminescence Spectra

The optical absorption spectra of the thiophene-quinoxaline copolymers in dilute, 10^{-5} M, solution and solid-state are shown in Figures 2.2 and Figure 2.3, respectively. Additionally, the solution photoluminescence spectra are shown in Figure 2.2. All of the pertinent optical and electrochemical data is shown in Table 2.1. For **PTHQx**, the lowest energy absorption band in solution is broad, extending from 420 to 670 nm with an absorption maximum (λ_{max}) at 545 nm with high intensity absorption peaks at 300 and 350 nm. Since **PTHQx** TFA solutions are acidic, the resulting solution absorption spectra is red-shifted due to protonation. The lowest energy absorption band in solid state is broad, extending from 420 to 720 nm with an absorption maximum (λ_{max}) at 636 nm and a vibronic peak at 572 nm. The optical band gap derived from the absorption edge of the thin film spectrum is 1.75 eV. No photoluminescence in solution or thin film was observed for **PTHQx**.

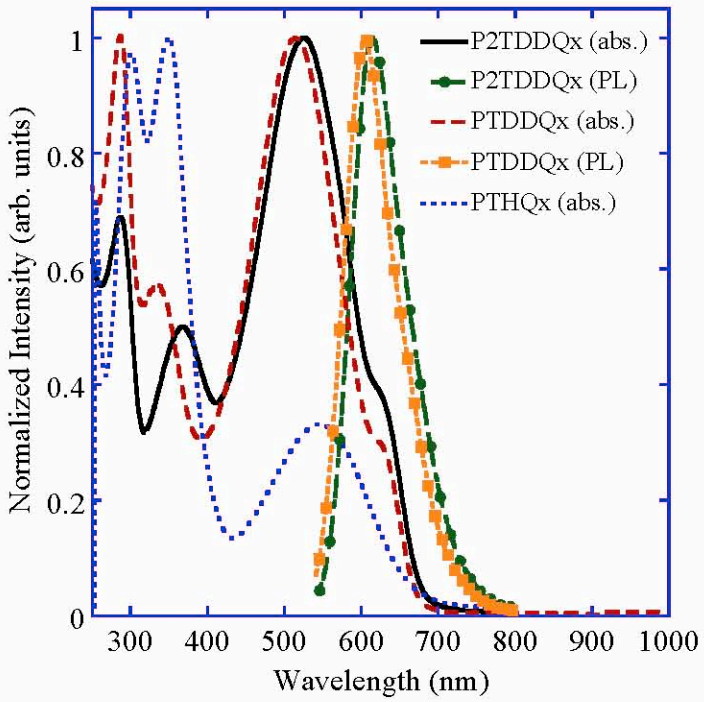

Figure 2.2. Optical absorption and photoluminescence spectra of thiophene-quinoxaline copolymers. Shown are TFA solutions of **PTHQx** and $CHCl_3$ solutions of **PTDDQx** and **P2TDDQx** (10^{-5} M).

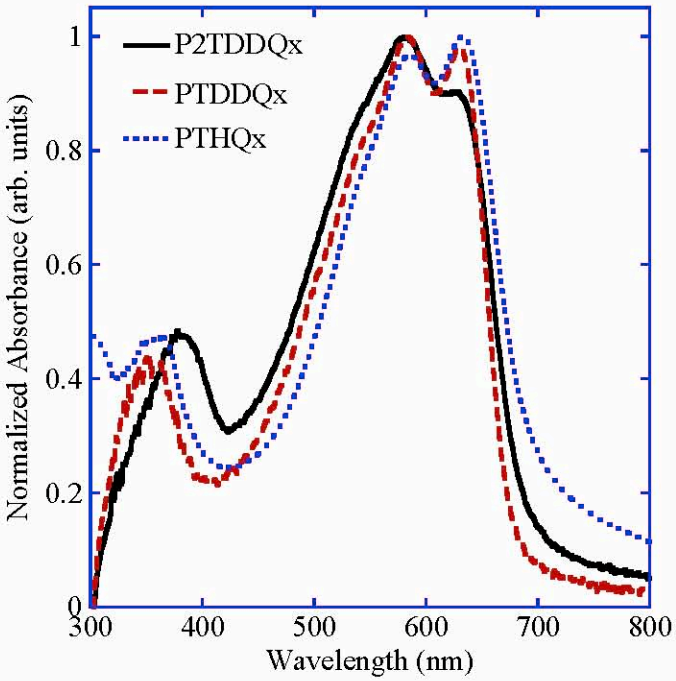

Figure 2.3. Optical absorption spectra of thiophene-quinoxaline copolymers thin films on glass.

Table 2.1. Optical and Redox Properties of Thiophene - Quinoxaline Copolymers

Copolymer	λ_{max}^{abs} (nm)		E_g^{opt} (eV)	$E_{ox\ a}^{onset}$ (V)	$E_{ox}^{o\text{-}b}$ (V)	IP[c] (eV)	$E_{red}^{onset\ a}$ (V)	$E_{red}^{o\text{-}b}$ (V)	EA[d] (eV)	E_g^{el} (eV)
	solution	film								
PTHQx	545	636	1.75	0.67	0.83	5.07	-1.62	-1.80	2.78	2.36
PTDDQx	514	583	1.83	0.60	0.92	5.00	-1.74	-1.90	2.66	1.84
P2TDDQx	527	583	1.80	0.49	0.74	4.89	-1.71	-1.85	2.69	2.20

[a] Onset oxidation and reduction potentials vs SCE. [b] Formal oxidation and reduction potentials vs SCE. [c]Ionization potential was obtained based on IP = E_{ox}^{onset} + 4.4 eV. [d]Electron affinity was obtained based on EA = E_{red}^{onset} + 4.4 eV.

For **PTDDQx**, the lowest energy absorption band in solution is broad, extending from 410 to 690 nm with an absorption maximum (λ_{max}) at 514 nm with a shoulder from 600 - 630 nm. The lowest energy absorption band in solid state is broad, extending from 410 to 690 nm with a low energy peak at 632 nm and an vibronic peak at 583 nm, which was the absorption maximum (λ_{max}).The optical band gap derived from the absorption edge of the thin film spectrum is 1.83 eV. Solution photoluminescence was observed for **PTDDQx** with an emission maximum (λ_{max}) at 604 nm. Weak photoluminescence for **PTDDQx** thin films was observed, but the poor signal to noise ratio made it difficult to discern a emission maximum.

For **P2TDDQx,** the lowest energy absorption band in solution is broad, extending from 410 to 690 nm with an absorption maximum (λ_{max}) at 527 nm with a shoulder from 600 - 630 nm. The lowest energy absorption band in solid state is broad, extending from 410 to 690 nm with a low energy shoulder at 605-640 nm and an vibronic peak at 583 nm, which was the absorption maximum (λ_{max}). The optical band gap derived from the absorption edge of the thin film spectrum is 1.80 eV. Solution photoluminescence was observed for **P2TDDQx** with an emission maximum (λ_{max}) at 615 nm. Weak photoluminescence for **P2TDDQx** thin films was observed, but the poor signal to noise ratio made it difficult to discern a emission maximum.

In comparison, the λ_{max} of the parent polythiophene and poly(quinoxaline) thin films are 490 and 375 nm, respectively.[5a] The significantly larger λ_{max} of the thiophene-quinoxaline copolymers than those of the corresponding parent homopolymers shows

that intramolecular charge transfer between the thiophene and quinoxaline moieties is large.

2.3.2 – Copolymer Electrochemical and Thermal Properties

The electrochemistry of **PTHQx** had been studied previously by the Yamamoto group[1d], but was verified. The cyclic voltammogram of **PTHQx**, shown in Figure 2.4, match up well with those previously reported with an oxidative doping at a half-wave potential ($E_{1/2}^{ox}$) of 0.83 V (vs. SCE) and a broad undoping at a half-wave potential ($E_{1/2}^{ox}$) of 0.69 V (vs. SCE). Similarly the reduction doping at a half-wave potential ($E_{1/2}^{red}$) of -1.80 V (vs. SCE) and undoping at half-wave potentials ($E_{1/2}^{red}$) of -1.58 and -1.28 V (vs. SCE) match up quite well with those previously reported. The experimental EA and IP levels of 2.78 and 5.07 eV, and therefore a bandgap, Eg, of 2.29 eV correlate well with our reported calculated EA and IP energy levels of 2.73 and 4.91 eV and Eg of 2.18 eV for the related **PTQx** copolymer.[7]

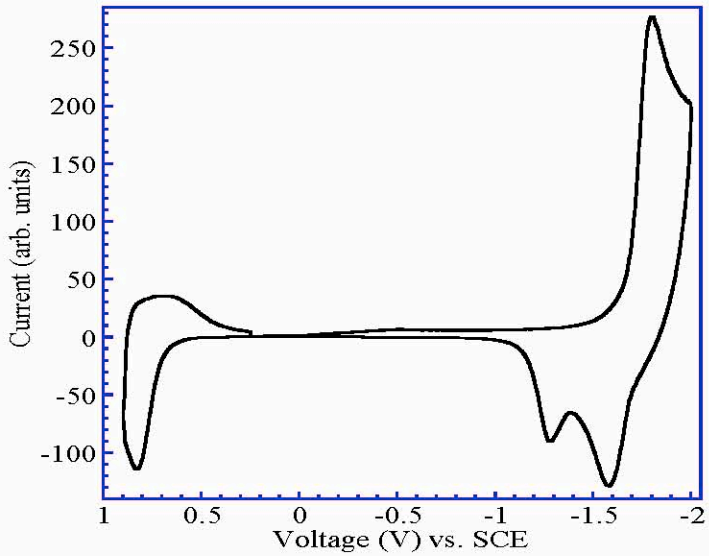

Figure 2.4. CV curves of **PTHQx** film on Pt electrode in 0.1 M $TBAPF_6$ solution in acetonitrile at a scan rate of 40 mV/s.

The electrochemistry of **PTDDQx** and **P2TDDQx** were also quite similar in their EA and IP energy levels to both the experimental results for **PTHQx** and those calculated for **PTQx**. An initial scanning of **PTDDQx**, Figure 2.5, revealed a major oxidative doping and shoulder at half-wave potentials ($E_{1/2}^{ox}$) of 1.09 and 0.92 V (vs. SCE) with and single oxidative undoping at a half-wave potential ($E_{1/2}^{ox}$) of 0.77 V (vs. SCE). Upon a second oxidation scan the doping converges at a half-wave potential ($E_{1/2}^{ox}$) of 0.92 V (vs. SCE), while the undoping potential and intensity are unchanged. This shift is also represented in a shift in the oxidation onset from a half-wave potential ($E_{1/2}^{ox}$) of 0.68 to 0.60 V (vs. SCE). **PTDDQx** had a singular reduction doping at a half-wave potential ($E_{1/2}^{red}$) of -1.90 V (vs. SCE) and a single undoping at a half-wave potential ($E_{1/2}^{red}$) of -1.70 V (vs. SCE) with a reduction onset at a half-wave potential

($E_{1/2}^{red}$) of -1.74 V (vs. SCE). Thus the experimental EA and IP energy levels were 2.66 and 5.08 or 5.00 eV (based on either the first oxidation or subsequent oxidations) and therefore had an electrochemical bandgap of 2.42 or 2.36 eV.

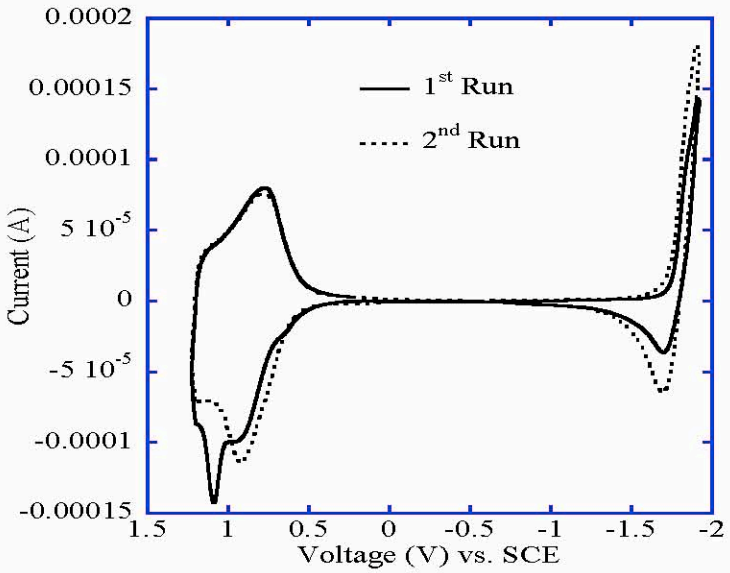

Figure 2.5. CV curves of **PTDDQx** film on Pt electrode in 0.1 M $TBAPF_6$ solution in acetonitrile at a scan rate of 20 mV/s. (first and second scans)

The cyclic voltammograms of **P2TDDQx**, Figure 2.6, are quite similar to those previously reported herein. The **P2TDDQx** thin films showed a single oxidative doping at a half-wave potential ($E_{1/2}^{ox}$) of 0.74 V (vs. SCE) and undoping at a half-wave potential ($E_{1/2}^{ox}$) of 0.63 V (vs. SCE) with the oxidation onset at a half-wave potential ($E_{1/2}^{ox}$) of 0.49 V (vs. SCE). **P2TDDQx** showed a single reduction doping at a half-wave potential ($E_{1/2}^{red}$) of -1.85 V (vs. SCE) and undoping at a half-wave potentials ($E_{1/2}^{ox}$) of -1.70 and -1.81 V (vs. SCE) with the oxidation onset at a half-wave potential

($E_{1/2}^{ox}$) of -1.71 V (vs. SCE). Thus the experimental EA and IP energy levels were 2.69 and 4.89 eV and therefore had an electrochemical bandgap of 2.20 eV. All of the reported IP levels, 4.9-5.1 eV, make for the subsequent use of gold electrodes (work function, Φ = 5.2 eV) in OFETs an optimal choice.

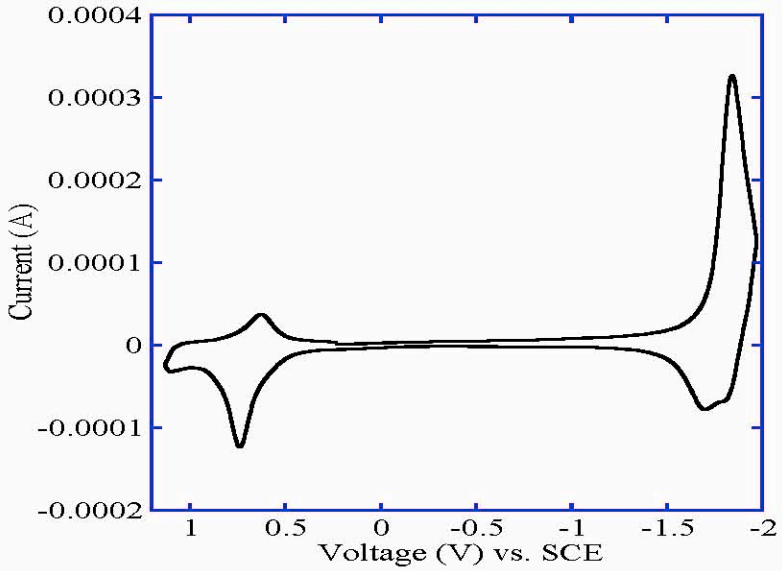

Figure 2.6. CV curves of **P2TDDQx** film on Pt electrode in 0.1 M $TBAPF_6$ solution in acetonitrile at a scan rate of 20 mV/s.

Thermogravimetric analysis (TGA) of **PTHQx**, Figure 2.7, shows an onset decomposition temperature (T_d) of 413 °C. The high T_d observed in the **PTHQx** suggests robust thermal stability, which is essential for prevention of decomposition due to joule heating in OFETs, especially at high current densities.

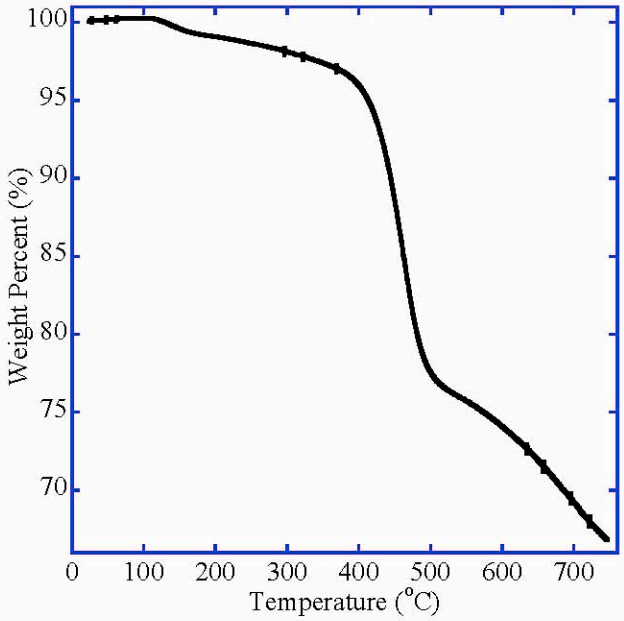

Figure 2.7. TGA thermogram of **PTHQx**; heating rate of 20°C/min.

2.3.3 - Copolymer Thin Film Morphology

Previous powder X-ray diffraction of **PTHQx** revealed strong peaks which evidenced a high degree of crystallinity.[1c] We used AFM imaging to directly observe the morphology of **PTHQx** thin films spin-coated on the surfaces of substrates employed in OFETs. The AFM topographic and phase images of **PTHQx** thin films on untreated SiO_2/Si and on OTS-8 SAM-modified SiO_2/Si are shown in Figure 2.8. Densely packed spherical grains of about 100-nm average diameter were observed in thin films deposited on untreated SiO_2 dielectric (Figures 2.8.A and 2.8.B). The morphology of **PTHQx** thin films on OTS-8 SAM-modified SiO_2 dielectric also consisted of densely packed crystalline spherical grains (Figure 2.8.C and 2.8.D).

However, these latter grains were about 20-50 nm in diameter and appear to be more densely packed than those on the untreated SiO_2/Si surface (Figures 2.8.A and 2.8.B). The observed morphology of **PTHQx** thin films on both substrates is very different from those commonly observed in AFM images of regioregular poly(3-hexylthiophone) and other conjugated polymer semiconductors used in OFETs.[10] In fact, the morphology of **PTHQx** thin films is reminiscent of that commonly observed for thermally evaporated small molecule semiconductors such as pentacene.[11] One implication of the polycrystalline grain morphology of **PTHQx** thin films is that advances in processing this copolymer could directly improve OFETs made from it. Broader scans of **PTHQx** thin films, Figure 2.9, reveal much larger aggregates of the copolymer. On OTS-8 SAM-modified SiO_2 dielectric, the aggregate features were up to 200 nm in height and grew in directions more parallel to the dielectric surface, whereas on an untreated dielectric the **PTHQx** copolymer aggregates grew more vertically, reaching heights of 250 nm and had a more ribbon-like appearance. Such large copolymer aggregates were not observed on the other thiophene-quinoxaline copolymer thin films.

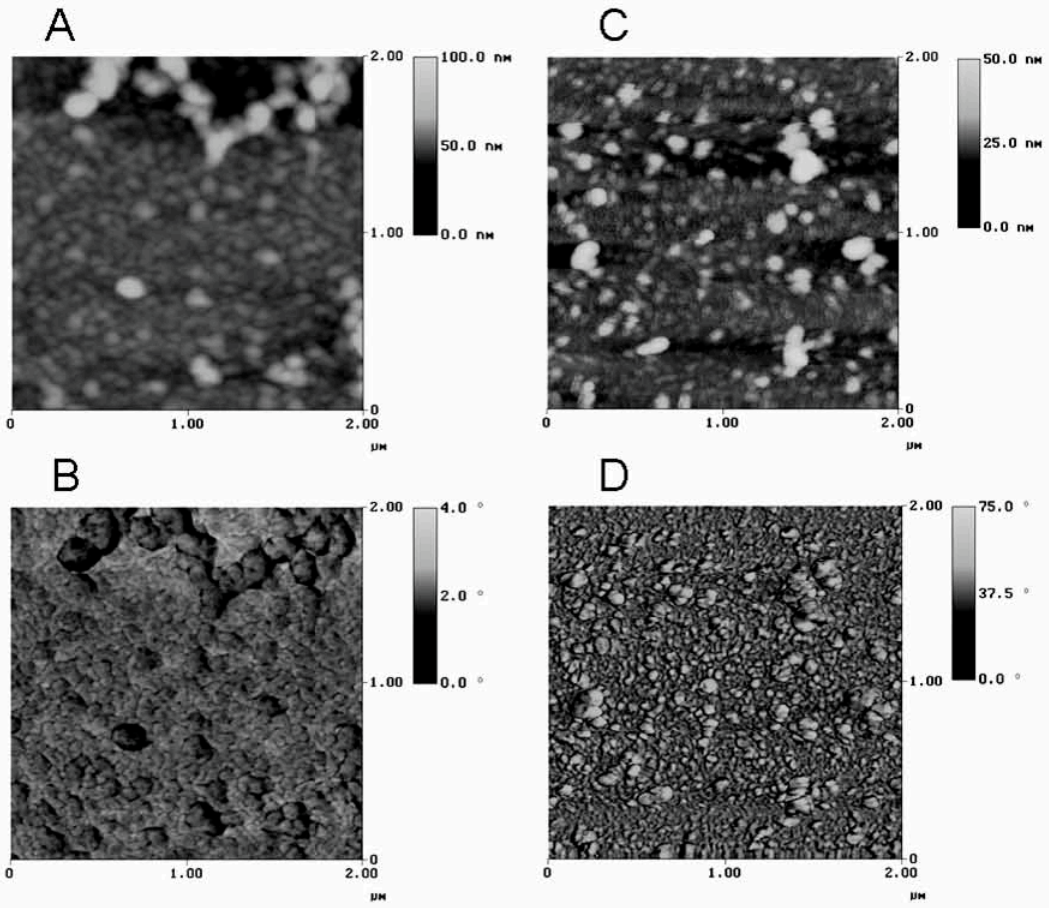

Figure 2.8. Topographical (A, C) and phase (B, D) 2 µm x 2 µm AFM images of **PTHQx** thin films on an untreated SiO_2 surface (A, B) and OTS-8 SAM-treated SiO_2 surface (C, D).

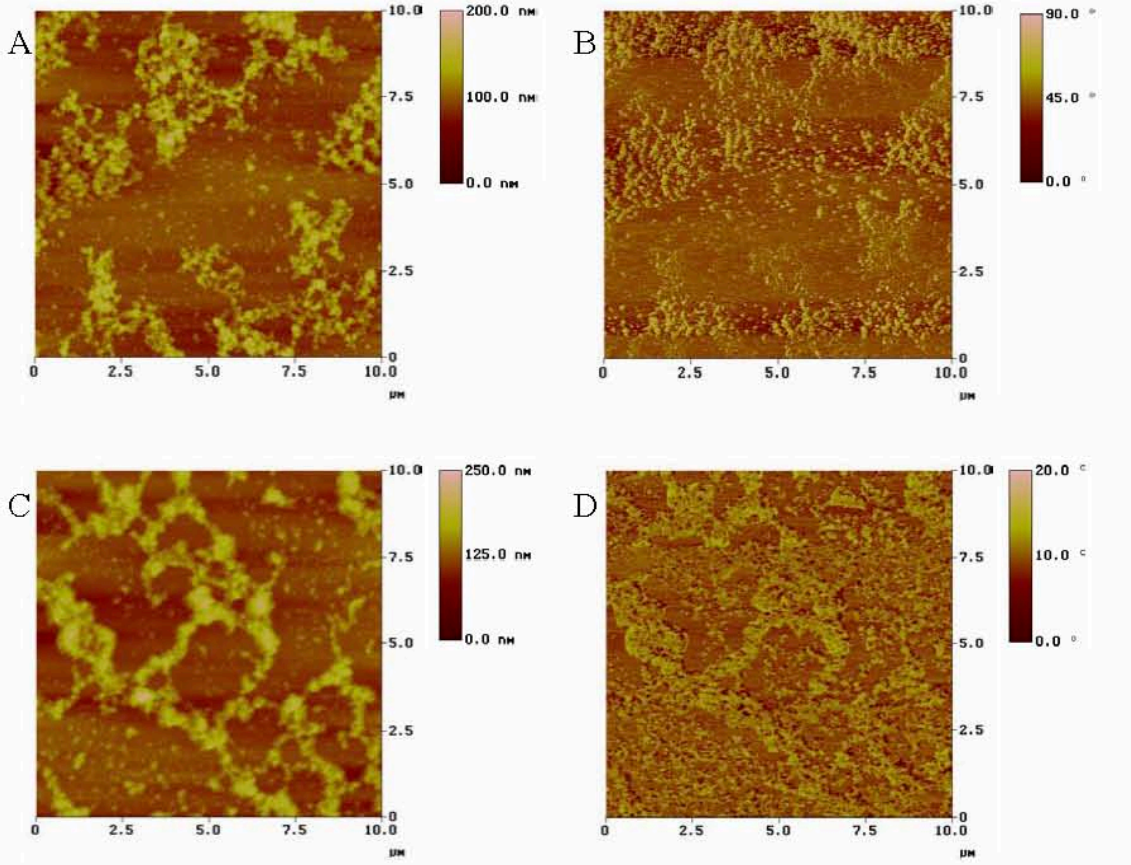

Figure 2.9. Topographical (A, C) and phase (B, D) 10 µm x 10 µm AFM images of **PTHQx** thin films on an OTS-8 SAM-treated SiO_2 surface (A, B) and untreated SiO_2 surface (C, D).

AFM analysis of **P2TDDQx** cast from TCB (Figure 2.10), on both untreated and OTS-8 SAM-treated SiO_2 dielectric surfaces, revealed a morphology similar to jagged cloud features with the aggregated copolymer only 15-20 nm in height. **PTDDQx** from a TCB solution on an OTS-8 SAM-modified SiO_2 dielectric displayed an interconnected web structure of aggregated copolymer of about 20 nm in height (Figure 2.11). Also shown in Figure 2.11, is the AFM morphology data of **PTDDQx** from a TCB on an untreated SiO_2 dielectric which is more amorphous with much larger

aggregates, as compared to the SAM-treated surface, with sizes of about 0.75 x 0.25 μm, but with a web of the copolymer between the larger aggregates. Additionally, **PTDDQx** from a TFA solution (Figure 2.12) was also studied on unmodified or OTS-8 SAM-modified SiO_2 dielectrics. thin films spin-cast from TFA did not have an interconnected topology, but had isolated aggregates with heights of 50 nm and diameters of 50-100 nm These observed morphologies lie somewhere between the bulk of previously reported semiconductive polymers[10], which are amorphous, and **PTHQx** which has a densely-packed polycrystalline morphology.[7]

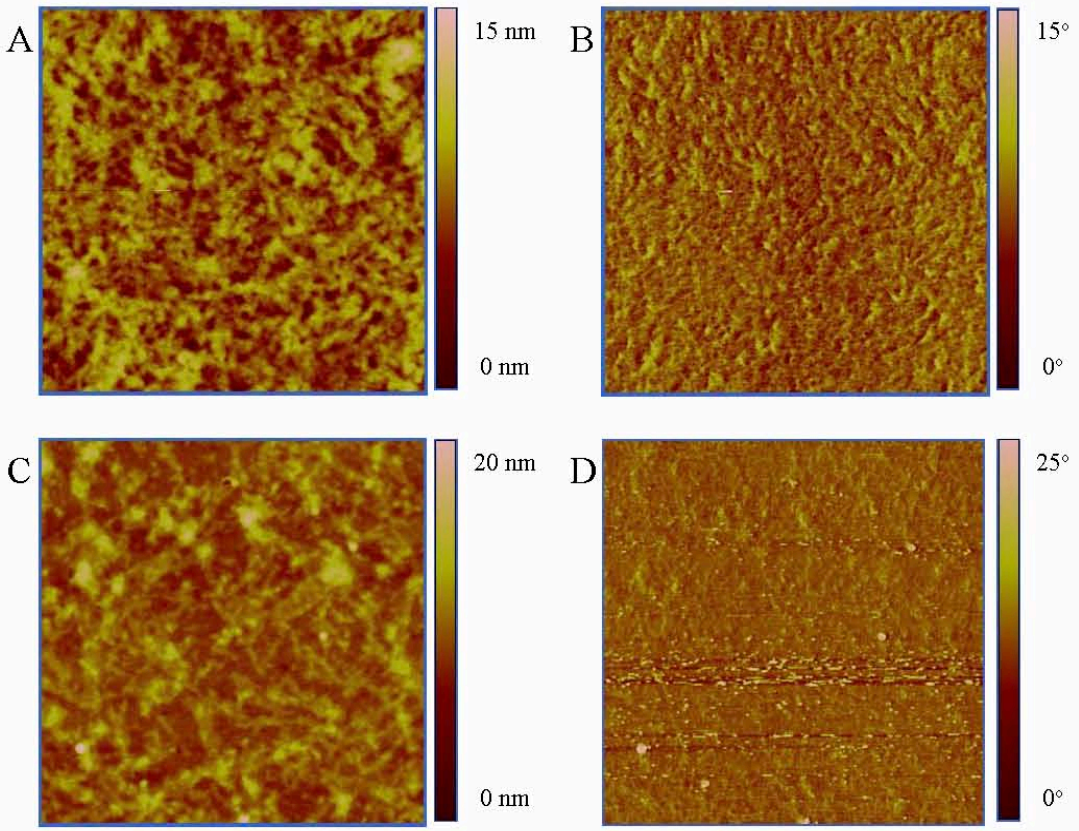

Figure 2.10. Topographical (A, C) and phase (B, D) 2 μm x 2 μm AFM images of **P2TDDQx** (from TCB solution) thin films on an OTS-8 SAM-treated SiO_2 surface (A, B) and untreated SiO_2 surface (C, D).

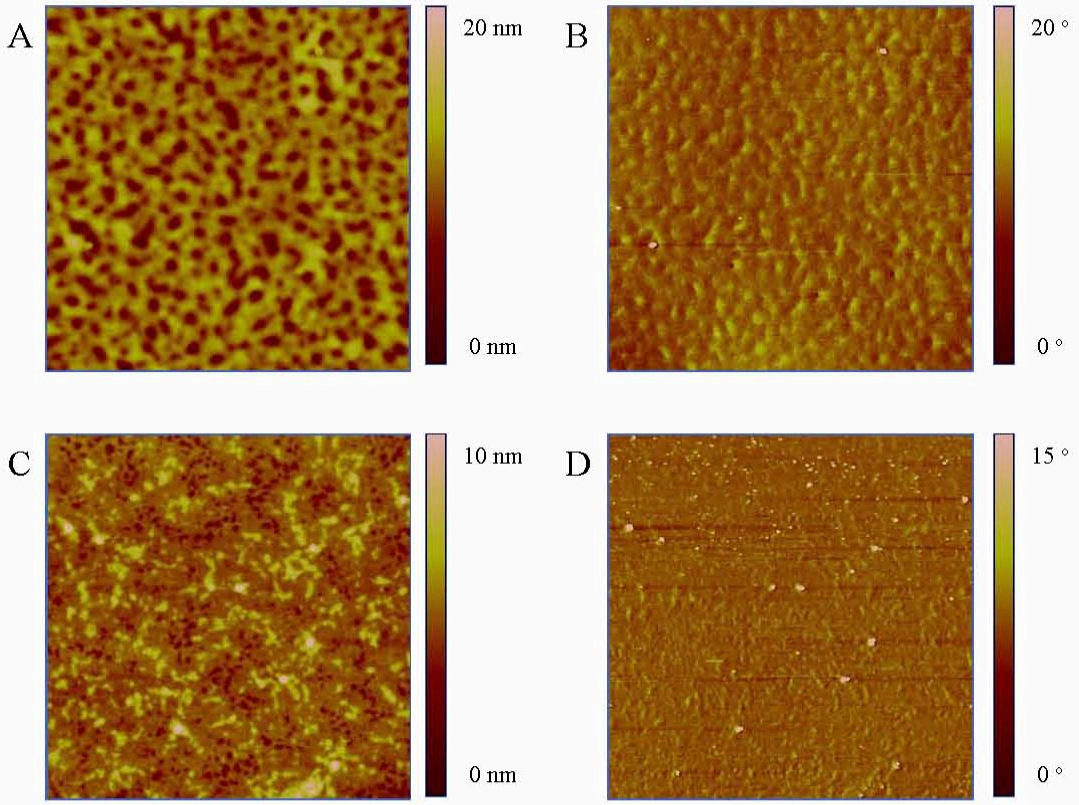

Figure 2.11. Topographical (A, C) and phase (B, D) 2 μm x 2 μm AFM images of **PTDDQx** (from TCB solution) thin films on an OTS-8 SAM-treated SiO_2 surface (A, B) and untreated SiO_2 surface (C, D).

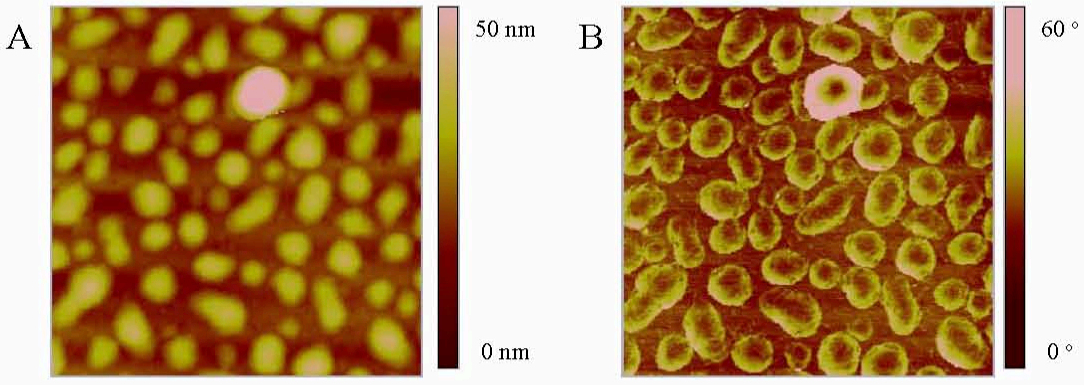

Figure 2.12. Topographical (A) and phase (B) 2 μm x 2 μm AFM images of **PTDDQx** (from TFA solution) thin films on an OTS-8 SAM-treated SiO_2 surface.

2.4 - Conclusions

A thiophene-quinoxaline donor-acceptor conjugated copolymers **PTHQx**, **PTDDQx**, and **P2TDDQx** have demonstrated as being promising p-channel semiconductors for field-effect transistors. OFETs fabricated from **PTHQx** thin films had the maximum saturation hole mobility of 8.3×10^{-3} $cm^2/(Vs)$ with an on/off current ratio of 10^6. Spin-coated **PTHQx** thin films were found to have a densely packed polycrystalline grain morphology, whereas the **PTDDQx** and **P2TDDQx** had networks of copolymer aggregates. The studied thiophene-quinoxaline copolymers displayed electrochemical reduction indicating such polymer systems have potential as n-type and ambipolar field-effect transistors. The temperature dependence of **PTHQx** FET performance was explored, which showed a unique termination of hole conduction above 410 K. The accounting for occurrence will be explored in the future.

Notes to Chapter 2

(1) (a) Agrawal, A. K.; Jenekhe, S. A. *Macromolecules* **1993**, *26*, 895. (b) Karikomi, M.; Kitamura, C.; Tanaka, S.; Yamashita, Y. *J. Am. Chem. Soc.* **1995**, *117*, 6791. (c) Lee, B.-L.; Yamamoto, T. *Macromolecules* **1999**, *32*, 1375. (d) Kanbara, T.; Miyazaki, Y.; Yamamoto, T. *J. Polym. Sci. A: Polym. Chem.* **1995**, *33*, 999. (e) Jenekhe, S. A.; Lu, L.; Alam, M. M. *Macromolecules* **2001**, *34*, 7315.

(2) (a) Zhang, X.; Jenekhe, S. A.; *Macromolecules* **2000**, *33*, 2069. (b) Ego, C.; Marsitzky, D.; Becker, S.; Zhang, J.; Grimsdale, A. C.; Müllen, K.; MacKenzie, J. D.; Silva, C.; Friend, R. H.; *J. Am. Chem. Soc.* **2003**, *125*, 437. (c) Thompson, B. C.; Madrigal, L. G.; Pinto, M. R.; Kang, T.-S.; Schanze, K. S.; Reynolds, J. R. *J. Polym. Sci. A: Polym. Chem.* **2005**, *43*, 1417. (d) Kulkarni, A. P.; Zhu, Y.; Jenekhe, S. A.; *Macromolecules* **2005**, *38*, 1553.

(3) (a) Babel, A.; Jenekhe, S. A. *J. Am. Chem. Soc.* **2003**, *125*, 13656. (b) Yamamoto, T.; Kokubo, H.; Kobashi, M.; Sakai, Y. *Chem. Mater.* **2004**, *16*, 4616. (c) Yoon, M.-H.; DiBenedetto, S. A.; Facchetti, A.; Marks, T. J. *J. Am. Chem. Soc.* **2005**, *127*, 1348. (d) Ando, S.; Nishida, J.-I.; Tada, H.; Inoue, Y.; Tokito, S.; Yamashita, Y. *J. Am. Chem. Soc.* **2005**, *127*, 5336. (e) Babel, A.; Wind, J. D.; Jenekhe, S. A. *Adv. Funct. Mater.* **2004**, *14*, 891. (f) Kunugi, Y.; Takimiya, K.; Negishi, N.; Otsubo, T.; Aso, Y. *J. Mater. Chem.* **2004**, *14*, 2840. (g) Chua, L.-L.; Zaumseil, J.; Chang, J.-F.; Ou, E. C.-W.; Ho, P. K.-H.; Sirringhaus, H.; Friend, R. H. *Nature* **2005**, *434*, 194. (h) Yamamoto, T.; Yasuda, T.; Sakai, Y.; Aramaki, S. *Macromol. Rapid Commun.* **2005**, *26*, 1214.

(4) (a) Yu, G.; Gao, J.; Hummelen, J. C.; Wudl, F.; Heeger, A. J. *Science* **1995**, *270*, 1789. (b) Jenekhe, S. A.; Yi, S. *Appl. Phys. Lett.* **2000**, *77*, 2635. (c) Alam, M. M.; Jenekhe, S. A. *J. Phys. Chem. B* **2001**, *105*, 2479. (d) Alam, M. M.; Jenekhe, S. A. *Chem. Mater.* **2004**, *16*, 4647.

(5) (a) Yamamoto, T.; Zhou, Z.-H.; Kanbara, T.; Shimura, M.; Kizu, K.; Maruyama, T.; Nakamura, Y.; Fukuda, T.; Lee, B.-L.; Ooba, N.; Tomaru, S.; Kurihara, T.; Kaino, T.; Kubota, K.; Sasaki, S. *J. Am. Chem. Soc.* **1996**, *118*, 10389. (b) Yasuda, T.; Imase, T.; Sasaki, S.; Yamamoto, T. *Macromolecules* **2005**, 38, 1500. (c) Tsai, F.-C.; Chang, C.-C.; Liu, C.-L.; Chen, W.-C.; Jenekhe, S. A. *Macromolecules* **2005**, *38*, 1958. (d) Liu, C.-L.; Tsai, F.-C.; Chang, C.-C.; Hsieh, K.-H.; Lin, J.-L.; Chen, W.-C. *Polymer* **2005**, *46*, 4950.

(6) (a) Horowitz, G.; Hajlaoui, R.; Delannoy, P. *J. Phys. III* **1995**, *5*, 355. (b) Knipp, D.; Street, R. A.; Volkel, A. R. *Appl. Phys. Lett.* **2003**, *82*, 3907.

(7) Champion, R. D., Cheng, K.-F., Pai, C.-L., Chen, W.-C., Jenekhe, S. A. *Macromol. Rapid Commun.* **2005**, *26*, 1835.

(8) Agrawal, A. K.; Jenekhe, S. A.; *Chem. Mater.* **1996**, *8*, 579.

Chapter 3: Adsorption Kinetics of Ion-Exchange of Organic Cationic Materials in Cellulosic Fiber Matrices

3.1 – Introduction

There have been previous studies regarding the kinetics of metal cation adsorption onto cellulosic fibers. For a well-mixed metal ion-exchange process, many studies have established that the rate–determining step of the process is the diffusion of the ions that are being exchanged, or counter ions, rather than the chemical reactions at the fixed ionic groups.[1,2] Furthermore, the possible rate-limiting step has been concluded to be either the intraparticle diffusion or the film diffusion models if not both.[3,4] Intraparticle diffusion is the diffusion of counter ions within the ion exchanger.[3] Film diffusion is the diffusion of counter ion through the liquid boundary layer surrounding the particle.[4] In the bulk liquid, the metal ion concentration differences are constantly leveled out by agitation.

Because the electroneutrality must be preserved throughout the system, the charge transfer by of the ion not of interest, in this case ammonium or n-substituted pyrrolidine molecules or macromolecules, is balanced by the equivalent charge transfer of the previously adsorbed metal ions. The anions (e.g. Cl^- or Br^-) do not participate in the cation ion exchange. Furthermore, ion exchange is a stoichiometric process. The stoichiometry of ion exchange requires that the fluxes of the two exchanging counter ions be equal although the two ions may have different mobilities. The net transfer of

electric change due to the unequal mobilities produces the electric force which slows down the faster ion and accelerates the slower ion so that the fluxes become equal. Consequently, for modeling the steady-state rate of adsorption one need not consider the rate of counter ion desorption.

Based upon the above description of ion-exchange processes, two models have been developed to predict the ion adsorption kinetics on wood pulp: the intraparticle diffusion model and the convective mass transfer model.

3.2 – Intraparticle Diffusion

The intraparticle diffusion model considers the unsteady state diffusion of ions from the bulk solution (source) to the pore solution within the pulp fibers (sink). A time-dependent concentration profile developes as the metal ions penetrate into the liquid filled pores within the pulp fibers. At long times, the unsteady state diffusion process reaches the equilibrium. The following derivations are coalesced from the work of Yantasee and others.[5-8]

The development of the intraparticle diffusion model for organic ion (solute "1") adsorption kinetics assumes that:

1. The pulp fibers are uniformly cylindrical.

2. The organic ions in the solution are dilute.

3. The concentration of the metal ions in the bulk solution initially is denoted by $C_{1,0}$ and

the pulp is initially free of organic ions.

4. The solution is well-mixed so that the concentration of the metal ion in the solution is always uniform.

5. The bulk diffusion rate is much faster than the intraparticle diffusion rate, so that

the concentration of organic ions in the bulk solution is equal to the organic ion concentration at the particle surface.

6. There is a limited volume of solutions, hence the concentration of the organic ion in the solution falls as the solute diffuses and adsorbs into the pulp fibers.

7. The concentration of the free organic ion, $C_{r,1}$, inside a cylindrical particle is a function of the radial position from the center of the cylinder and the contact time, that is:

$$C_{r,1} = C_{r,1}(r, t) \qquad (1)$$

8. The concentration of adsorbed organic ion, $q'_{r,t}$, inside a cylindrical particle is also a function of the radial position and the contact time, that is:

$$q'_{r,t} = q'_{r,t}(r,t) \qquad (2)$$

9. The rate of adsorption is instantaneous relative to the rate of the diffusion, so that the concentrations of the free organic ion, $C_{r,1}$, and the adsorbed organic ion, $q'_{r,t}$, anywhere inside the particle remain in equilibrium with the partition factor K_1.

$$q'_{r,t}(r,t) = K_1 C_{r,1}(r,t) \qquad (3)$$

One considers that the mass transfer process consists of two systems. The first system represents the bulk solution. The second system represents the molecular diffusion of the organic ions within the liquid pores within the cylindrical pulp fibers and the adsorption of organic ions within the fibers.

For the first step the material balance of the organic ion in the bulk solution is

Metal ion accumulation	=	Rate of organic ion diffusion
in the bulk solution		into the particle at $r = a$
(internal → external)		(external → internal)

For this material balance:

$$V\frac{\partial C_1}{\partial t} = n_p(2\pi al)j_{r,1}|_{r=a} \qquad (4)$$

where n_p is the total number of pulp fibers in the pulp suspension, V is the bulk solution volume, l is the fiber length and, $j_{r,1}$ is the molar diffusion flux of the organic ions, defined as:

$$j_{r,1} = -D_1 \frac{\partial C_{r,1}}{\partial r} \tag{5}$$

For diffusion inside porous media, the diffusion coefficient D_1 in equation (5) is replaced by the effective diffusion coefficient, $D_{e,1}$

$$j_{r,1} = -D_{e,1} \frac{\partial C_{r,1}}{\partial r} \tag{6}$$

Substituting equation (6) into equation (4), one gets:

$$V \frac{\partial C_1}{\partial t} = -AD_{e,1} \left(\frac{\partial C_{r,1}}{\partial r}\right)|_{r=a} \tag{7}$$

where A is the total external surface area of all pulp fibers.

$$A = n_p(2\pi al) \tag{8}$$

Then one must come to a material balance of the organic ions within a differential volume element within the cylindrical particle.

Organic accumulation	=	Rate of diffusion	-	Rate of diffusion
Inside the cylindrical shell		into the shell at r		out of the shell at $r + \Delta r$

$$\varepsilon_p \frac{\partial}{\partial t} 2\pi r l \Delta r C_{r,1}(r,t) + \frac{\partial}{\partial t} 2\pi r l \Delta r q'_{r,1}(r,t) =$$

$$2\pi r l \, j_{r,1}|_{r=r} - 2\pi r l \, j_{r,1}|_{r=r+\Delta r} \qquad (9)$$

where $q'_{r,1}$ is the concentration of adsorbed organic ion (mmol organic ion adsorbed/cm^3 pore solution) and $\varepsilon_p$is the pulp porosity, given by:

$$\varepsilon_p = 1 - \frac{\rho_p}{\rho_s} \qquad (10)$$

where ρ_p is the bulk density of pulp (including pores) and ρ_s is the solid density of pulp (excluding pores). Dividing equation (9) by the shell volume and taking the limit as $\Delta r \to 0$,

$$\varepsilon_p \frac{\partial C_{r,1}}{\partial t} + \frac{\partial q'_{r,1}}{\partial t} = -\frac{1}{r}\frac{\partial r j_{r,1}}{\partial r} \qquad (11)$$

Substitute in $j_{r,1}$ into equation 11, the diffusion equation is

$$\varepsilon_p \frac{\partial C_{r,1}}{\partial t} + \frac{\partial q'_{r,1}}{\partial t} = D_{e,1}\frac{1}{r}\frac{\partial}{\partial r}\left(r\frac{\partial C_{r,1}}{\partial r}\right) \qquad (12)$$

The equations (6) and (12) subject to the initial conditions:

$$C_1(t) = C_{1,o} \qquad \text{(t=0)} \qquad (13)$$

$$C_{r,1}(r,0) = 0 \qquad \text{(t=0, } 0 \le r \le a\text{)} \qquad (14)$$

$$q'_{r,1}(r,0) = 0 \qquad \text{(t=0, } 0 \le r \le a\text{)} \qquad (15)$$

and the boundary conditions

$$\frac{\partial C_{r,1}}{\partial r} = 0 \qquad (r=0,\ t > 0) \qquad (16)$$

$$C_{r,1}(a,t) = C_1(t) \qquad (r = a, t > 0) \qquad (17)$$

To facilitate mathematical solution Wilson[6] defined the total amounts of free ions, $y_{r,1}(r,t)$, and adsorbed ion, $z_{r,1}(r,t)$, as:

$$y_{r,1}(r,t) = n_p 2\pi l \int_0^r r C_{r,1}(r,t)dr \qquad (18)$$

$$z_{r,1}(r,t) = n_p 2\pi l \int_0^r r q_{r,1}(r,t)dr \qquad (19)$$

Furthermore, equation (3) can be rewritten as

$$z_{r,1} = K_1 y_{r,1} \qquad (20)$$

and the corresponding equation (12) can be rewritten as

$$\frac{\partial y_{r,1}}{\partial t} = \frac{D_{e,1}}{K_1+\varepsilon_p} r \frac{\partial}{\partial r}\left(\frac{1}{r}\frac{\partial y_{r,1}}{\partial r}\right) \qquad (21)$$

Differentiating and rearranging equation (18) yields the concentration of the free ions at the surface of the cylinder

$$C_{r,1}(a,t) = \frac{1}{n_p 2\pi a l}\left(\frac{\partial y_{r,1}}{\partial r}\right)_{r=a} \qquad (22)$$

The amount of ions in both systems always remains constant and is given by the overall material balance:

$$VC_{1,o} = VC_{r,1}(a,t) + \varepsilon_p y_{r,1}(a,t) + z_{r,1}(a,t) \tag{23}$$

Substituting equations (20), and (22) into equation (23) yields

$$\frac{V}{n_p 2\pi a l}\frac{\partial y_{r,1}}{\partial r} + \left(K_1 + \varepsilon_p\right) y_{r,1} = VC_{1,o} \qquad (r = a) \tag{24}$$

It is necessary to define a new independent variable $f_1(r,t)$, so that $y_{r,1}(r,t)$ is now:

$$y_{r,1}(r,t) = \frac{VC_{1,o} n_p \pi r^2 l}{(K_1+\varepsilon_p) n_p \pi a^2 l + V} + f_1(r,t) \tag{25}$$

Where V_P is the total volume of pulp fibers, given by:

$$y_{r,1}(r,t) = n_p \pi a^2 l \tag{26}$$

the variable $f_1(r,t)$ satisfies the differential equation:

$$\frac{\partial f_1}{\partial t} = \frac{D_{e,1}}{K_1+\varepsilon_p} r \frac{\partial}{\partial r}\left(\frac{1}{r}\frac{\partial f_1}{\partial r}\right) \tag{27}$$

is subject to the boundary condition:

$$\frac{V}{A}\frac{\partial f_1}{\partial r} + \left(K_1 + \varepsilon_p\right) f_1 = 0 \qquad (r = a) \tag{28}$$

and the initial condition:

$$\frac{VC_{1,o}\pi r^2}{(K_1+\varepsilon_p)V_p+V} + f_1(r,0) = 0 \qquad (0 \le r \le a) \qquad (29)$$

The solution of the differential equation (27, 28, 29) provided by Wilson[5] is:

$$\frac{M_{1,t}}{M_{1,\infty}} = 1 - \sum_{n=1}^{\infty} \frac{4\alpha(1+\alpha)}{4+4\alpha+\alpha^2 q_n^2} \exp\left(-\beta\, q_n^2 t\right) \qquad (30)$$

where $M_{1,t}$is the total amount of ions inside the cylindrical pulp fibers at time *t*, $M_{1,\infty}$ is the total amount of ions inside the pulp cylinders at infinite time, α and β and defined as:

$$\alpha = \frac{V}{(K_1+\varepsilon_p)V_p} = \frac{V}{m_p/\rho_p(K_1+\varepsilon_p)V_p} = \frac{\rho_p}{C_p(K_1+\varepsilon_p)} \qquad (31)$$

$$\beta = \frac{D_{e,1}}{a^2(K_1+\varepsilon_p)} \qquad (32)$$

where $C_p$is the pulp consistency (g of dry pulp/cm^3 of solution). The terms $q_n s$ are the positive, non-zero roots of:

$$\alpha q_n J_o(q_n) + 2J_1(q_n) = 0 \qquad (33)$$

The roots of equation (33), listed by Crank[6], are provided in Table 3-1.

An ion material balance on the whole pulp suspension is:

$$M_{1,t} = \varepsilon_p C_{r,1}(a,t)V_p + q_{r,1}(a,t)V_p = (K_1 + \varepsilon_p)y_{r,1}(a,t) \qquad (34)$$

where $C_{r,1}$and $q_{r,1}$are the average free and adsorbed ion concentration inside the pulp fibers, respectively, and are given by

$$C_{r,1}(r,t) = \frac{1}{a}\int_0^r rC_{r,1}(r,t)dr \tag{35}$$

$$q_{r,1}(r,t) = \frac{1}{a}\int_0^a rq_{r,1}(r,t)dr \tag{36}$$

Based on equation (37) above, at equilibrium,

$$y_{r,1}(a,\infty) = \frac{VV_pC_{1,o}}{(K_1+\varepsilon_p)V_p+V} \tag{37}$$

Therefore, $M_{1,\infty}$, the total amount of the ions in the pulp at equilibrium, is

$$M_{1,t} = (K_1+\varepsilon_p)y_{r,1}(a,t) = \frac{(K_1+\varepsilon_p)V\cdot V_pC_{1,o}}{(K_1+\varepsilon_p)V_p+V} = \frac{VC_{1,o}}{1+\alpha} \tag{38}$$

Finally, $M_{1,t}$ is related to the adsorption capacity of metal ion at any time ($q_{r,t}$, mmol ion/g of dry pulp) by:

$$q_{1,t} = \frac{M_{1,t}-M_{1,o}}{m_p} \tag{39}$$

where $M_{1,o}$, the total amount of ion inside the fibers at time zero, is assumed to be zero.

The value of the linear partition factor K_1 is estimated from the ion adsorption isotherm. We force a linear relationship between the molar adsorption capacity of ions on the wood pulp at equilibrium ($q_{1,e}$, mmol ion/g of dry pulp) and the molar concentration of ions in the solution at equilibrium ($C_{1,e}$, mmol ion/L),

$$q_{1,e} = K'_1 C_{1,e} \tag{40}$$

Therefore, the linear parameter K'_1 is obtained from the adsorption isotherm by:

$$K'_1 = \frac{q_{1,e}}{C_{1,e}} \tag{41}$$

Equation (41) requires that the values of $q_{1,e}$ at a given $C_{1,e}$ are known. The best estimates are obtained from the Freundlich adsorption model[7]:

$$q_{1,e} = K''_1 C_{1,e}^{n_1} \tag{42}$$

Estimates for the Freundlich adsorption constant K''_1 and the fitting constant n_1 were obtained from the least-squares intercept and slope respectively of $\ln q_{1,e}$ vs. $\ln C_{1,e}$ data.[8] Once K''_1 and n_1 are known, $q_{1,e}$ at any $C_{1,e}$ is calculated., and K'_1 is then obtained from equation (41). In practice, K'_1 is the average value of the slopes of two straight lines on the iso therm curve: one line connecting points (0,0) and $(C_{1,o}, q_{1,o})$ and the other line connecting point (0,0) and $(C_{1,f}, q_{1,f})$. Note that $C_{1,o}$ and $C_{1,f}$ are the initial and final solution concentrations of the ion from the kinetics experiment, whereas $q_{1,o}$ and $q_{1,f}$ are their corresponding adsorption capacities. Finally, the linear partition factor, K_1 $(\frac{mmol\ ion\ adsorbed/cm^3\ pulp}{mmol\ ion/cm^3\ pore\ solution})$ is related to the linear adsorption isotherm constant, K'_1 $(\frac{mmol\ ion\ adsorbed/cm^3\ dry\ pulp}{mmol\ ion/L\ solution})$ as:

$$K_1 = \rho_p K'_1 \tag{43}$$

To correct for the situation at hand, it must be considered that wood pulp fiber is recognized as a porous material. Some of the pores exist in the wood and some are generated in the pulping and bleaching process.[7] The porosity and pore distribution of wood pulp fibers has been studied.[8,9] For diffusion of ions through porous pulp fibers, the apparent or effective diffusion coefficient of the ions is required. The effective diffusion coefficient of a solute within the pore structure is normally smaller than that in the external solution, depending on the relative sizes of the diffusing solute, the solvent, and the pore. Because the pores are not straight and the solid fraction is not permeable, the diffusion takes place over a longer distance and a smaller cross-sectional area than in a homogeneous material of equivalent outer dimensions. Consider a case where the molecular diameter of solute is less than the pore diameter but comparable to it, and the solute is assumed to be a rigid sphere in the solvent continuum that fills the pore. In this case, the effective diffusion coefficient that factors in the combined effects of the steric hindrance at the entrance to the pores and the frictional resistance within the pores by:

$$D_{1,e} = D^{o}_{1-2}\varepsilon_p^2 F_1(\lambda)F_2(\lambda) \qquad (44)$$

where the subscript "2" denotes the solvent molecule, in all experiments this was water. λ is the reduced pore diameter, given by

$$\lambda = \frac{d_{solute}}{d_{pure}} \qquad (45)$$

where d_{solute} is a diameter of the hydrated solute, and d_{pure} is the median diameter of pulp fibers. The term $F_1(\lambda)$ is a steric partition coefficient, given by:

$$F_1(\lambda) = (1-\lambda)^2 \tag{46}$$

and $F_2(\lambda)$ is the Renkin equation,[5] given by:

$$F_1(\lambda) = 1 - 2.104\lambda^2 - 2.09\lambda^3 - 0.95\lambda^5 \tag{47}$$

In an electrolyte solution, the anions and cations travel together to maintain charge neutrality. Therefore, d_{solute} is assumed to be the diameter of hydrated electrolyte molecules (e.g. $CaCl_2$ or NH_4Cl) rather than individual ions. The radius of each hydrated ion (Ca^{2+}, NH_4^+, Cl^-, etc.) is determined from the relationship:[10]

$$\frac{4}{3}\pi\left(R_{o,i}^3\right) = \frac{4}{3}\pi\left(R'_{o,i}\right)^3 + n\left(\frac{V_{H_2O}}{N}\right) \tag{48}$$

where $R_{o,i}$ is the radius of the hydrated anion or cation, $R'_{o,i}$ is the true ionic radius provided by Shannon,[11] n is the hydration number, V_{H_2O} is the molar volume of water, and N is Avagadro's number. The radius of a hydrated electrolyte molecule (r_{solute}) is assumed to be the sum of the hydrated radii of anions and cations composing the molecule (e.g. one hydrated Ca^{2+} and two hydrated Cl^- for $CaCl_2$).

The molecular diffusion coefficient (D_{1-2}^{o}) is a direct function of temperature (T) and inverse function of solvent viscosity (η). To scale-up the molecular diffusion coefficient at temperature T_1 to that at temperature T_2, the relationship is given by

$$D^{o}_{1-2}(T_2) = D^{o}_{1-2}(T_1) \cdot \frac{T_2}{T_1}\frac{\eta_1}{\eta_2}$$

(49)

The water viscosity (η) decreases as temperature increases. For example, η decreases from 1.0 centipoises at 25 °C to 0.4 centipoises at 75 °C.[12]

3.2 – Convective Mass Transfer

For a well-mixed closed system consisting of liquid and fiber phases, the material balance on the adsorbing metal ion (species "1") is:

$$(C_{1,o} - C_1)V = q_1 m_p \tag{50}$$

Initially, the rate of ion adsorption is assumed to be limited by the convective mass transfer of ions from the bulk liquid phase to the fiber surface.

In the liquid phase, the material balance on species 1 within a well-mixed closed vessel is

$$-N_1 A = \frac{d(C_1 V)}{dt} \tag{51}$$

where N_1 is the convective mass transfer flux, given by:

$$N_1 = k_L(C_1 - C_{1,s}) \tag{52}$$

If V is constant, substituting equation (52) into equation (51) yields:

$$\frac{dC_1}{dt} = \frac{k_L A}{V}\left(C_{1,s} - C_1\right) \tag{53}$$

The Freundlich adsorption isotherm is:

$$q_1 = K''_1 C_{1,s}^n \tag{54}$$

or

$$C_{1,s} = \left(\frac{q_1}{K''_1}\right)^{1/n} \tag{55}$$

Subsititution of equations (50), (54), and (55) into equation (53) results in

$$\frac{dC_1}{dt} = \frac{k_L A}{V}\left\{\left[\left(C_{1,o} - C_1\right)\frac{V}{K''_1 m_p}\right]^{\frac{1}{n}} - C_1\right\} \tag{56}$$

with:

$$k_L a = \frac{k_L A}{V} \tag{57}$$

The initial condition is $t = 0$, $C_1 = C_{1,o}$. The mass transfer coefficient, $k_L a$, can be estimated by fitting C_1 vs. t data to the integrated form of equation (56).

At low ion concentration in solution, a linear relationship represents the equilibrium between the ion and the fiber and in the solution phases

$$C_{1,s} = \frac{q_1}{K'_1} \tag{58}$$

Substitution of equations (50) and (58) into equation (53) results in

$$\frac{dC_1}{dt} = k_L a \left[\left(C_{1,o} - C_1 \right) \frac{V}{K_1' m_p} - C_1 \right] \quad (59)$$

The analytical solution is:[13]

$$\frac{C_{1,t}}{C_1} = \frac{1}{1+C_p K_1'} + \frac{C_p K_1'}{1+C_p K_1'} \exp\left(-\frac{1+C_p K_1'}{C_p K_1'} k_L a t \right) \quad (60)$$

Finally, the adsorption capacity at any time is obtained from:

$$q_{1,t} = \left(C_{1,o} - C_1 \right) \frac{V}{m_p} + q_{1,o} \quad (61)$$

3.3 – Literature Cationic Adsorption Kinetics

The adsorption kinetics of metal cations onto cellulosic fibers has been explored previously.[13-15] Researchers found that the adsorption process is very rapid, occurring typically within 2 minutes, at which point equilibrium of the metal cation(s) being studied had been reached between those cations within the cellulosic fibers and those in the exterior solution. In Figure 3.1, it may be observed that equilibrium between two metal cations, in this case nickel and calcium, is reached quickly with the relative concentrations of the metal cations exchanged out of the cellulosic fiber volumes, in this case calcium, based upon the initial concentration of the displacing cation, in this case nickel. As it can be roughly surmised from these graphs that the Donnan equilibrium is

upheld as greater amounts of cations in solution displaces a greater amount of adsorbed cations.

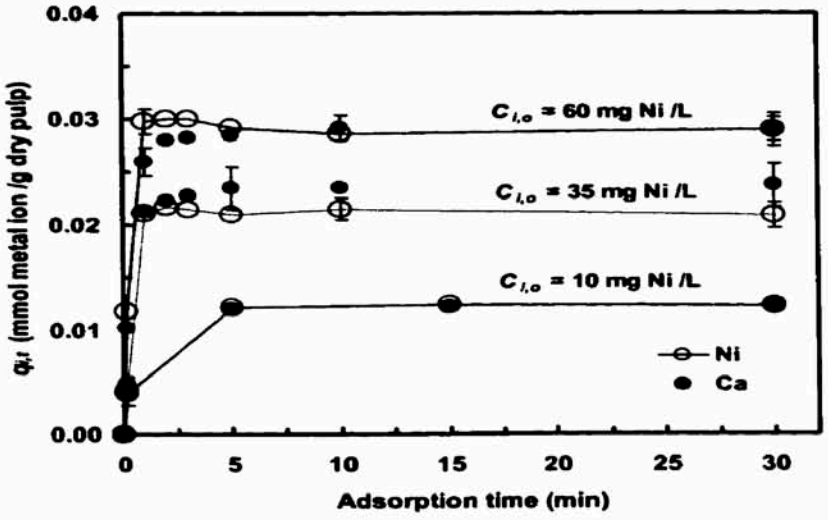

Figure 3.1 Nickel adsorption 10, 30 and 60 mg/L adsorbed onto calcium exchanged pulp[5]

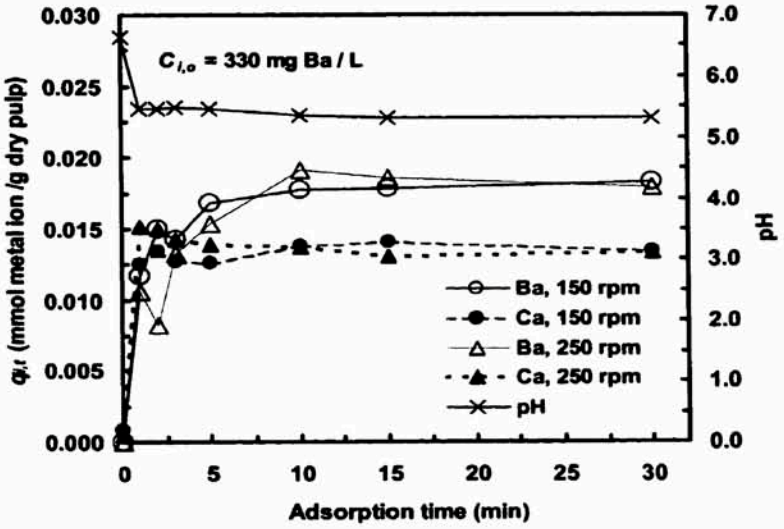

Figure 3.2 Adsorption kinetics of Ba^{2+} on Ca-exchanged pulp at mixing speeds of 150 and 250 rpm.[5]

In Figure 3.2, we can see the kinetics of barium adsorption onto calcium-exchanged pulp at mixing speeds of 150 and 250 rpm.[5] It can be readily recognized that equilibrium between the barium and calcium ions is reached readily at both speeds. Additionally, there is no apparent difference in the kinetics of this ion-exchange at 150 or 250rpm. This study and others work clearly exhibits no dependence upon mixing speed.[16] Thus, it has been stated that competitive adsorption of metal ions in wood pulp does not follow the Convective Mass Transfer Model. This is due to the model being based on a convective mass flux and mass transfer coefficient, which can be minimized to be (m/s) and, therefore, velocity of the solution would prove determinative, but that has not been observed in purely metal-metal ion-exchanges in cellulosic fibers.

Therefore for metal-metal systems the intraparticle diffusion model was tested and proved valid for metal-metal ion-exchange in cellulosic fiber matrices.

For the intraparticle diffusion model, as discussed earlier, the Freundlich isotherm model is used to derive estimates of K_i'. In order to obtain K_i', one must do a best-fit of the Freundlich equation to the adsorption data. Conversely, for reference, when applying the convective mass transfer model, one must use the Freundlich isotherm model is used to derive estimates of $k_L a$, as discussed earlier.

3.4 – Experimental

The cellulose pulp used in the following examples was a standard bleached kraft southern softwood market pulp, Grade NB 416, available from Weyerhaeuser Company, New Bern, N.C. It has an alpha cellulose content of about 88-89% and a D.P. of about 1200. Using the TAPPI method[16] it was the samples were determined to have 4.0 meqs/100g of carboxyl content. The pulp was prepared by first acid washing the pulp, initially at a 3.0wt% consistency, with dilute hydrochloric acid to a final pH of 1.8. This was to remove all metal ions initially adsorbed to the carboxylic acid groups.[4,5] Then 1.0 N HCl was added to adjust the pH to the desired level. This resulting mixture was then stirred continuously for 30 minutes and then the pulp was vacuum-filtered and rinsed with copious amounts of deionized (DI) water. To prepare a pulp sample with uniform calcium adsorption to the carboxylic acid groups contained therein, first the acid-washed pulp and a 0.01 M calcium chloride solution ($CaCl_2$) was

mixed at a 1.0 wt. % consistency for 30 minutes. The pulp was then rinsed with DI water until the washwater contained no detectable amount of calcium. This process exchanged the hydrogen atoms on the carboxylic acid groups with calcium cations. The calcium content at this stage was determined by atomic absorption to be 1.5 meq/100g of pulp.

The process conditions for measurement of the organic or polymeric cationic adsorption kinetics onto cellulosic fibers first involved using a 1.0 wt. % suspension of calcium-exchanged NB 416 kraft pulp fibers in a beaker. Then mixing this suspension at a specified rotary speed using a vertical stirrer of 0, 100 or 200 rpm. To this stirring mixture 2 equivalents of cationic material was added, that is the cationic groups of the added chemicals or polymers was twice the number of carboxylic acid groups present in the pulp sample. The materials were tetramethyl ammonium chloride (TMAC), tetrabutyl ammonium choride (TBAC), benzalkonium chloride (BAC), hexadimethrine bromide (also known as polybrene), and Polydiallyldimethylammonium chloride (also known as PolyDADMAC). A 1.0 mL sample of the stiring solution was taken at 0 (before the cationic organic chemicals or polymers were introduced), 1, 2, 4, 8, 15, 30, 60, 120, 240, 360, 720, and 1440 minutes. After the 1 day, or 1440 minutes, sample was taken, samples were taken every 24 hours. A Varian ICP Emission Spectrometer (Liberty 150) was used to measure the metal ion content of the aqueous samples taken.

3.5 – Results

To determine if the convective mass transfer model was applicable to the adsorption of organic and polymeric cationic, first the experiments done using the same organic or polymeric materials with varying mixing speeds were analyzed.

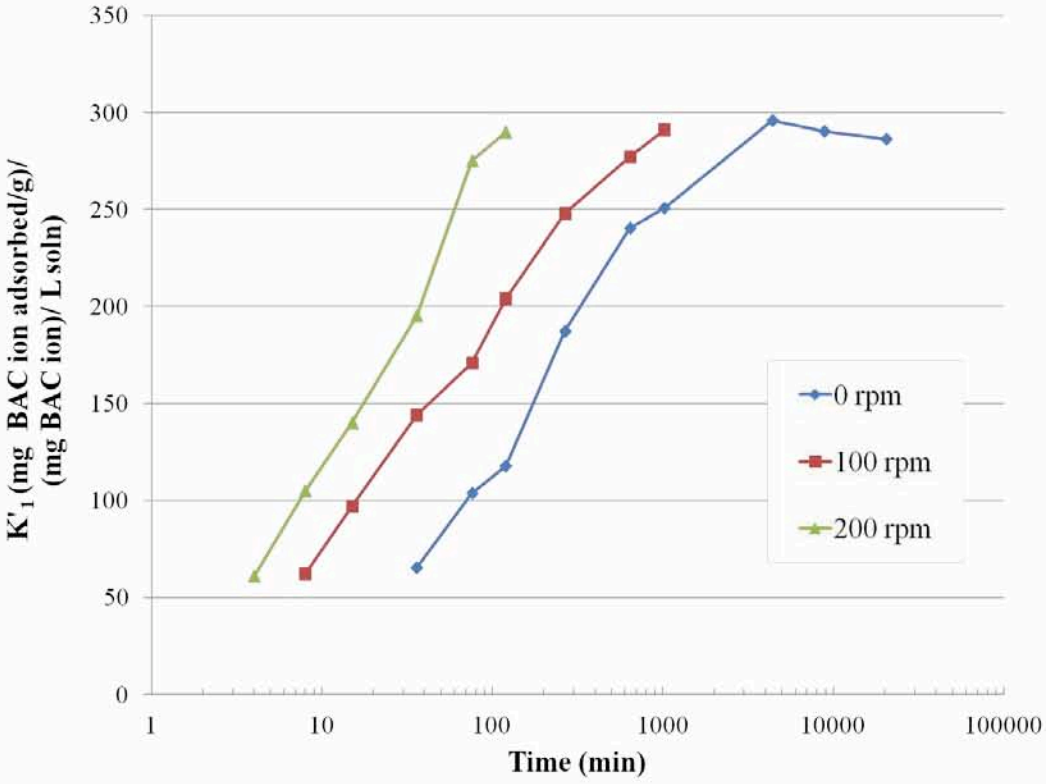

Figure 3.3 Adsorption kinetics of BAC on Ca-exchanged pulp at mixing speeds of 0, 100, and 200 rpm.

In Figure 3.3 we observe that the kinetics of adsorption of BAC was dependent upon the mixing speed used. For this reason the intraparticle diffusion model can be eliminated as a possible means of modeling the adsorption process. Thus the convective

mass transfer model was tested. It is worthy of note to state that for all of the organic and polymeric materials studied this same phenomenon, that being the dependency upon mixing speed, was observed.

As stated previously, to text the convective mass transfer model when applying the convective mass transfer model, one must use the Freundlich isotherm model to derive estimates of $k_L a$. This is done by integrating equation (59) and using the best-fit of C_l vs. t to derive $k_L a$. As a reminder, C_l is the solution concentration and $k_L a$ is the mass transfer coefficient.

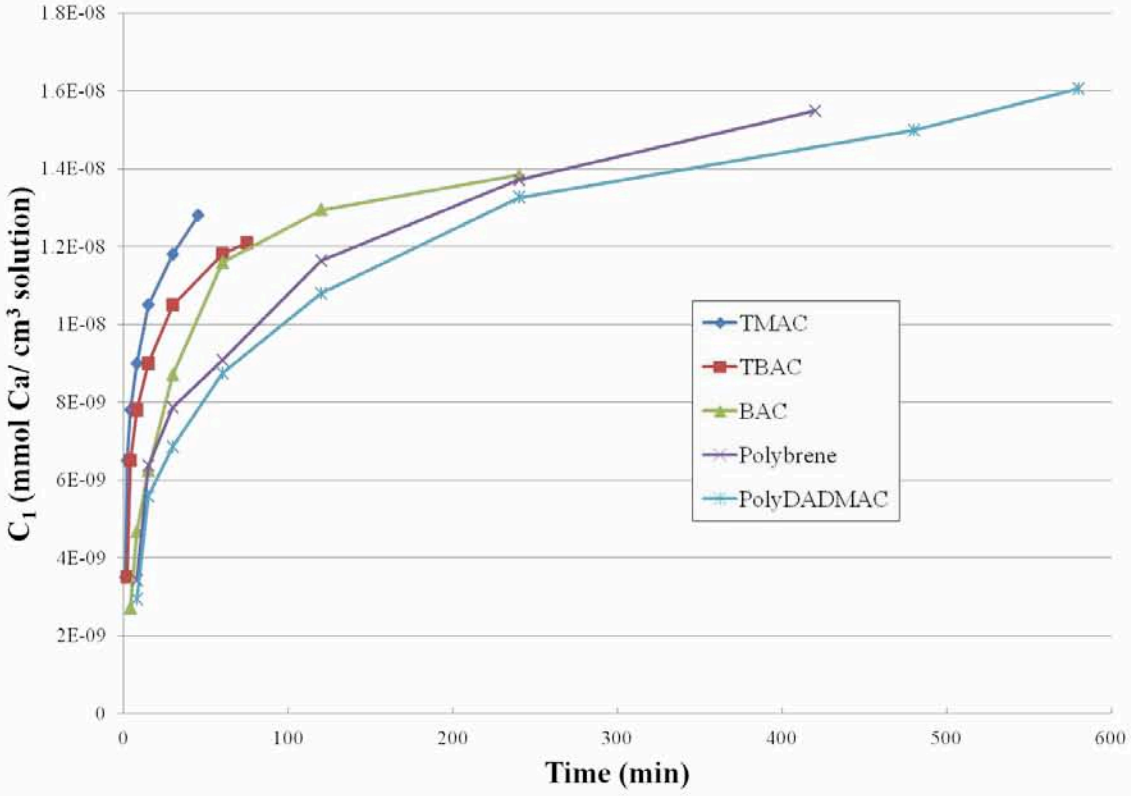

Figure 3.5 Solution concentration of calcium vs. time in ion-exchanges between TMAC, TBAC, BAC, Polybrene and PolyDADMAC solutions and calcium-exchanged NB 416 kraft wood pulp fibers at a mixing speed of 200 rpm.

Figure 3.5 shows the solution concentration of calcium, C_1, vs. time in ion-exchanges of TMAC, TBAC, BAC, Polybrene and PolyDADMAC solutions and calcium-exchanged NB 416 kraft wood pulp fibers at a mixing speed of 200 rpm. Clearly it can be observed that the size of the molecules or polymers being exchanged affected the resulting time necessary to reach equilibrium, with the smallest molecules, TMAC, reaching equilibrium in less than 50 minutes, while the largest polymer, PolyDADMAC, requiring almost 10 hours. This can be understood by the increasing steric hindrances upon transport through the pores of the cellulosic fibers.

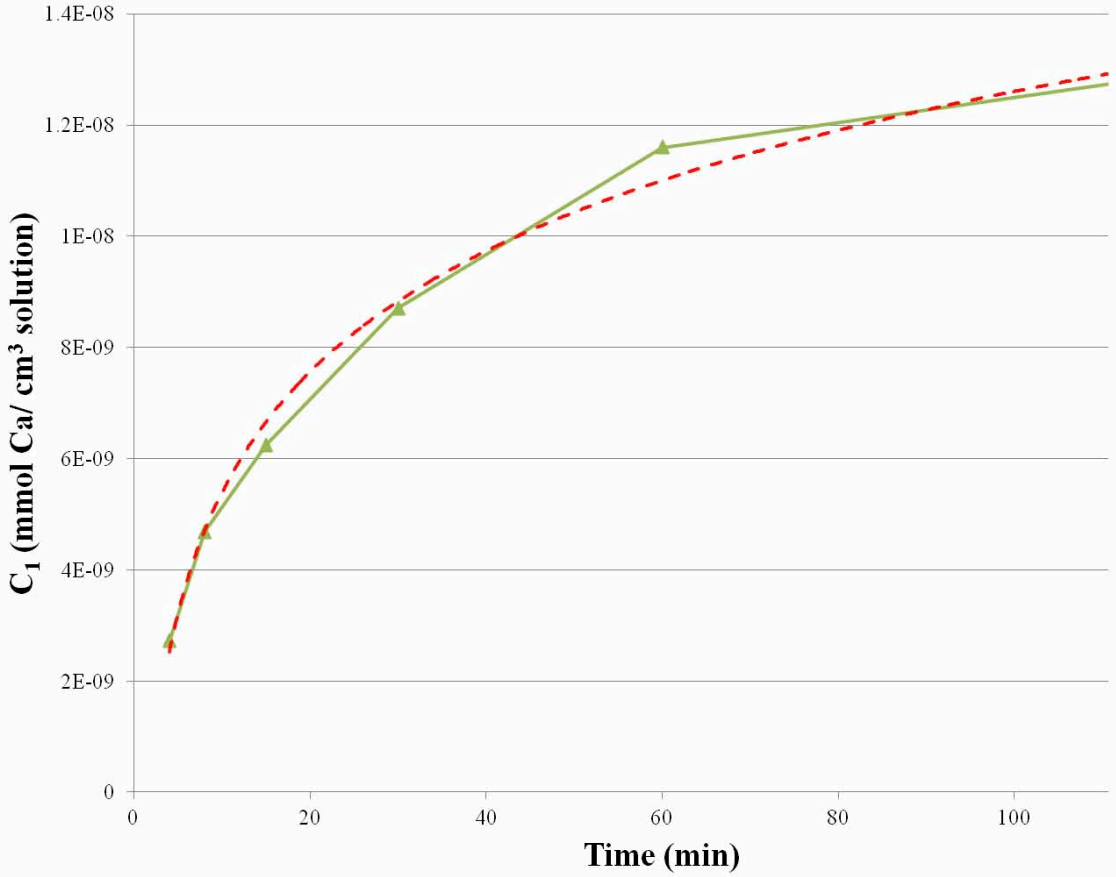
1.4E-08
1.2E-08
1E-08
8E-09
6E-09
4E-09
2E-09
0
0
20
40
60
80
100
C1 (mmol Ca/ cm3 solution)
Time (min)

Notes to Chapter 3

(1) Yantasee, W.; and Rorrer, G.L. J. Wood Chem. Tech., 22, 157 (2002).

(2) Rudie, A.W.; Ball, A.; and Patel, N. J. of Wood Chem. Tech., 26, 259 (2006).

(3) Yantasee, W. *"Kinetic and Equilibrium Analysis of Metal Ion adsorption onto Bleached and Unbleached Kraft Pulps"*. PhD Thesis, OSU, Corvallis, OR (2001).

(4) Schindler, P.W.; and Gamsjöger, H. *Kolloid Z. u. Z. Polymere*, **250**, 759 (1972).

(5) Nilsson, N.; Persson, P.; Lövgern, L.; and Sjöberg, S. *Geochim. Cosmochim. Acta* **60**, 4385 (1996).

(6) Yates, D.E.; Levine, S.; and Healy, T.W. *J. Chem. Soc. Faraday Trans.1*, **70**, 1807 (1974).

(7) Davis, J.A.; James, R.O.; and Leckie, J.O. *J. Colloid Interfae Sci.* **63**, 480 (1978).

(8) Towers, M.; and Scallan, A.M. *J. Pulp Paper Sci.*, **22**, 332 (1996).

(9) Räsänen, E.; and Stenius, P. *"The sorption of Na^{+}, Ca^{2+}, Mg^{2+} and Mn^{2+} on cellulose fibres: Prediction and analysis of sorption equilibrium with electrostatic models"*, 9th ISWPC, 94 (1997).

(10) Donnan, F.G.; and Harris, A.B. *J. Chem. Soc.* **99**, 1554 (1911).

(11) Doering, H. *Das Paper*, **10**, 140 (1956).

(12) Wilson, K. *Svensk Papperstidn*, **51**, 45 (1948).

(13) Wilson, W.K.; and Mandel, J. *Tappi*, **44**, 131 (1961).

(14) Rebek, M.; Klaus, K.; and Baumgartner, H. *Das Paper.*, **10**, 91, (1956).

(15) Forsling, W.; Hietanen, S.; and Sillén, L.-G. *Acta Chem. Scand.* **1952**, *6*, 901.

Chapter 4: Competitive Adsorption of Quaternary Ammonium Cations onto Cellulosic Fibers

4.1 – Introduction

Disposable antimicrobial wipes are an article of commerce that is made by impregnating a non-woven substrate with a solution containing one or more quaternary ammonium salts (hereafter referred to as quat salts). The non-woven substrate typically contains a blend of cellulose fibers, such as wood pulp fibers, and one or more synthetic fibers, such as polypropylene fibers.

The quat salts usually used are variants of BAC and DDAC (BAC's are benzyl-alky dimethyl ammonium chlorides, where the alkyl chain lengths range from 8 to 16 carbons, though usually 12 or 14 (average molecular mass ~ 365 g/mol). DDAC's are dialkyl-dimethyl ammonium chlorides, again with the same range in the alkyl chain lengths, but in this case typically with 8 or 10 carbons (average molecular mass ~ 345 g/mol). The structures of these quat salts are shown in Figure 1.

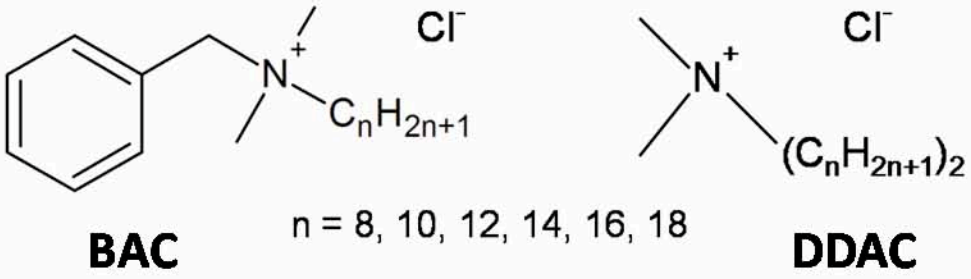

Figure 1. Molecular structures of Quat salts.

In order for the wipes to have effective antimicrobial action, a sufficient concentration of quat salts must be present in the solution squeezed from the wipes during their use.[1] In practice it is found that a high percentage of quat salts are irreversibly adsorbed onto the fibers of the non-woven substrate and are thus not available to provide antimicrobial action to the surface being disinfected. It is, therefore, necessary for the manufacturers of the disinfectant wipes to compensate for this by using a more concentrated solution of quat salts than is theoretically necessary to provide sufficient antimicrobial action. This requirement adds considerable expense to the cost of the wipes.

This research describes compositions for antimicrobial wipes that significantly inhibit the adsorption of quat salts by the fibers during use so that a greater percentage of the quat salts are available to provide antimicrobial action. This research will reduce the amount quat salts that must be added and, thereby, lower the overall cost of the microbial wipe composition.

4.2 – Theory

It is known that vast majority of pulp from hardwoods and softwoods is cellulose (> 80%), which, if not chemically modified, has no charged species on its polymer chains. That being said, there is a significant minority constituent, even after pulping, of hemicellulose. A large component of that hemicellulose fraction is composed of glucuronoxylans, which possess pendant 4-O-methyl-α-D-glucuronic acid groups, shown in Figure 2. These 4-O-methyl-α-D-glucuronic acid groups have been estimated to account for between 5 and 25 meqs/100g (acid groups per 100g wood) before pulping and as low as 3 meqs/100g of pulp after pulping conditions (meqs are millimolar equivalents). It is possible to reduce the hemicellulose content, and thereby number of acidic groups, in wood pulp by more exhaustive pulping methods. However, these methods reduce yield and increase the cost to manufacture pulps. In addition, there are other sources of acid groups in the pulp such fatty acids as well as oxidized lignin and cellulose, which are generated during pulping and bleaching. Currently, most bleached kraft softwood pulps will contain between 2 and 4 meq/100g of carboxyl (and other acid) groups.

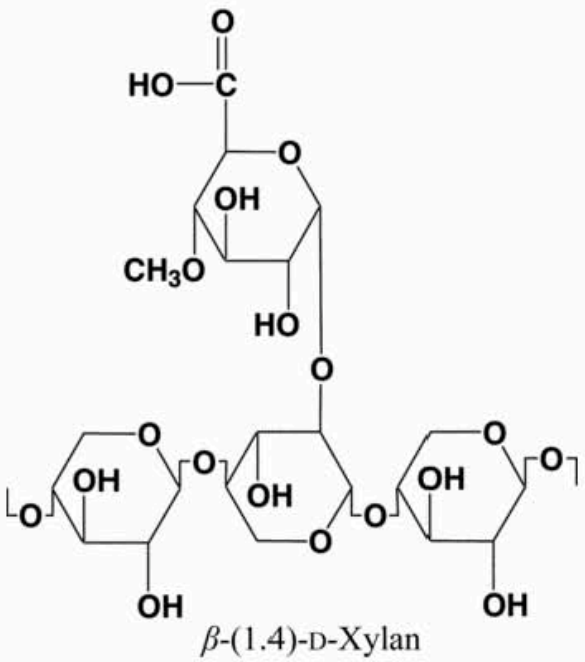

Figure 2. Molecular Structure of Glucuronoxylan.

Under neutral and alkaline conditions, these carboxylic acid groups are deprotonated, pKa = 4-5, and, therefore, carry a single negative charge. These negative charges have an inherent electrostatic attraction to positive charges or cations, such as quat salts. The hypothesis is that these carboxylic acid groups (and other acid groups) are electrostatically attracting the quat salts in the antimicrobial solutions, which are then irreversibly adsorbed onto the pulp, through a process of ionic bonding, and thus, those quat salts that are adsorbed are not capable of being present in solutions expressed from the wipes during use.

There is a phenomenon known as a Donnan Equilibrium wherein there is an equilibrium reached between charged species present in a free solution and those

absorbed onto an oppositely charged material. This explains, in part, why there is never a complete, that is 100%, adsorption of quat salts onto pulp, even at very low concentrations of quat salt. For example, typically a solution expressed from a pulp sheet is only about 250 ppm quat salt, if the initial concentration of quat salt solution exposed to the pulp was 1000 ppm.

A solution to the above problem described in this work is to use dissolved metal salts, which exist as metal cations in aqueous solutions ($M^{x+}_{(aq)}$), to essentially occupy the acid groups on the pulp by "out competing" quat salts for adsorption onto the pulp at those sites. The metal cations would "out compete" the quat salts through both the pulp's inherent greater affinity for the metal cations as well as through a numeric advantage by exceeding both the number of quat salts in the disinfectant solution as well as the amount of acid groups present.

The theory of Donnan equilibria states that an individual cation's affinity, in this case a metal cation, for an anion, in this case the deprotonated carboxylic acid groups, is specific to the cation itself and, therefore, each metal cation should have a different affinity for the pulp. Simply put, the concentration of quat salt present in solution expressed from pulp exposed to both metal salts and quat salts, regardless of when the pulp is exposed to these materials, is greater than the concentration of quat salt present in solution expressed from pulp exposed to only quat salts.

4.2 – Previous Work

Buckeye Technologies has patented several inventions wherein they impregnate wood pulps with precipitated aluminum compounds. In "Method for treating pulp to reduce disintegration energy"[3] precipitates aluminum compounds onto wood pulp at the wet-end by increasing the pH of a previously soluble aluminum slurry with wood pulp. This is technique is performed to have the precipitated aluminum act as a debonder, which decreases the amount of energy required to defribate the wood pulp, in place of other forms of debonders. These products were actually tested for the rejection of quat salts (by us, not Buckeye, that is) but while there was greater quat salt rejection, there was not the degree as seen in aluminum sulfate samples cited herein. This is because the insoluble aluminum, likely aluminum hydroxide ($AlOH_3$) cannot interact with the wood pulp's carboxylic acid groups, and therefore cannot obtain the benefit of it competing with quat salts for adsorption onto the pulp. The increased rejection in these materials over untreated pulp is likely due to the significant amount of sodium present, which is another soluble metal cation, like Al^{3+} from aluminum sulfate, but the pulp fibers' carboxylic acid groups don't have as great an affinity for sodium as it does for aluminum. The sodium present in these pulp materials likely comes from the basic salts, such as NaOH, to increase the pH to precipitate the aluminum. Also, in Buckeye's patent "Cementitious material reinforced with chemically treated cellulose fiber"[4] they added aluminum, either in the form of aluminum chloride, aluminum hydroxide, or aluminum sulfate, to wood pulp fibers and again raised the pH, as done in the previous patent described. Then they acid treated this aluminum precipitate-pulp fiber slurry with

an acid treatment, which was meant to buffer it against the harsh alkaline cementitious environment. These materials were then used as additives for cement slurries providing them with a structural reinforcement that degrades more slowly than cellulosic materials that are not chemically treated. In Buckeye's patent "Absorbent structures of chemically treated cellulose fibers"[5] they again added aluminum, from the same compounds stated previously, as well as other polyvalent metal cations to wood pulp fibers. These metal salts were again then precipitated onto the pulp fibers. These materials were then used as cellulosic materials in diapers and other similar product to maintain absorbent structure, meaning avoiding "gel block" with the super-absorbent polymers added to these products. This means that the product would maintain permeability allowing for better wicking and, therefore, better performance.In addition to the work done by Buckeye Technologies, there has been a lot of work with creating antibacterial wood pulp or cellulosic materials by altering the pulp itself. Patents have shown some examples of these.[6-10] They devise several techniques of modifying cellulosic materials to have quaternary ammonium salt moieties or other similar antibacterial compound on the surface of the fibers. While they are related to the desire for antibacterial wipe, their goals differ from ours in that they wish to make the wipe or other absorbent material antibacterial, whereas we wish to create an absorbent material that releases antibacterials.

A patent that supports our concept of an overall cationic substrate repelling quat salts and inhibiting their adsorption is "Cationic Fibrous Sanitizing Substrate".[11] Herein the investigators are trying to solve the same problem we are, which is avoiding the

adsorption of quaternary ammonium salts by a material when stored in said solution. They tackled the problem by using a cationic polymer, chitosan, mixed with other synthetic polymer fibers, including polyethylene terephthalate (PET) and rayon, which might actually be better described as semi-synthetic. The amount of chitosan was generally kept between 5 and 60% of total mass, but displayed very good performance even at $\leq$ 15% (wt.) For example, a 5% chitosan/40% PET/55% rayon substrate had 90% rejection after 1 hour, while a 35% rayon/35% tencel/30% PET substrate only had 62%.

There is a decent amount of literature available discussing the Donnan equilibrium in wood pulps, but all of them pertain to metal adsorption or their competition with other metals or $H^{+)}$ (due to varied pH). Our solution, conversely involves the competition between inorganic (metal) cations and organic (quat salt) cations for adsorption onto the wood pulp fibers. In Towers' and Scallan's research[12] a model was developed for predicting the amount of certain metal cations (Na^{+}, Ca^{2+}, Mg^{2+}, and Mn^{2+}) that would adsorb onto unbleached craft pulps depending on pH. "Interactions between divalent metal ions and oxygen-delignified draft pulps" by Karin Athley and Per Ulmgren explored the adsorption of calcium or manganese cations in a strong sodium solution, with manganese displaying a slightly greater affinity for adsorption.[13] Norberg, Lindén and Öhman's research studied a much more complicated situation where not only is the a competition for adsorption onto the pulp by Ca^{2+} and Mg^{2+}, but there is also the complicating factors of precipitation (due to change in pH) as well as complexation by chelating materials also added.[14] In "Acid/base and metal

adsorption properties of CMC-type softwood Kraft pulps of different charge" by Ola Sundman and Lars-Olof Öhman the researchers looked at the effect of pH upon the adsorption of the metal cations: Na^{+}, K^{+}, Mg^{2+}, and Ca^{2+}.onto pulp with varying degrees of chemical modification to increase the number of carboxylic acid groups on the pulp.[15] Their results found trends of the adsorption of metal cations with varying pH depended greatly upon the number of acid groups present on the pulp. These results for high-carboxylic content pulp did not exhibit the general under-prediction of metal uptake predicted by previous Donnan models. In "Ion Exchange of H^{+}, Na^{+}, Mg^{2+}, Ca^{2+}, Mn^{2+}, and Ba^{2+}, on Wood Pulp" by Alan W. Rudie, Alan Ball, and Narendra Patel was similar in some respects to the previously mentioned study, but was expanded to a greater number of metal cations, as described in the title, but was done upon Kraft pulp with far lower Kappa numbers.[16] Also, much of the study did not just involve the competition for adsorption between H+ and a metal cation, but also between the metal cations themselves. It was found that affinity of the pulp for the metal cations generally was $Ca^{2+} > Na^{+} > Mg^{2+} > Ba^{2+} > Mn^{2+}$.

There have also been a few papers on the study of the adsorption of aluminum (our best mode) onto wood pulps. In "Studies on Interactions between Aluminum Compounds and Cellulosic Fibers in Water by means of ^{27}Al-NMR" by Kato, Isogai, and Onabe the adsorption of Al^{3+} from the soluble salt aluminum sulfate was studied.[17] It was found that no aluminum was adsorbed onto pure cellulose materials regardless of pH, which supports the claim that it is dependent upon the carboxylic acid groups present in the hemicellulose of the adsorption of metal cations. Also, it was found that

the Al^{3+} complexed with 3 different carboxylic acid groups, meaning that there are few "dangling" positive charges from the aluminum adsorbed meaning that the overall charge of aluminum sulfate doped pulp is close to zero. Bottero and Fiessinger's "Aluminum Chemistry in Aqueous Solution" (Nordic Pulp and Paper, 1989, 2, p. 81) is general background upon the different hydrates, flocculants and colloids present in aluminum solutions depending upon pH and ionic strength.

4.3 – Results

The following examples show that the addition of metal cations to compositions containing quat salt and wood pulp fibers significantly reduces the amount of quat salt adsorbed onto the pulp fibers compared to compositions containing only wood pulp fibers and quat salts alone. Further, it will be shown that a range of metal cations and metal cation concentrations are effective. The metal salts evaluated were calcium chloride, magnesium chloride and aluminum sulfate. The range of metal salt concentrations evaluated was from 0.001 moles of metal salt per 100 grams of oven dry wood pulp fiber to 0.02 moles of metal salt per 100 grams of oven dry fiber. The authors believe that the effective range of metal ion could be as low as 0.0001 moles of metal salt per 100 grams of oven dry wood pulp fiber. The upper range of metal salt addition is only restricted by the solubility of the metal salt chosen and other, primarily commercial and not performance, considerations, such as, discoloration, softness or health issues.

The examples will show that the manner in which the metal cations are added to the composition is not important. Examples are given simulating addition during the wet-laid sheet forming process during pulp fiber manufacturing. Other examples simulate addition after the wood pulp fibers have been dried in sheet form via spray or shower addition. In another example, the metal cations were added directly to a mixture containing the wood pulp and quat salts.

Other examples will show that the wood pulp fibers in the mixture containing fibers, quat salts and metal cations can be in sheet form or singulated fiber form. Finally, examples are given with pure quat salts as well as commercial antimicrobial (with quat salts as the active ingredient) products.

Example 1 The Effect of Various Metal Ions on Quat Rejection Efficiency

In the following examples the terms such as "percent BAC rejected" and "percent quat rejected" refer to the percentage of quat salts, either a specific variety, such as BAC, or a combined DDAC and BAC solution referred to as "quat salts", that are added to the compositions that are not adsorbed on the wood pulp fibers when liquid is squeezed out of the mixture containing pulp fibers, dissolved quat salts and, possibly, dissolved metal ions. For example, if pulp fibers in sheet form are exposed to a solution containing 1000 ppm of a quat salt, and the concentration of the quat salt in the solution that has been squeezed out of the mixture is 250 ppm, then the %quat rejection is said to be 25%. That is, 25% percent of the quat salt has not been adsorbed onto the fibers.

The amounts of metal salts added to the compositions described in the following examples are expressed in equivalents of charge. The equivalents of charge is the ratio of the moles of "positive charges" in the metal salt to the moles of "negative charges" on the pulp fibers. For example, if the pulp fibers have a carboxyl content of 4 meq/100g, their negative charge equates to 4 millimoles/100g, since carboxylic acids are univalent, that is having a single negative charge. One equivalent of a metal salt with a metal with an oxidation state of 2, meaning it produces a +2 charged metal ion when dissolved, would be 2 millimoles/100g. In other words, 2 millimoles/100 g of a +2 metal ion is equivalent to the charge on a pulp fiber having a carboxyl content of 4 meq/100 g. The carboxyl content of the wood pulps used in the following examples were measured by TAPPI Method – T237 cm-08.[17]

In Example 1, various metal ion salts were added to CF416 wood pulp in a manner meant to mimic wet-end addition on a paper machine. CF416 is a bleached southern pine kraft wood pulp manufactured by Weyerhaeuser NR in Columbus MS. The effectiveness of 3 different metal soluble salts were compared. These were magnesium chloride, calcium chloride, and aluminum sufate. Used delivered from Sigma-Aldrich in the forms of magnesium chloride-hexahydrate, calcium chloride-anhydrous, and aluminum sulfate-octadecahydrate, respectively.The CF416 pulp sheet was cut into small pieces and soaked in a solution of the appropriate metal ion salt, which when added at a 3:1 mass ratio of metal salt solution to wood pulp for 1 charge equivalent when using 4 meqs/ 100 g carboxylic acid pulp, typical for CF416, is 1904, 2220, and 2281 ppm of $MgCl_2$, $CaCl_2$, and $Al_2(SO_4)_3$ – as calculated vs. anhydrous

forms of the metal salts. The experiment durations of these pulp soaking in aqueous metal salt solutions were typically between 1-2 hours, took place within plastic syringes (BD Medical), and done at room temperature. Afterwards the wetted 416 pulp sheet had the metal salts solutions (though depleted by the metal cation adsorption onto the pulp) expressed from them using a caulking gun and was then washed a number of times with DI water, and dried. A control samples (CF416 with no exposure to any metal salts) as well as the dried metal salt treated samples were then ready to be treated with quat salts to observe the effectiveness of the metal salt treatments.Four quat salt solutions were prepared having the following concentrations; 100 ppm, 200 ppm, 500 ppm and 1000 ppm by dissolving the appropriate weight of BAC (MW 365 g/mole) in deionized water. The BAC was used as delivered from Sigma-Aldrich in its neat form (a waxy solid), CAS # 8001-54-5. The quat solutions were placed in separate plastic syringes (BD Medical) to which a known quantity of pulp sheet pieces prepared in the above manner had been added. The mass to mass ratio of the quat salt solution to the dry mass of the pulp was 3:1 in all cases. Thus, for example, one syringe contained calcium chloride treated pulp plus 3 times its mass of 100 ppm BAC solution, while the next syringe contained calcium chloride treated pulp plus 3 times its mass of 200 ppm BAC solution and so on until all combinations of pulp treatments and BAC solution concentrations were prepared.

The syringes containing quat salt solution plus pulp were allowed to stand for about 1.5 hours at room temperature. At the end of the exposure time each syringe was placed in a calking gun and pressure was applied to the syringe plunger until the free quat salt

solution could be collected for analysis. The unadsorbed quat salt concentration was measured by CE as described in Example 5.

Figure 3 shows that all three metal salts ($CaCl_2$, $MgCl_2$, and $Al_2(SO_4)_3$) had significant effects upon the percentage of BAC rejected. Thus, in all these cases these metal salts were effective in ameliorating the issue at hand, with aluminum sulfate being the most effective salt of the three shown. This may be due to greater affinity of the pulp's carboxylic acid groups for Al^{3+} cations as well as the greater charge of a metal (III) cation, which might have greater repulsion of other cations, i.e. quat salts, if they are not completely coordinated with the pulp's carboxylic acids, which would result in free or dangling positive charges.

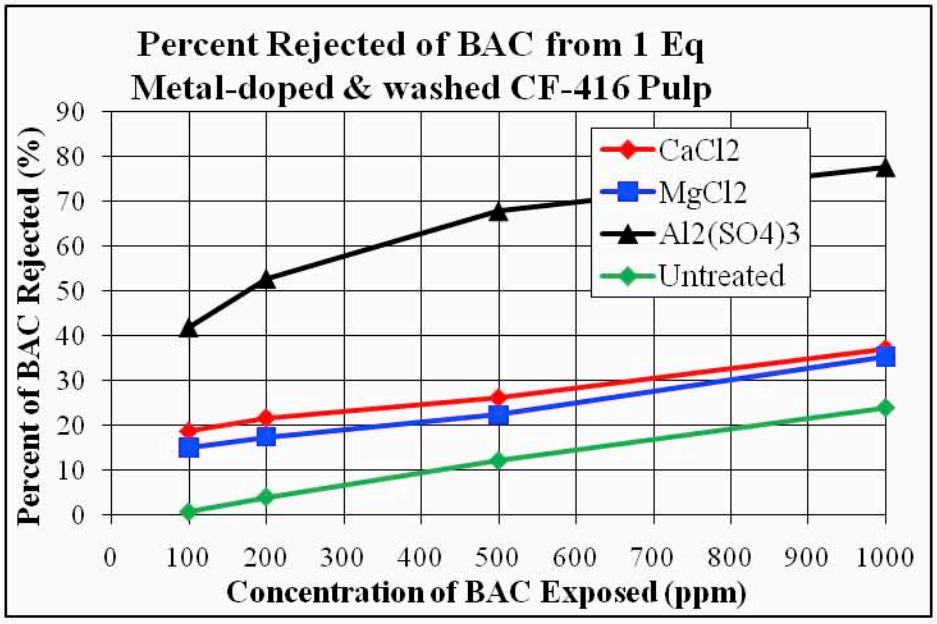

Figure 3. Percent Rejection of BAC in relation to its initial concentration upon exposure to 1 Equivalent of charge Metal-doped, then washed, 416 pulp sheet.

Example 2 The Effect of Salt Addition Mode on Quat Rejection

In Example 2, the method by which the metal is added to composition containing quat salt and pulp fibers was studied. The first series of samples was prepared in the manner described in Example 1. These samples were meant to simulate salt addition in the wet-end of the papermaking process. The second series of samples was prepared by squirting a much smaller volume of a much more concentrated metal salt solution onto the pulp sheet with a syringe in parallel streaks, and allowing the sample to air dry without washing. This method was meant to simulate addition of the metal salts at the dry-end pulp sheet making process or during the non-woven manufacturing process as might be accomplished by a spray bar. In these series the treated pulp samples and the quat salt solutions were combined in the same manner described in Example 1.

In the third series, the metal ion salt was added directly to the quat salt solutions. The quat salt / metal ion combined solutions were added to untreated pulp pieces in syringes as described in Example 1. In all 3 sample series, 1 equivalent of aluminum sulfate was used. The concentration of rejected quat salt was measured by potentiametric titration as described in ASTM D 5806-95.

Figure 4 compares the percent BAC rejection levels for 3 series described above with a control without metal ion addition. All of these aluminum sulfate treated samples had 1 equivalent of charge of aluminum sulfate applied. These results demonstrate that all 3

methods of metal salt addition were effective in reducing the amount of quat salt that was adsorbed onto the pulp fibers.

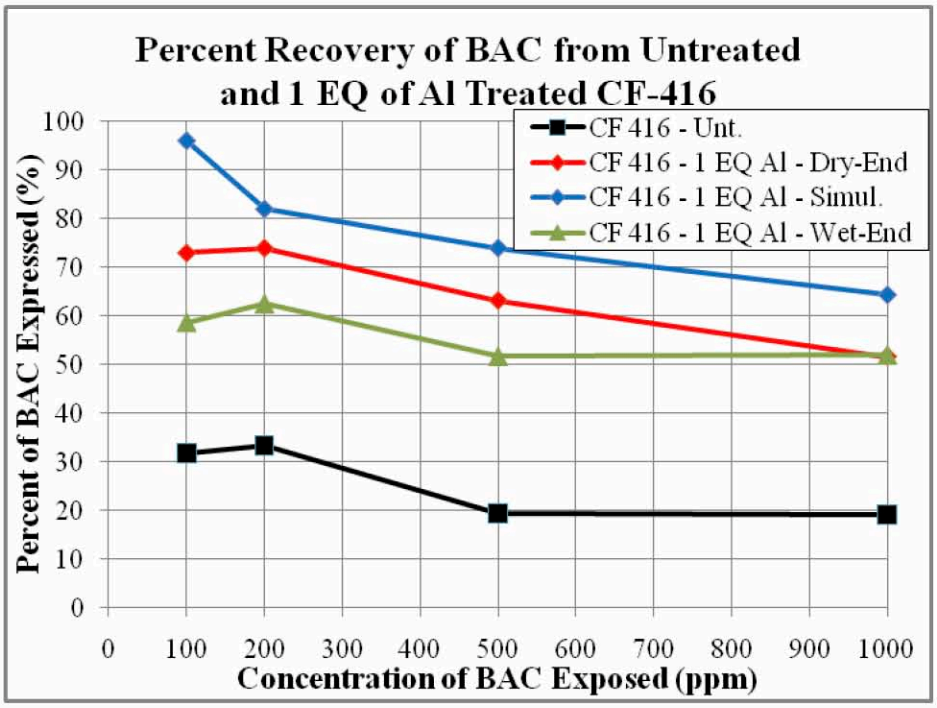

Figure 4. Percent Rejection of BAC in relation to its initial concentration upon exposure to 1 Equivalent of charge Al-treated CF416 pulp sheet by simulated: dry-end, simultaneous (with BAC), or wet-end

Example 3 Singulated Fiber vs. Sheet Form Comparison

In the preceding experiment the wood pulp fibers were in a wet-laid sheet form when they were exposed to the solutions containing quat salts. In this example, compositions in which the fibers were in sheet form were compared with compositions where the fibers were in singulated fluff form. The singulated fibers had a much greater

absorbency for the quat salt solution than the fibers in sheet form. Therefore, it was necessary to increase the liquid to fiber ratio in order assure all of the fibers would be wetted. A 6:1 liquid to fiber ratio was found to be necessary to wet out the singulated fiber samples.

In order to understand the effect of the liquid to fiber ratio separate from the effect singulated fiber vs. sheet form, a comparison was done with pulp sheet samples at both 3:1 and 6:1 liquid to fiber ratios. The wood pulp fibers used for these experiments were CF405 and CF416. Both are bleached kraft southern pine pulps manufactured by Weyerhaeuser NR Co at Columbus MS. CF405 contains a debonder to make the wet-laid pulp sheet softer and easier to defibrate, while CF416 does not. The aluminum sulfate solutions were applied to dry pulp sheets with a syringe, as done in Example 2. The aluminum sulfate treated pulp sheet samples were exposed to quat salt solutions as described in Example 1. The percentage of quat salts present in the expressed solution were measured by ASTM method D 5806-95 using potentiometric titration.

The results in Figure 5 indicate that a higher percentage of the quat salts are rejected when the liquid to fiber level was increased from 3:1 to 6:1 due to an increased ratio of total quat salt molecules to carboxylic acid groups on the fiber. There is a spike in the rejection numbers at low concentrations of quat salt in the case of the 3:1 samples, but not in the case of the 6:1 samples. This is likely due to the pulp fluff samples not being entirely wetted, thus not all of the quat salt molecules are capable to interact with all the pulp fiber's carboxylic acid groups.Thus, when the solution is

expressed from the pulp material contains a portion of quat salts that never interacted with carboxylic acid groups and are still in solution; which produces an artificially high number of quat salts that are expressed from the pulp resulting in and artificially high rejection number.

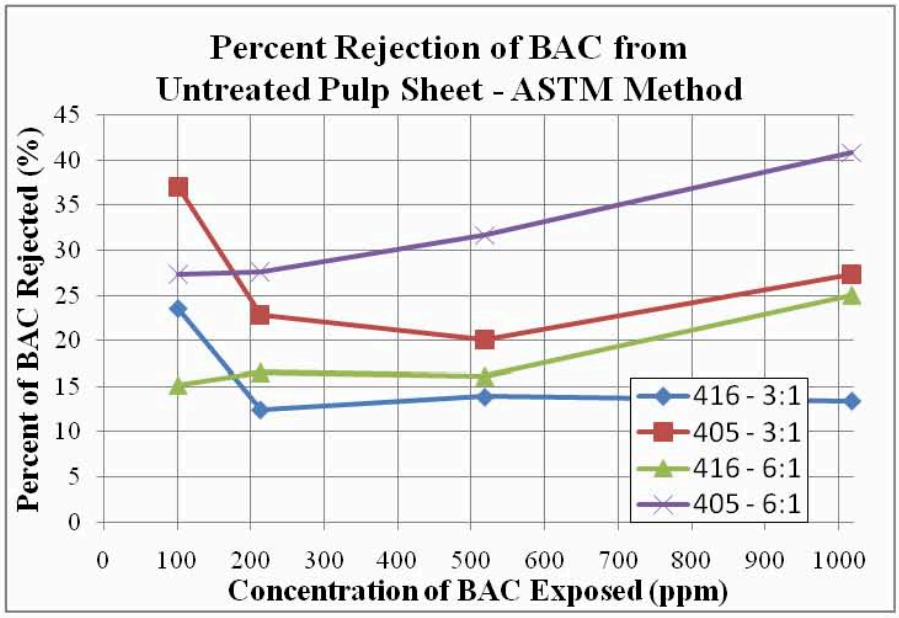

Figure 5. Percent Rejection of BAC in relation to its initial concentration upon exposure to Untreated Pulp Sheet using ASTM Method.

Next, CF416 and CF405 pulp sheets were treated with 3 equivalents of aluminum sulfate with a syringe as described earlier and in Example 2. Part of the aluminum treated 405 and 416 material was then fiberized in a Kamas laboratory hammermill to yield a singulated fiber fluff. Also untreated pulp sheets were similarly fiberized as controls. The untreated fluff, aluminum treated fluff, and the aluminum

treated sheet samples were exposed to quat salt solutions as described in Example 1 except that a 6:1 liquid to fiber ratio was used for the fluff samples and half of the aluminum treated sheet samples. The other half of the aluminum treated sheet samples was exposed to 3:1 ratio of the quat solutions. The concentration of the rejected quat in the expressed solutions was measured by ASTM method D 5806-95.

The results are summarized in Figures 6 and 7 for CF416, and CF405 respectively. In these figures, PS is used to designate the pulp sheet samples and PF the pulp fluff samples. Clearly, as shown before, the addition of aluminum sulfate significantly improved the percentage of BAC rejected by the pulp fibers. These results also showed that the untreated fluff samples gave higher rejection levels than the untreated sheet samples. This was attributed to the difficulty in fully wetting the pulp fluff with the quat salt solution as well as the difficulty of flow through essentially a plug of pulp fluff that exists in the syringe during the experiment. This would hypothetically result in quat salt depleted regions, due to interaction with carboxylic acid group in the pulp, but due to very slow diffusion these regions would not be equilibrated with portions of the solution that had not come into contact with the pulp carboxylic acid groups and were thus not depleted of quat salts. Thus, over the period of the experiment, it is our belief that the pulp fluff is not allowed to reach its Donnan Equilibrium due to slow diffusion.

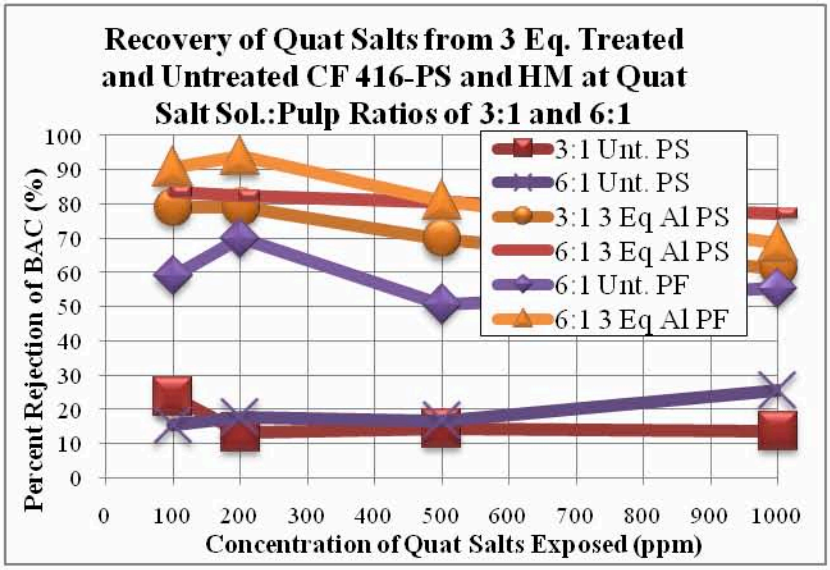

Figure 6. Percent Rejection of BAC in relation to its initial concentration upon exposure to Untreated and 3 Equivalents of charge from Al^{3+} treated 416 Pulp Sheet and Pulp Fluff at 3:1 and 6:1 mass ratios

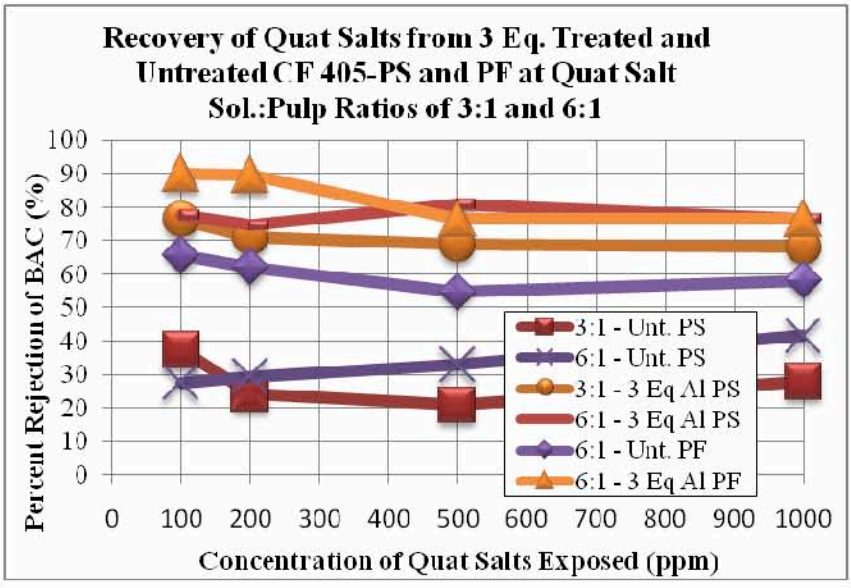

Figure 7. Percent Rejection of BAC in relation to its initial concentration upon

exposure to Untreated and 3 Equivalents of charge from Al^{3+} treated 405 Pulp Sheet and Pulp Fluff at 3:1 and 6:1 mass ratios

Example 4 Comparison of Results With Different Quat salt and Different Aluminum Salt Treatment Levels.

In this example, the percent quat rejection was tested using BAC, DDAC, and Virex. Virex is a commercially available antimicrobial solution made by Johnson Wax. According to the MSDS it contains a 1:1 mixture of BAC and DDAC as well as other ingredients. Aluminum sulfate treated wood pulp samples were produced from NB416 and NF405, which are southern pine bleached kraft wood pulps manufactured by Weyerhaeuser NR in New Bern North Carolina. NF405 contains a debonder, whereas NB416 does not. A commercial solution of aluminum sulfate (26.8% $Al_2(SO_4)_3$) was sprayed onto the pulp sheet as the sheet was being rewound from one spool to another. The amounts deposited upon the pulp sheet were calculated as being 3 and 5 charge equivalents of Al^{3+} with those samples being designated as MOD 3 and MOD 5, respectively. These amounts were calculated by knowing both the pump rate of aluminum sulfate solution at a certain RPM of the pump as well as the sheet velocity. Aluminum sulfatepulp sheet samples prepared in the above manner as well as untreated pulp sheet samples were exposed to quat salt solutions as described in Example 1. The concentration of rejected quat salts in the expressed solutions was measured by ASTM method D 5806-95. In this case, one series of experiments was performed with BAC,

another was performed with DDAC and another was performed with Virex. The results are compared in Figures 8 and 9 for NB416 and NF405.

In Figure 8, the rejection levels of Virex and BAC were compared for compositions containing a quat salt solution and either untreated NB416, or NB416 treated with either 3 or 5 equivalents of aluminum. The untreated NB416 compositions rejected about 18 to 38% of the BAC and 5 to 20% of the Virex. The aluminum sulfate treated NB416 compositions rejected 60-90% of the BAC and 32 to 55% of the Virex. The NB416 treated with 5 equivalents of aluminum sulfate provided slightly better performance than the samples treated with 3 equivalents.

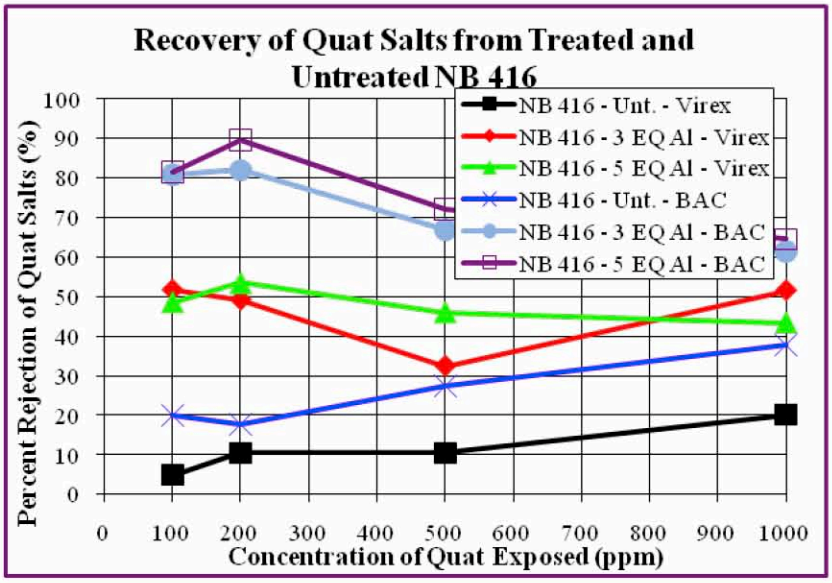

Figure 8. Percent Rejection of Quats Salts in relation to their initial concentration upon Exposure to Untreated, MOD 3, and MOD 5 modified 416 Pulp Sheet.

In Figure 9, the rejection levels of Virex and DDAC were compared for composition containing a quat salt solution and either untreated NF405 or NF405 treated with either 3 or 5 equivalents of aluminum. The untreated NF405 compositions rejected about 5-33% of the DDAC and 10-14% of the Virex. The aluminum sulfate treated samples rejected about 75-90% of the DDAC and 30-65% of the Virex. Again the samples with the samples with 5 equivalents of aluminum tended to perform better than the samples with 3 equivalents of aluminum.

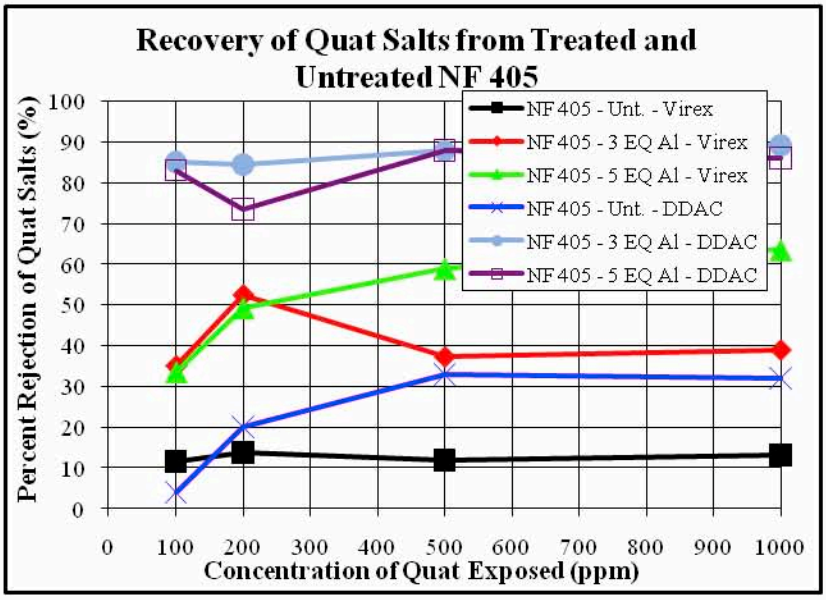

Figure 9. Percent Rejection of Quats Salts in relation to their initial concentration upon Exposure to Untreated, MOD 3, and MOD 5 modified 405 Pulp Sheet.

Overall, the results show that the compositions containing aluminum ions rejected quat salts much better than the compositions without aluminum ions. In both the circumstances with and without aluminum ions a higher proportion of the pure quat salts (BAC and DDAC) were rejected than observed with quat salts from Virex.

ICP Analysis of Treated and Untreated Pilot Line Pulp - Blended				
Client ID	Lab ID	Al	Theoretical/Expected Amount (mg/kg)	Percent Deviation (%)
		mg/kg, as-received basis		
NB 416 - MOD 3	001	590	1079.26	-45.33
NB 416 - MOD 5	002	2340	1798.77	30.09
NF 405 - MOD 3	003	910	1079.26	-15.68
NF 405 - MOD 5	004	1430	1798.77	-20.50
NB 416 - Untreated	005	< 20	0.00	
NF 405 - Untreated	006	< 20	0.00	

Table 4.1. ICP analysis of the Aluminum content in treated and untreated pilot rolls along with comparisons to theoretical Aluminum contents.

Table 4.1 contains the results of the ICP analysis of the Aluminum content in the aluminum sulfate-treated and untreated pulps. ICP stands for Inductively-Coupled Plasma, is an analytical method used for the detection of, primarily, trace metals. The method for digesting the pulp and the ICP analysis of it come from Methods 3050B and 6010C, respectively, of the EPA's "Test Methods for Evaluating Solid Waste, Physical/Chemical Methods" or SW-846. The results indicate that we were successful in achieving within a 15-45% of the theoretically expected amount of aluminum delivered to the pulp sheet using the spray-bar. It is likely that the actual number is even

closer to the expected value, as there were some difficulties samples of pulp sheet with our ICP work.

Example 6 CE Test Method For Analyzing Quat Salts in Solution

4.4 – Method

This method is applicable to the determination of alkylbenzyldimethyl ammonium chlorides in reagent water and to aqueous client matrices after recovery confirmation via sample spiking . Alkyl groups ranging from n-$C_{12}H_{25}$ to n-$C_{16}H_{33}$ have been shown in the literature to be separated by this method. The present application is limited to n-$C_{12}H_{25}$ and n-$C_{14}H_{29}$ alkyl substituents as these are the ones present in the BAC supplied by the client. It is based on the work of Ya-Hui, et al. adapted for the Agilent G1600A Capillary Electrophoresis System. Analytes C12-BAC and C14-BAC both work used in the concentration range of 1.0-30 µg/mL

In capillary electrophoresis (CE), solutes are separated in an electrolyte-filled fused silica capillary due to differences in their electrophoretic mobilities. Useful features of CE include: the ability to determine the type and number of anions, cations, and neutral species in a sample using the various modes of separation with short analysis times, high efficiency separations, selective or universal detection modes (using a photodiode array detector(DAD)), the ability to analysis complex matrices with little sample preparation, and the use of simple commercially-available buffers and inexpensive capillary columns. The Agilent CE system has an autosampler carousel,

which provides for unattended operation. Each analytical method provides a recommended technique for dilution and, occasionally, derivatization of the samples to be analyzed. Before the prepared sample is introduced into the CE, a procedure for standardization must be followed to determine the recovery and the limits of detection for the analytes of interest. Following sample introduction into the CE, analysis proceeds with a comparison of sample values with standard values. Qualitative identification is by means of migration time (MT) and quantitative analysis is achieved through integration of peak area which is normalized by migration time.

The present application uses a simple phosphate buffer modified with acetonitrile. This modification disrupts BAC micelle formation and adsorption of BAC to the capillary wall. For this method, the buffer is 40 mM sodium phosphate (pH 4.0) in 40% acetonitrile. At pH 4.0, the BAC migrates toward the detector where they are detected by direct absorbance at 200 nm. Caution is warranted regarding BAC levels higher than 50 ug/mL. Preliminary work using higher concentrations fouled the capillary to the point of no migration being seen within a reasonable time. Replacing the capillary column was required.

For Hazard Information related to this method, please see section 8. It is expected that any user of this method be fully informed of the potential hazards before preparing the buffer or standard solutions.

Following is a list of possible interfeneces:

1 Thus far, there have been no interferences noted. The samples are prepared at a dilution of at least 20 to 1, due to expected levels being higher than the calibrated range.

The initial samples are likely to be sufficiently clean as to not present an interfering matrix.

2 Fresh buffer and column conditions typically provide a stable baseline near the analyte migration times. As the buffer is used over the course of a series of runs, artificial responses will be seen both early and late in the separation. As the baseline stabilizes and migration times don't shift, this is generally of little concern. Initial analyses indicate buffer stability for up to 13 runs. After buffer vial replacement, migration times become stable after an initial standard run.

3 Changes in migration times and resolution are symptoms of buffer deterioration or may be caused by the buildup of contaminants on the inner capillary wall. Refer to the manufacturer's guidelines for instructions on column cleaning. If these guidelines do not restore the retention times, replace the column.

4 The presence of air bubbles or particulants in the column may cause baseline fluctuations, low current readings, or peak variability. All samples require filtration to 0.45 um. Commercial buffer systems are already filtered. The use of degassed water for dilution may help to minimize the introduction of air. Freshly prepared buffer must be degassed ultrasonically during filtration.

A sample of 40 mL is preferred. The amount of diluted sample required depends on vial type used. It is recommended that glass vials be used. They require 500 uL. The actual criterion is the sample vials need to be filled to a level 1.4 cm from the base. This is a requirement of the CE injection system. Always using the same vial volume helps maintain injection reproducibility. Thus far, samples from the clients have required two dilutions: a 1 to 25 dilution for BAC when it is known present; and a 1 to 5 dilution for a good detection limit for others. Hence, the actual minimum volume requirement has been determined by filtration needs and is likely to be on the order of 1 mL.

Samples were stored in plastic bottles with no apparent deleterious effect. The sample should be stored at 4 °C (39 °F) and returned to the lab for analysis as soon as possible. There is no known holding time for BAC solutions. Commercially available aqueous solutions are stable at a 50 % concentration when refrigerated. Material Safety Data Sheets for various BAC mixtures also state these are stable compounds.

The Agilent G1600A Capillary Electrophoresis System contains in one cabinent an autosampling carosel, a thermostatted capillary column cassette, A Diode Array Detector (DAD) operating in the UV-Visible range, an integral high voltage power supply capable of both positive and negative inlet electrode voltages, and a buffer solution replenishment system (if needed). The ChemStation data acquisition and analysis system is supported by a PC running Windows XP Professional SP 2.

The capillary column used for this application is the Agilent P/N G1600-61232. It is a bare fused silica capillary with a 50 um internal diameter, a length of 56 cm, and

an extended light path bubble cell. The bubble cell is an internal bubble blown into the detector region of the column. As it widens the inner channel, it produces an extended path for absorbance detection. An attribute of laminar flow in CE keeps the analyte zone from mixing in the larger volume and thus maintains the concentration within the zone.

The DAD is used with a signal wavelength of 200 nm and bandwith of 20 nm. The reference wavelength is 425 nm (50 nm). The detection method uses the direct scheme in which a UV absorbing analyte creates an absorbance signal. The reference wavelength helps compensate for minor shifts in the buffer background.

The Agilent G1600A Capillary Electrophoresis System includes a version of ChemStation software configured for use with CE. In one PC environment are combined instrument control, raw data acquisition and reduction, and report generation. All aspects are included in a single method file: for example, the file stored as C:\HPCHEM\1\METHODS\CE\BAC3.m.

If one is preparing a CE buffer system from individual components, it is generally recommended to use polypropylene volumetric flasks dedicated to each aqueous buffer. This avoids trace contamination from the glass surface which could affect migration time stability and cleanliness of the electropherogram baseline. This method uses an operator-prepared buffer system.

Following is a list of glassware used:

9-mL borosilicate glass culture tube, VWR, 47729-572.

14-mL borosilicate glass culture tube, VWR, 47729-576.

Polyethylene Cap for 14-mL Tube, Becton Dickinson, Falcon 352030.

2-mL (3 mL) Norm-Ject disposable syringe with Luer adapter.

GHP Acrodisc 25 mm 0.45 micron syringe filter,

2-mL clear (glass) wide opening crimp vial, Agilent 5181-3375.

Snap caps, polyurethane for 2-mL vials, Agilent 5181-1512.

Microduster III, CleanTex, inert gas for glassware dust purging.

To avoid particulate contamination, it is a good idea to purge test tubes and vials with a quick burst of inert Microduster III gas just prior to use. Calibration standards and samples are prepared in disposable glass ware. The final dilutions of standards and samples are filtered using disposable filter cartridges and dispensed into disposable glass sample vials. Volumetric pipettes should be used to measure stock solutions. The pipettes may be either fixed or variable volume and preferably those with disposable tips in order to reduce contamination.

The buffer is based on a 66.7 mM $NaH_2PO_4 \cdot H_2O$ solution adjusted to pH 4.0 using phosphoric acid. It is then mixed with actonitrile to a final concentration of 40 mM. (There remains a non-standard definition in the literature regarding the concentration of mixed solvent buffers. The 40 mM (final) concentration used in this method produced acceptable results.)

Following is a list of chemicals used:

Sodium Phosphate, Monobasic,monohydrate ($NaH_2PO_4 \cdot H_20$), 100.7%, JTBACer

3818-01/Lot Y10145. Formula weight is137.99 g/mol.

Phosphoric acid, 85.2%, JT BACer 0260-05/ Lot N08803. Formula weight is 98.0 g/mol.

Acetonitrile (ACN), B&J, Biosyn Grade, BB017-4 Lot CM370.

Distilled deionized water, use the distilled water available from SLM 212S-5. It has been demonstrated as clean for CE work. If used immediately as a water blank, it requires filtration.

To make a buffer stock solution place 1.058 gm $NaH_2PO_4 \cdot H_2O$ in a 100 mL polypropylene volumetric flask and add ca. 90 mL of distilled deionized water. Swirl until dissolved, then carefully dispense into a 100 mL plastic beaker and add a small Teflon-coated stir bar. Use a pH meter calibrated for measurement between pH 4 and 7 to measure the initial pH. It should read about pH 4.3. Take a disposable glass pipet and just wet it with conc. phosphoric acid. A quick dip into the buffer should lower its pH significantly. Less than a drop of acid is required to adjust the pH to 4.0. Use dilute NaOH solution to raise the pH, if needed. Once adjusted, redispense the buffer into the 100 mL volumetric, fill to volume, shake well, then pour into a 4 oz. plastic bottle.

The run buffer is composed as 40:60 ACN:Phosphate solution (described above). A convenient volume is composed by placing 2400 uL ACN into a 14 mL tube

with 3600 uL pH 4.0 phosphate buffer, capping, then mixing well by inversion. This volume is immediately vacuum filtered through a 0.45 um filter with ultrasonic degassing for about a minute. Significant degassing is seen initially. This filtered buffer is immediately dispensed into the glass CE sample vials as determined by the method run table. Currently, there is need for 4 buffer vials. Fill them to 1.0 ml and cap them with polyurethane caps.

The stock standard solution is best prepared as needed within the week of its use. The working standard is a dilution which is completely used to make the calibration standards. The calibration standards are prepared in sufficient volume for a single filtration and use. It may be best to consider these solutions as replaceable after one week. Store the solutions at 4°C in freshly-capped CE sample vials.

Following is a list of chemicals used:

Benzalkonium Chloride (BAC), 100%, Alpha Easar 41339 (current lot: E22R060). Label only states a range for alkylation, but analysis has demonstrated this is 60% dodecyl (C12) form and 40% is tetradecyl (C14) form. As this is a mixture, there is no single formula weight. The calibration is performed in units of ug/ml.

Distilled water, use the distilled water available from SLM 212S-5. It has been demonstrated as clean for CE work. If used immediately as a water blank, it requires filtration.

Methanol, B&J, Purge and Trap Grade, 232-1 (current lot: CN637).

70:30 Methanol:Water. A convenient volume is prepared by adding 3.0 mL of Distilled water to 7.0 mL P&T methanol. This is the CE sample diluent and further protects the BAC from micelle formation.

The BAC stock standard is prepared 70:30 methanol:water. Place 8.0 mg BAC in a 4 mL screw cap vial and add 4.0 ml using a pipet for a concentration of 2000 ug/mL. A working 500 ug/mL standard is prepared using 250 ul of this stock in 1000 mL total volume of 70:30 MeOH:H_2O. A final volume of 1 mL is likely stable to evaporation for the short period it is needed to make the calibration standards.

The six calibration standards currently defined in the method are then prepared using aliquots of the 500 ug/mL (or 10 ug/mL) working standard added to separate 9-mL borosilicate glass culture tubes for final dilution to 1000 or 3000 uL in 70:30 MeOH:H_2O according to the following table.

Standard #	#1	#2	#3	#4	#5	#6
Final Conc, ug/mL	1	5	10	15	20	30
Final	1000	1000	3000	1000	1000	1000

Volume, uL						
Stock Conc, ug/mL	10	10	500	500	500	500
Volume Stock, uL	100	500	60	30	40	60
C12-BAC, ug/mL	0.60	3.0	6.0	9.0	12	18
C14-BAC, ug/mL	0.40	2.0	4.0	6.0	8.0	12

Table 4.2 Dilution Table

After all additions have been made, the tube is briefly hand shaken or vortexed then the contents immediately drawn into 3-mL disposable syringe. A 0.45 um filter is added and 0.5 mL filtered directly into the CE autosampler vial.

Samples have been provided for analysis in polyethylene sample bottles with no apparent deleterious effects. The best CE operability has been found using the 2-mL glass vials sealed with the polyurethane snap caps. Proper sealing is essential as the system uses pressure for sample injection and monitors system pressure for failure.

4.4 – Conclusions

The process provides a composition for antimicrobial wipes that significantly increases the proportion of the quaternary ammonium compounds that are not adsorbed onto the substrate and, therefore, remain in the solution when it is squeezed out of the wipes. In its simplest form, the composition of the invention contains water, wood pulp fibers, one or more quaternary ammonium salts, and a soluble ionic salt, such as aluminum sulfate.

The composition of the best mode of the invention contains a 3 to 1 weight/weight (w/w) ratio of water to wood pulp fibers which are in sheet form either by themselves or in a blend with synthetic fibers. The concentration of the quaternary ammonium compounds in the solution is between 100 and 200 ppm (weight basis) The quaternary ammonium salts are benzylalkyldimethyl ammonium chloride (BAC), dialkyldimethyl ammonium chloride (DDAC), or Virex. Virex is a commercial antimicrobial cleaner manufactured by Johnson Wax. It contains a 1:1 mixture of BAC and DDAC as well as other proprietary ingredients.

The most effective soluble ionic salt explored thus far is aluminum sulfate, $Al_2(SO_4)_3$. The w/w range that has been investigated was between 0.002281 and 0.011407. Aluminum sulfate has been found to be effective in reducing the percentage of quaternary ammonium salts that are irreversibly absorbed to the substrate over this entire range. Presumably higher levels of aluminum sulfate would also be effective up to the solubility limits of the aluminum sulfate. However, high levels of aluminum salts may cause discoloration or other problems in the use of the wipes.

It is believed that the aluminum cations in this composition of the invention compete with the quaternary ammonium salts for the anionic sites, typically carboxylic acid groups, that are present on the surface of the wood pulp fibers and, thereby, inhibit the quaternary ammonium ions from adsorbing onto the fibers.

In the best mode of the invention, an aluminum sulfate solution is applied to the wood pulp fibers prior to the manufacture of the disposable wipes. However, experiments have shown that it is equally effective to add the aluminum sulfate directly to the solution containing the quaternary ammonium salts in a solution exposed to the wipe substrates at the end of the manufacturing process. Thus, the mode and timing of the aluminum sulfate addition are not important. It is only important that a sufficient quantity of soluble aluminum is present in the antimicrobial composition containing pulp fibers and quaternary ammonium salts.

Notes to Chapter 4

(1) FDA Code of Regulations – Title 21 – Chapter I – Subchapter B – Part 178 – Section 178.1010 Sanitizing Solutions).

(2) Eklund, Dan; Lindström, Tom. Paper Chemistry: An Introduction. DT Paper Science Puplications, Grankulla, Finland (1991)).

(3) Patent # 6,159,335 - Dec. 12, 2000

(4) Patent # 6,942,726 B2 - Sep. 13, 2005

(5) Patent # 6,562,743 B1 - May 13, 2003

(6) Patent # 2006/0141015 A1.

(7) Patent #3,018,192.

(8) Patent # 4,035,146.

(9) Patent # 2,585,048.

(10) Patent # 4,311,479.

(11) Patent # 7,485,589 B2 – Feb. 3, 2009.

(12) Katz, H.E. *Chem. Mater.* **2004,** *16,* 4748;

(13) Journal of Pulp and Paper Science, 1996, 22(9), p. J332.

(14) Nordic Pulp and Paper, 2001, 16(3), p. 204.

(15) Journal of Pulp and Paper Science, 2001, 27(9), p. 296.

(16) Nordic Pulp & Paper, 2006, 21(3), p. 372.

(17) Journal of Wood Chemistry and Technology, 2006, 26, p. 259.

(18) Journal of Wood Science, 2000, 46, p. 310.

(19) TAPPI Method – T237 cm-08.

(20) Ya-Hui Hou, Chien-Yi Wu, and Wang-Hsien Ding. Development and validation of a capillary zone electrophoresis method for the determination of benzalkonium chlorides in ophthalmic solutions. , J Chrom A, 976(2002), 207-213..

(21) Agilent Technologies, Agilent Capillary Electrophoresis System User's Guide, PN G1600-90009, April 2000, 1-270..

(22) Agilent Technologies, Agilent ChemStation for CE Systems, PN G2172-90006, November 2001, 1-160.

(22) Agilent Technologies, Agilent ChemStation. Understanding Your ChemStation, PN G2070-91114, August 2001, 1-278.

Chapter 5: Published Patent No.: US 20110220311 A1

Reduction of the Adsorption of Quaternary Ammonium Salts onto Cellulosic Fibers

Inventors: Richard D. Champion, Federal Way, WA (US); James H. Wiley, Tacoma, WA (US)

Assignee: Weyerhaeuser NR Company, Federal Way WA (US)

Appl. No.: 12/724,208

Filed: Mar. 15, 2010

Publication Classification

Int. Cl. D21H 17/66 (2006.01)

U.S. Cl. 162/181.2

5.1 – Abstract

A product comprising cellulosic fiber in sheet form, 0.0001 to 0.03 moles of water soluble metal salt per 100 grams of cellulosic fiber, based on oven dry weight of cellulosic fiber, water and a quantity of quaternary ammonium salt to provide 100 to 3000 ppm of quaternary ammonium salts in solution. A process for making the product.

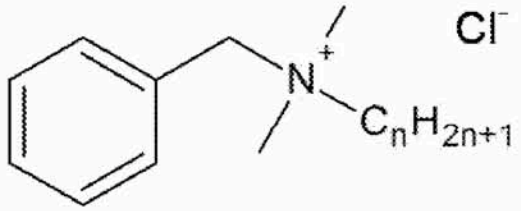

BAC n = 8, 10, 12, 14, 16, 18

Figure 1.

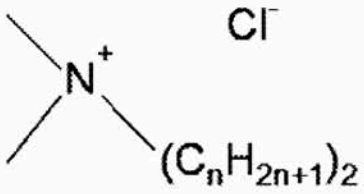

DDAC n = 8, 10, 12, 16, 18

Figure 2.

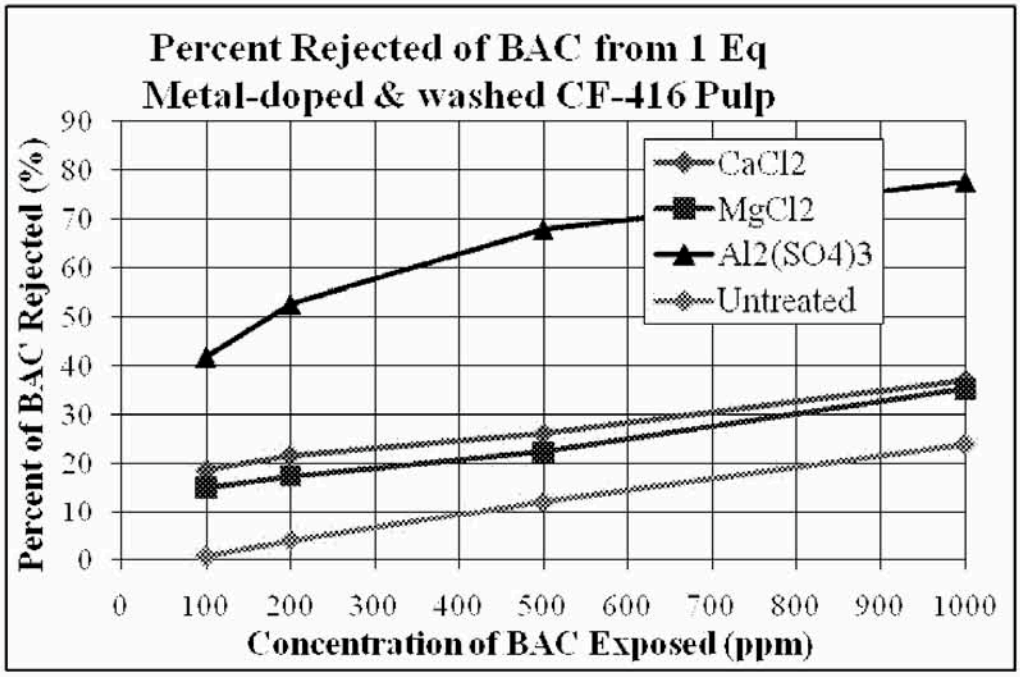

Figure 3.

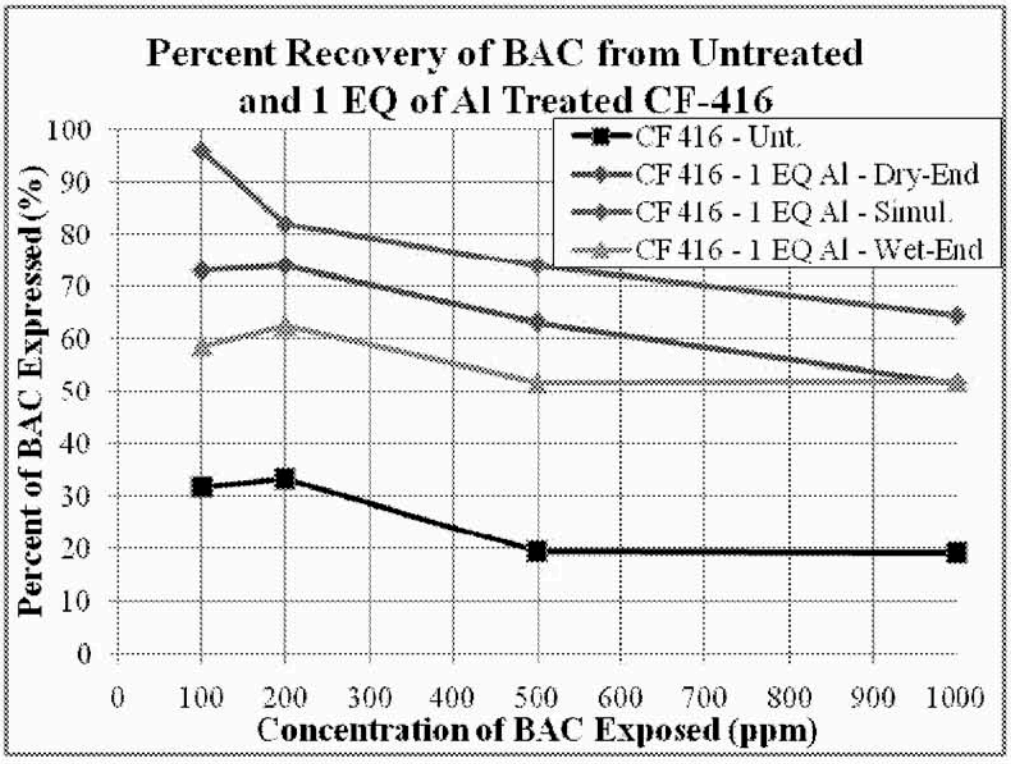
Percent Recovery of BAC from Untreated and 1 EQ of Al Treated CF-416
Percent of BAC Expressed (%)
100
90
80
70
60
50
40
30
20
10
0
0
100
200
300
400
500
600
700
800
900
1000
Concentration of BAC Exposed (ppm)
CF 416 - Unt.
CF 416 - 1 EQ Al - Dry-End
CF 416 - 1 EQ Al - Simul.
CF 416 - 1 EQ Al - Wet-End

Figure 4.

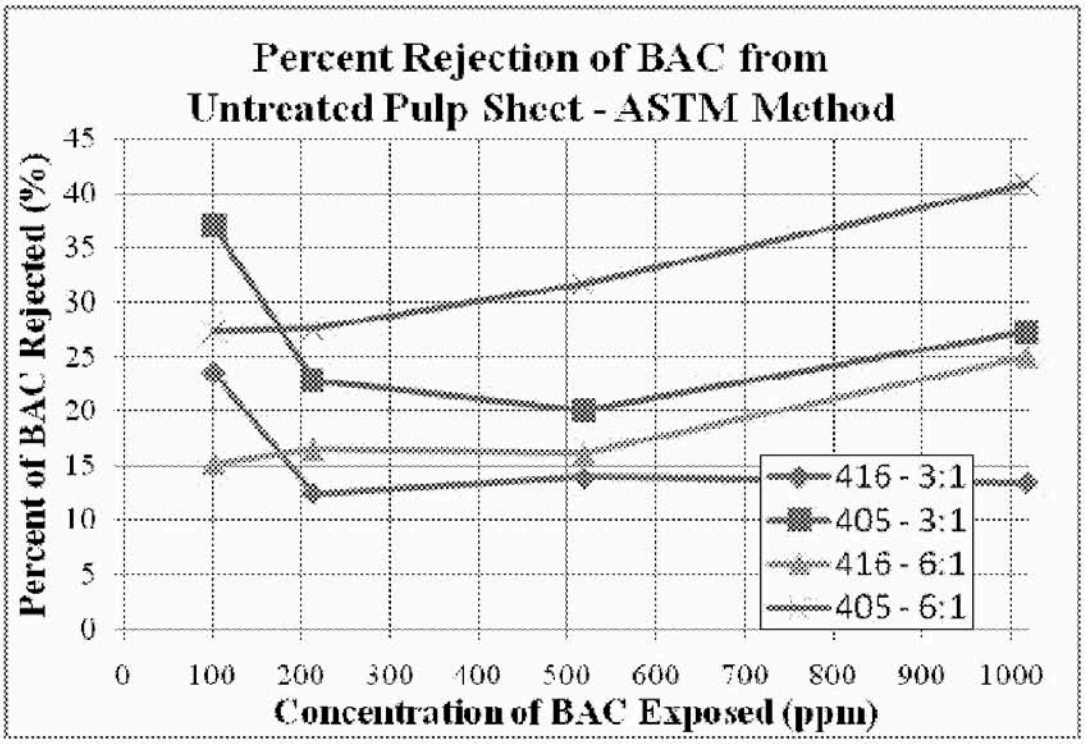

Figure 5.

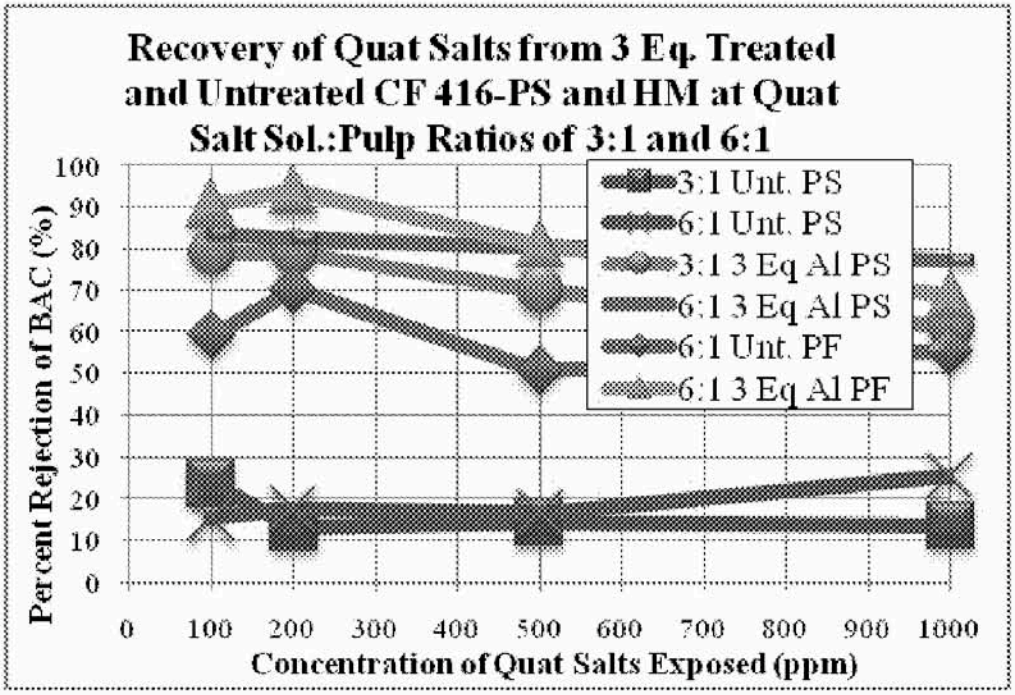

Figure 6.

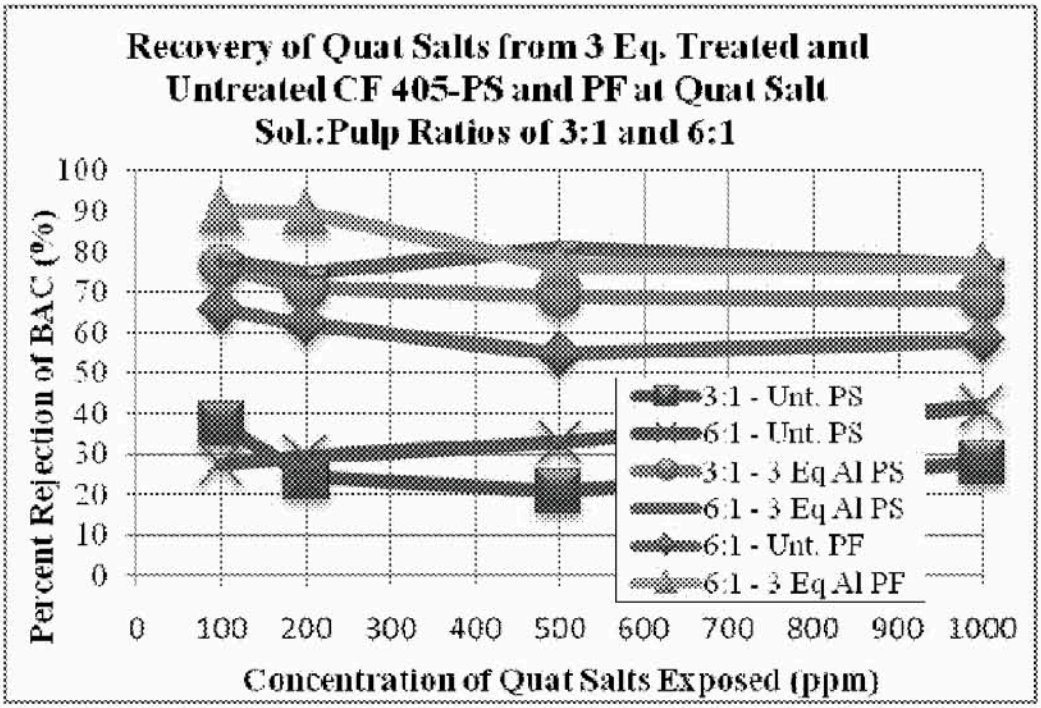

Figure 7.

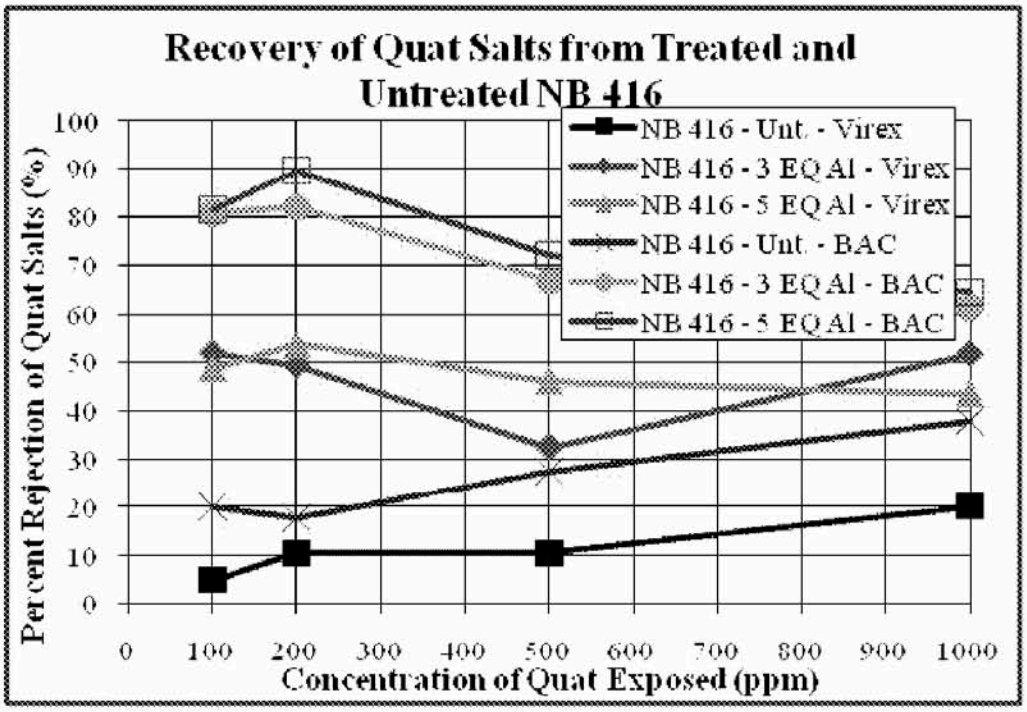

Figure 8.

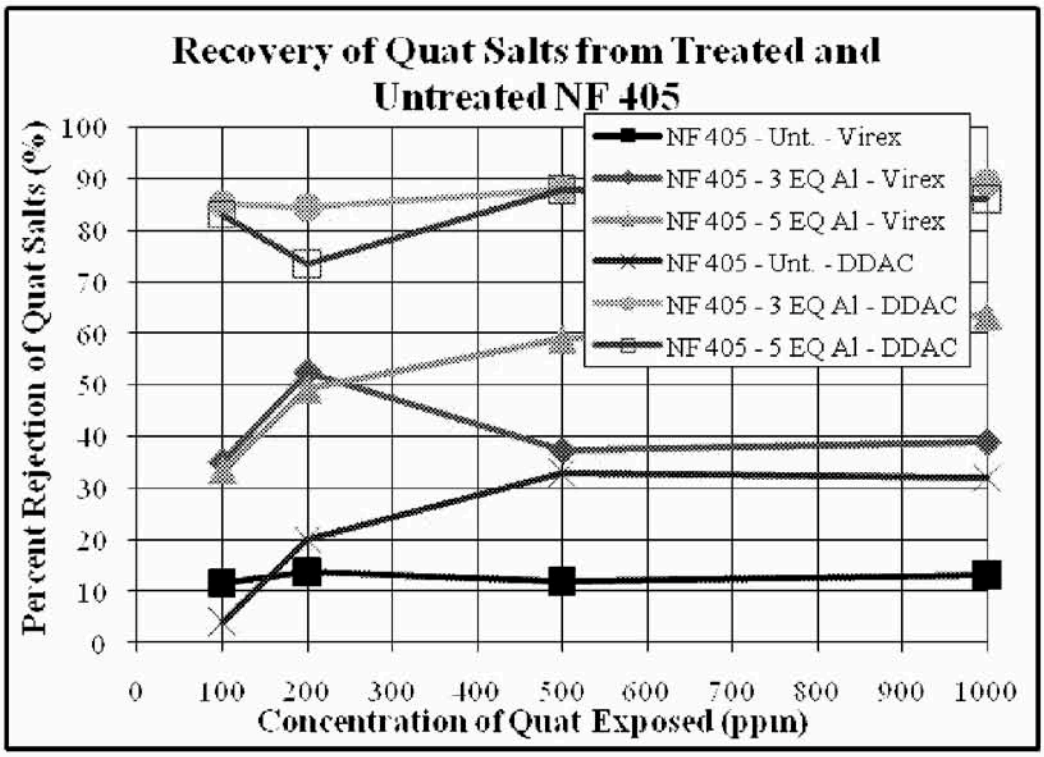
Recovery of Quat Salts from Treated and Untreated NF 405
Percent Rejection of Quat Salts (%)
100
90
80
70
60
50
40
30
20
10
0
0
100
200
300
400
500
600
700
800
900
1000
Concentration of Quat Exposed (ppm)
NF 405 - Unt. - Virex
NF 405 - 3 EQ Al - Virex
NF 405 - 5 EQ Al - Virex
NF 405 - Unt. - DDAC
NF 405 - 3 EQ Al - DDAC
NF 405 - 5 EQ Al - DDAC

Figure 9.

5.2 – Description

[0001] The field of the invention is quaternary ammonium slats used with cellulosic fibers. An embodiment is an antimicrobial wipe.

[0002] Disposable antimicrobial wipes are an article of commerce that is made by saturating a non-woven substrate with a solution containing one or more quaternary ammonium salts. The non-woven substrate contains cellulosic fibers and possibly one or more synthetic fibers, such as polypropylene fibers, in a blen. Cellulosic fibers contain both cellulose and hemicelluloses. Wood pulp fibers are one example of cellulosic fibers.

[0003] In the United States, the compounds and the amounts of active ingredient present in an antimicrobial wipe solution is specified in EPA docket numbers: EPA-HQ-OPP-2006-0339 and EPA-HQ-OPP-2006-0338 and 21 Code of Federal Regulations §178.1010(b) and (c). The FDA regulation applies to "food-processing equipment and utensils, and on other food-contact articles as specified", whereas the EPA regulations covers most of the other uses, primarily sanitation wipes for use with hard surfaces. §178.1010(b) specifies the compounds which can be used and §178.1010(c) specifies the amounts of the active ingredients in the solution in "at least" amounts and "not to exceed" amounts, whereas the EPA regulations specify the maximum quaternary ammonium salt concentrations.

[0004] Broadly, the quaternary ammonium salts listed are (1) n-alkyl benzyl dimethyl ammonium chlorides; (2) di-n-alkyl dimethyl ammonium chlorides; and (3) n-alkyl dimethyl ethylbenzyl ammonium chlorides.

[0005] Another name for n-alkyl benzyl dimethyl ammonium chloride is benzyl-alkyl-dimethyl ammonium chloride. It is also known as BAC or ABDAC. BAC alkyl chains may be of any length. BAC alkyl chains may range, typically, from 8 to 18 carbons in length. Other typical BAC alkyl chain lengths are 12 to 16 carbons in length and 8 and 10 carbons in length. Alkyl dimethyl ethylbenzyl ammonium chlorides, also known as ADEBAC, are grouped with BAC in the aforementioned EPA regulations, but are kept separate in the FDA code. ADEBAC have alkyl chains of any length, but principally of 12 or 14 carbons. The present invention applies to all BAC, including ADEBAC, compounds of any chain length.

[0006] Di-n-alkyl dimethyl ammonium chloride compounds are also known as dialkyl-dimethyl ammonium chloride compounds. They are also called DDAC. DDAC alkyl chains may be of any length. DDAC molecules may have, for example, alkyl chains in the range of 8 to 16 carbons in length. DDAC typically have alkyl chains in the range of 8 to 10 carbons in length.

[0007] The structures of these quaternary ammonium salts are shown in FIGS. 1 and 2. FIG. 1 shows the structure of BAC and FIG. 2 shows the structure of DDAC.

[0008] Quaternary ammonium salts, also known as "quat salts", are used as (1) single quaternary ammonium salt molecule, (2) a single type of quaternary ammonium salt though with a range of alkyl chains present, or (3) used in combination with other

types of quaternary ammonium salts. Often all of these quaternary ammonium salt preparations are used in combination with other compounds, such as ethyl alcohol or isopropyl alcohol.

[0009] The effective amounts of quaternary ammonium salts in solution are also specified in the FDA Code, while the EPA regulations specify maximum concentrations. The amount is dependent on the specific quaternary ammonium salt. Some of the amounts are at least 150 ppm, a level of 150 ppm, not less than 150 ppm, 200 parts per million (ppm), not more than 200 ppm, or not more than 400 ppm. In some instances the "at least" and "not more than" amounts are listed for the same quat salt solution. In the EPA regulations for "wiping," the maximum concentrations are 2400 ppm for DDAC and for 3000 ppm BAC, including ADEBAC.

[0010] Although BAC, ADEBAC, and DDAC are discussed in detail in this application, the chemistry, and this application, applies to all quaternary ammonium salts when used with cellulosic fibers.

[0011] In order for wipes to have effective antimicrobial action, a sufficient concentration of quaternary ammonium salts must be present in the solution squeezed from the wipes during their use. In practice, a high percentage of quaternary ammonium salts are adsorbed onto the cellulosic fibers of the substrates, which may be non-woven, and the quaternary ammonium salts are, thus, unavailable to provide antimicrobial action to the surface being disinfected. It is, therefore, necessary for the manufacturers of disinfectant wipes to compensate for this by using a more concentrated solution of quaternary ammonium salts than is theoretically necessary to provide sufficient

antimicrobial action. This requirement adds considerable expense to the cost of the wipes. In some instances, the FDA Code specifies the maximum amount present in the solution so there is a need to provide a concentration in the solution that is effective, but not greater than specified by the Code.

[0012] This illustrates that a large amount of quaternary ammonium salt is required to obtain a sufficient amount of quaternary ammonium salt in solution. This raises the cost of the product because of the large amount of unusable quaternary ammonium salt which must be included in the product in order to obtain a usable amount of quaternary ammonium salt.

[0013] The inventors hypothesized that one possible reason for adsorption of the quaternary ammonium salts is the possibility of an electrostatic attraction between the cellulosic fiber and the quaternary ammonium salt. They reasoned that cellulosic fiber--including most bleached kraft softwood pulps, and other wood pulps--will contain acid groups, particularly carboxylic acid groups, which under neutral and alkaline conditions, will carry a single negative charge. These negative charges would have an inherent electrostatic attraction to positive charges or cations, including quaternary ammonium salts which are cations.

[0014] The inventors' hypothesis is these acid groups on the cellulosic fiber are electrostatically attracting the quaternary ammonium salts present in the solutions and the quaternary ammonium salts are adsorbed onto the cellulosic fiber through a process of ionic bonding. Those quaternary ammonium salts that are adsorbed onto the

cellulosic fiber are, therefore, not capable of being present in solutions expressed from the wipes during use. Only those salts that remain in solution are available for use.

[0015] The inventors reasoned that there was a Donnan equilibrium between the amount of quaternary ammonium salts present in solution and the amount of quaternary ammonium salts absorbed onto the cellulosic fiber. There is never a complete 100% adsorption of quaternary ammonium salts onto cellulosic fiber. For example, three-quarters of the quaternary ammonium salt may be absorbed on the cellulosic fiber and one-quarter may remain in solution. This means that in this situation if the initial concentration of quaternary ammonium salt solution exposed to the cellulosic fiber is 1000 ppm then about 250 ppm quaternary ammonium salt will remain in solution and 750 ppm quaternary ammonium salt will be absorbed onto the cellulosic fiber.

[0016] It would be advantageous to provide a means for blocking the adsorption of the quaternary ammonium salts onto the cellulosic fibers.

BRIEF DESCRIPTION OF THE DRAWINGS

[0017] FIGS. 1 and 2 are diagrams of quaternary ammonium salts.

[0018] FIGS. 3-9 are graphs showing the percentage of quaternary ammonium salts rejected by cellulosic fiber under different conditions.

[0019] This invention describes compositions that significantly inhibit the adsorption of quaternary ammonium salts onto cellulosic fibers so that a greater

percentage of the quaternary ammonium salts remain in the solution and are available for their use in sanitation. This invention will, therefore, reduce the amount of quaternary ammonium salts that must be added and, thereby, lower the overall cost of any antimicrobial wipe containing both quaternary ammonium salts and cellulosic fibers.

[0020] The present invention proposes to add a small amount of metal cations in the form of dissolved metal salts, from a single or multiple metals, to the solution to prevent adsorption of quaternary ammonium salts by the cellulosic fibers. We have found that the cellulosic fiber acid groups have a greater affinity for the metal cations than they do for the quaternary ammonium salts and, thus, metal cations are absorbed by the cellulosic fibers in place of the quaternary ammonium salts. Therefore, less quaternary ammonium salts are required to be added initially to provide an adequate amount of quaternary ammonium salts in solution, because the equilibrium for the quaternary ammonium salt is now biased toward the quaternary ammonium salt being in solution because the acid ionic sites on the cellulosic fiber are now occupied by the metal cations the quaternary ammonium salts are blocked from these sites.

[0021] It is believed that the metal cations in the composition of the invention compete with the quaternary ammonium salts for the anionic sites, typically carboxylic acid groups, which are present on the surface of the wood pulp fibers and, thereby, inhibit the quaternary ammonium ions from adsorbing onto the fibers.

[0022] This blocking of quaternary ammonium salt adsorption can be further biased by providing more metal cations than quaternary ammonium salts. This blocking of

quaternary ammonium salt adsorption can also be biased by providing more metal cations than there are acid groups on the cellulosic fibers. For example, there are an estimated 3 to 5 meq (millimolar equivalents) of acid groups per 100 grams of bleached Southern Pine Kraft pulp, but other wood pulps may easily have tens of meqs of acid groups per 100 g of pulp. Unbleached pulps would have a higher number. The amount of metal salt can be in the range of 0.0001 to 0.03 moles of metal salt per 100 grams of cellulosic fibers, on an oven dry basis. In another embodiment the amount of metal salt can be in the range of 0.001 to 0.02 moles of metal salt per 100 grams of cellulosic fibers, on an oven dry basis.

[0023] The metal salt should be dissolvable in the solution. Metal cations that tend to be the most solvable are from the salts of alkali and alkali earth metals, but may also include, but not limited to, aluminum, manganese, and iron. Other metals are copper, chromium, nickel, cobalt, zinc, vanadium, tin. This could also be stated as alkali metals, alkali earth metals, first row (period 4) transition metals, tin and aluminum. Typically the most soluble metal salts are halides or sulfates. Other examples of soluble metal salts are acetates, hydroxides, phosphates, sulfites, and nitrates. This list is not inclusive.

[0024] The metal salts can be added before, during or after the addition of the quaternary ammonium salt without affecting their efficacy. The metal cations will prevent or reduce the adsorption of quaternary ammonium salt at the acid sites on the cellulosic fibers and can replace the quaternary ammonium salt if added afterwards.

[0025] The amounts of metal salts added to the compositions can be expressed in equivalents of charge. The equivalents of charge is the ratio of the moles of positive

charges in the metal salt to the moles of negative charges on the pulp fibers. For example, pulp fibers having a carboxylic acid content of 4 meq/100 g has 4 millimoles of negative charges per 100 grams of pulp fibers, based on oven-dried weight. It is worth noting that carboxylic acids are monoprotic acids, meaning they have a single negative charge when deprotonated, which is the case in all neutral or alkaline solutions. If 2 millimoles metal salt having an oxidation state of 2, which produces a +2 charged metal ion when dissolved, was added to 100 grams of pulp, there would be 4 millimoles of positive charges per 100 g. In other words, 2 millimoles/100 g of a +2 metal ion is 1 equivalent to the charge on a pulp fiber having a carboxylic acid content of 4 meq/100 g. The carboxylic acid content of the wood pulps used in the following examples was measured by TAPPI Method--T237 cm-08.

[0026] The cellulosic fiber can be wood pulp fiber. Cellulosic wood pulp can be a hardwood or softwood. Cellulosic wood pulp can be treated with a debonder. Debonders are surface active chemicals that are added prior to, or during the forming and drying operation of the cellulosic wood pulp manufacturing process. The purpose of debonders is to reduce the amount of fiber-fiber bonding that takes place during drying. Examples of debonding agents are Evonik Arosurf™ PA 777, Hercules ProSoft™ TQ 3190, Nalco DVP4V009, Eka Soft™ F509 HA, F587 and F639. Cellulosic wood pulp can be treated with other debonders as well.

[0027] Cellulosic wood pulp can be treated with one or more cationic polymers. Examples of cationic polymers are cationic starch and polydiallyldimethylammonium chloride (poly DADMAC). The cellulosic wood pulp can be treated with other cationic

polymers as well. The cellulosic wood pulp can be treated with clay. The cationic polymers, debonders, and clay have a small effect on blocking the absorption of quaternary ammonium salts by cellulosic fibers, as they all have positively charged elements within them.

[0028] In one embodiment, the invention provides a composition for antimicrobial wipes that significantly increases the proportion of the quaternary ammonium compounds that are not adsorbed onto the substrate, when the solution is squeezed out of the wipes. In its simplest form, the composition of the invention contains water, cellulosic fibers, one or more quaternary ammonium salts, and a soluble metal salt, such as aluminum sulfate. The cellulosic fibers can be wood pulp fibers.

[0029] In one embodiment of the invention the composition contain a 3 to 1 or 6 to 1 weight/weight (w/w) ratio of water to cellulosic fibers which are in sheet form either by themselves or in a blend with synthetic fibers. In one embodiment of the invention the concentration of the quaternary ammonium compounds in the solution is between 100 and 1000 ppm (weight basis). The quaternary ammonium salts explored were benzylalkyldimethyl ammonium chloride (BAC), dialkyldimethyl ammonium chloride (DDAC), or a commercial quaternary ammonium salt disinfectant. The commercial product was Virex, an antimicrobial cleaner manufactured by Johnson Wax. It contains an about a 1:1 mixture of BAC and DDAC, as well as other proprietary ingredients.

[0030] In one embodiment the soluble metal salt is aluminum sulfate, $Al_2(SO_4)_3$. In one embodiment the weight to weight (w/w) range of metal salt to cellulosic fiber can be 0.0001 to 0.03. In another embodiment the w/w range of metal salt to cellulosic fiber

was between 0.0023 and 0.011. Aluminum sulfate can be effective in reducing the percentage of quaternary ammonium salts that are absorbed to the substrate greater than these w/w ranges. Higher levels of aluminum sulfate would also be effective with the only restriction being to the solubility limits of the aluminum sulfate. However, high levels of aluminum salts, or in other embodiments other metal salts, may cause discoloration or other problems, including texture, in the wipes.

[0031] In one embodiment, a soluble metal salt solution is applied to the wood pulp fibers prior to the manufacture of the disposable wipes. However, it is equally effective to add the soluble metal salt directly to the solution containing the quaternary ammonium salts in a solution added to the wipe substrates at the end of the manufacturing process. It is important that a sufficient quantity of soluble aluminum, and/or other soluble metal cation(s), be present in the antimicrobial composition containing pulp fibers and quaternary ammonium salts.

[0032] In a wipe the cellulosic fiber can range from 10 to 100% of the weight of the wipe substrate, the fibrous material in the wipe. The cellulosic fiber can be a wood pulp fiber. The weight of the quaternary ammonium salt solution typically used for this invention can be from 2 to 10 times the weight of the dry substrate. The solution is water and quaternary ammonium salt. The quat salt, or mixture of quat salts, concentration in the wipe saturant can be 100 to 3000 parts per million (weight basis). The amount of metal salts or mixture of metal salts can be from 0.0001 to 0.03 moles per 100 grams of wood pulp fiber, measured on an oven-dried basis. The ratio of metal ion charge equivalents to wood pulp fiber charge equivalents is 0.1 to 45.

[0033] The addition of metal cations, from dissolved metal salts, to compositions containing quaternary ammonium salt and wood pulp fibers significantly reduces the amount of quaternary ammonium salt adsorbed onto the pulp fibers compared to compositions containing only wood pulp fibers and quaternary ammonium salts alone. A range of metal salts and metal salt concentrations have proved to be effective. The metal salts may be, for example, calcium chloride, magnesium chloride and aluminum sulfate. In one embodiment, the range of metal salt concentrations may be from 0.001 moles of metal salt per 100 grams of wood pulp fiber, based on oven-dried weight, to 0.02 moles of metal salt per 100 grams of pulp fiber, based on oven-dried weight. The effective range of metal ion could be as low as 0.0001 moles of applied metal ions per 100 grams of wood pulp fiber, based on oven-dried weight. Although the upper range of metal salt addition is only restricted by the solubility of the metal salt chosen and other considerations, such as, discoloration, softness or health issues, the reasonable upper limit could be 0.03 moles of metal salt per 100 grams of oven dry wood pulp fiber.

[0034] The metal salts can be added to the composition in several different ways without affecting their efficacy in preventing the adsorption of quaternary ammonium salts. The metal salts may be added, but are not limited to, at a point during the wet-laid sheet forming process during pulp fiber manufacturing, or after the wood pulp fibers have been dried in sheet form via spray or shower addition, or added directly to a mixture containing the wood pulp fibers and quaternary ammonium salts.

[0035] The wood pulp fibers in the mixture containing fibers, quaternary ammonium salts and metal cations can be in sheet form. Pulp sheets have basis weights of 250 to 900 g/m^2. The density of a wipe is 0.05 to 0.6 grams per cubic centimeter.

[0036] In the following examples the terms such as "percent BAC rejected" and "percent quaternary ammonium salt rejected" refer to the percentage of quaternary ammonium salts, either a specific variety, such as BAC, or a combined DDAC and BAC solution referred to as "quaternary ammonium salts", that are added to the compositions that are not adsorbed on the wood pulp fibers when liquid is squeezed out of the mixture containing pulp fibers, dissolved quaternary ammonium salts and dissolved metal ions. For example, if pulp fibers in sheet form are exposed to a solution containing 1000 ppm of a quaternary ammonium salt, and the concentration of the quaternary ammonium salt in the solution that has been squeezed out of the mixture is 250 ppm, then the percent quaternary ammonium salt rejection is said to be 25%. That is, 25% percent of the quaternary ammonium salt has not been adsorbed onto the fibers. Another way of expressing it is that 25% of the applied quaternary ammonium salts are in solution and, therefore, available for use as disinfectants.

EXAMPLE 1

The Effect of Various Metal Ions on Quaternary Ammonium Salt Rejection Efficiency

[0037] In Example 1, various metal salts were added to CF416 wood pulp in a manner meant to mimic wet-end addition on a paper machine. CF416 is a bleached southern pine kraft wood pulp manufactured by Weyerhaeuser NR in Columbus Miss. The effectiveness of each of 3 metal salts were compared. These were magnesium chloride (magnesium chloride hexahydrate from Sigma Aldrich), calcium chloride (calcium chloride anhydrous from Sigma Aldrich), and aluminum sulfate (aluminum sulfate octadecahydrate from Sigma Aldrich). The CF416 pulp sheet was cut into small pieces and soaked in a solution of the appropriate metal salt. The ratio of salt solution to pulp fiber was 3 to 1, weight to weight. The concentration of salt in solution was adjusted so that the ratio of metal charge to pulp charge was 1 equivalent. This equated to 1904 ppm of anhydrous magnesium chloride, 2220 ppm of anhydrous magnesium chloride and 2281 ppm anhydrous aluminum sulfate. The pulp fibers were allowed to soak in the metal salt solutions between 1 and 2 hours at room temperature in plastic medical syringes (BD medical).

[0038] After the pulp samples had been soaked in the metal salt solutions, the syringes were placed in a caulking gun, and the free liquid was expressed from the samples. This same procedure was then repeated several times, but with distilled water and then the samples were dried. Four quaternary ammonium salt solutions were prepared having the following concentrations; 100 ppm, 200 ppm, 500 ppm and 1000 ppm by dissolving the appropriate weight of BAC (Sigma Aldrich MW 365 g/mole) in deionized water. The quaternary ammonium salt solutions were placed in separate plastic syringes (BD Medical) to which a known quantity of pulp sheet pieces treated

with metal salts in the manner detailed above had been added. The weight to weight (w/w) ratio of the quaternary ammonium salt solution to the dry weight of the pulp was 3:1 in all cases. Thus, for example, one syringe containing calcium chloride treated pulp plus 3 times its weight of 100 ppm BAC solution, while the next syringe contained calcium chloride treated pulp plus 3 times its weight of 200 ppm BAC solution and so on until all combinations of pulp treatments and BAC solution concentrations were prepared.

[0039] The syringes containing quaternary ammonium salt solution plus pulp were allowed to stand for about 1.5 hours at room temperature. At the end of the exposure time each syringe was placed in a calking gun and pressure was applied to the syringe plunger until the free quaternary ammonium salt solution could be collected for analysis. The unadsorbed quaternary ammonium salt concentration was measured by CE as described in Example 5.

[0040] FIG. 3 shows that all three metal salts ($CaCl_2$, $MgCl_2$, and $Al_2(SO_4)_3$) had significant effects upon the percentage of BAC rejected. Thus, in all these cases these metal salts were effective in increasing the amount of quaternary ammonium salt in solution, with aluminum sulfate being the most effective.

EXAMPLE 2

The Effect of Salt Addition Mode on Quaternary Ammonium Salt Rejection

[0041] In Example 2, the method by which the metal is added to composition containing quaternary ammonium salt and pulp fibers was studied. The first series of samples was prepared in the manner described in Example 1. These samples were meant to simulate metal salt addition in the wet-end of the papermaking process (Al--Wet-End in FIG. 4). The second series of samples was prepared by squirting a known amount of metal salt solution onto the pulp sheet with a syringe in parallel streaks, and allowing the sample to air dry without washing. This method was meant to simulate addition of the metal salts at the dry-end pulp sheet making process or during a non-woven manufacturing process (Al--Dry-End in FIG. 4). In these series the treated pulp samples and the quaternary ammonium salt solutions were combined in the same manner described in Example 1.

[0042] In the third series, the metal salt was added directly to the quaternary ammonium salt solutions (Al--Simult. in FIG. 4). The quaternary ammonium salt/metal salt combined solutions were added to untreated pulp pieces in syringes as described in Example 1. In all 3 sample series, 1 equivalent of charge of aluminum sulfate was used. The concentration of rejected quaternary ammonium salt was measured by potentiometric titration as described in ASTM D 5806-95.

[0043] FIG. 4 compares the percent BAC rejection levels for 3 series described above with a control without metal salt addition (Unt. in FIG. 4). These results demonstrate that all 3 methods of metal salt addition were effective in reducing the amount of quaternary ammonium salt that was adsorbed onto the pulp fibers.

EXAMPLE 3

Singulated Fiber vs. Sheet Form Comparison

[0044] In the preceding experiment the wood pulp fibers were in a wet-laid sheet form when they were exposed to the solutions containing quaternary ammonium salts. In this example, compositions in which the fibers were in sheet form were compared with compositions where the fibers were in singulated fluff form. The singulated fibers had a much greater absorbency for aqueous solutions, including the quaternary ammonium salt solution used, than the fibers in sheet form. Therefore, it was necessary to increase the liquid to fiber ratio in order assure all of the fibers would be wetted. A 6:1 liquid to fiber ratio was found to be adequate in wetting the singulated fiber samples.

[0045] In order to understand the effect of the liquid to fiber ratio separate from the effect of singulated fiber vs. sheet form, a comparison was done with pulp sheet samples at both 3:1 and 6:1 liquid to fiber ratios. The wood pulp fibers used for these experiments were CF405 and CF416. Both are bleached kraft southern pine pulps manufactured by Weyerhaeuser NR Co at Columbus Miss. CF405 contains a debonder to make the wet-laid pulp sheet softer and easier to defibrate, while CF416 does not contain a debonder. The aluminum sulfate solutions were applied to dry pulp sheets with a syringe, as described in Example 2. The aluminum sulfate treated pulp sheet samples were exposed to quaternary ammonium salt solutions as described in Example

1. The percentage of quaternary ammonium salts present in the expressed solution were measured by ASTM method D 5806-95 using potentiometric titration.

[0046] The results in FIG. 5 indicate that a higher percentage of the quaternary ammonium salts are rejected when the liquid to fiber level was increased from 3:1 to 6:1 due to an increased ratio of total quaternary ammonium salt molecules to carboxylic acid groups on the fiber. There is a spike in the rejection numbers at low concentrations of quaternary ammonium salt in the case of the 3:1 samples (and are likely related to insufficient wetting issues), but not in the case of the 6:1 samples.

[0047] Next, CF416 and CF405 pulp sheets were treated with 3 charge equivalents of aluminum sulfate with a syringe as described in Example 2. Part of the aluminum treated 405 and 416 materials were then fiberized in a Kamas laboratory hammermill to yield a singulated fiber fluff. Also untreated pulp sheets were similarly fiberized as controls. The untreated fluff, untreated pulp sheet, aluminum treated fluff, and the aluminum treated sheet samples were exposed to quaternary ammonium salt solutions as described in Example 1 except that a 6:1 liquid to fiber ratio was used for the fluff samples and half of the aluminum treated sheet samples. The other half of the aluminum treated sheet samples were exposed to 3:1 ratio of the quaternary ammonium salt solutions. The concentration of the rejected quaternary ammonium in the expressed solutions was measured by ASTM method D 5806-95.

[0048] The results are summarized in FIGS. 6 and 7 for CF416 and CF405, respectively. In these figures, PS is used to designate the pulp sheet samples and PF the

pulp fluff samples. Clearly, as shown before, the addition of aluminum sulfate significantly improved the percentage of BAC rejected by the pulp fibers.

[0049] These results also showed that the untreated fluff samples gave higher rejection levels than the untreated sheet samples. This was attributed to the difficulty in fully wetting the pulp fluff with the quaternary ammonium salt solution as well as the difficulty of flow through essentially a plug of pulp fluff that exists in the syringe during the experiment. This would hypothetically result in quaternary ammonium salt depleted regions, not due to interaction with carboxylic acid group in the pulp, but due to very slow diffusion these regions would not be equilibrated with portions of the solution that had not come into contact with the pulp carboxylic acid groups and were thus not depleted of quaternary ammonium salts.

EXAMPLE 4

Comparison of Results With Different Quaternary Ammonium Salt and Different Aluminum Salt Treatment Levels

[0050] In this example, the percent quaternary ammonium salt rejection was tested using BAC, DDAC, and Virex. Virex is a commercially available antimicrobial solution made by Johnson Wax. According to the MSDS, it contains about a 1:1 mixture of BAC and DDAC, as well as other ingredients. Aluminum sulfate treated wood pulp samples were produced from NB416 and NF405, which are southern pine bleached kraft wood

pulps manufactured by Weyerhaeuser NR in New Bern N.C. NF405 contains a debonder, whereas NB416 does not contain a debonder. A commercial solution of aluminum sulfate (26.8% (wt.) $Al_2(SO_4)_3$) was sprayed onto the pulp sheet as the sheet was being rewound from one spool to another. The amounts deposited upon the pulp sheet were calculated as being 3 and 5 charge equivalents of Al^{3+}. These amounts were calculated by knowing both the pump rate of aluminum sulfate solution at a certain RPM of the pump as well as the sheet velocity. This is a good candidate for how this invention would be implemented in an industrial setting.

[0051] Aluminum sulfate pulp sheet samples prepared in the above manner as well as untreated pulp sheet samples were exposed to quaternary ammonium salt solutions as described in Example 1. The concentration of rejected quaternary ammonium salts in the expressed solutions was measured by ASTM method D 5806-95. In this case, one series of experiments was performed with BAC, another was performed with DDAC and another was performed with Virex. The results are compared in FIGS. 8 and 9 for NB416 and NF405.

[0052] In FIG. 8, the rejection levels of Virex and BAC were compared for compositions containing a quaternary ammonium salt solution and either untreated NB416, or NB416 treated with either 3 or 5 charge equivalents of aluminum. The untreated NB416 compositions rejected about 18 to 38% of the BAC and 5 to 20% of the Virex. The aluminum sulfate treated NB416 compositions rejected 60-90% of the BAC and 32 to 55% of the Virex. The NB416 treated with 5 charge equivalents of

aluminum sulfate provided slightly better performance than the samples treated with 3 charge equivalents.

[0053] In FIG. 9, the rejection levels of Virex and DDAC were compared for composition containing a quaternary ammonium salt solution and either untreated NF405 or NF405 treated with either 3 or 5 charge equivalents of aluminum. The untreated NF405 compositions rejected about 5-33% of the DDAC and 10-14% of the Virex. The aluminum sulfate treated samples rejected about 75-90% of the DDAC and 30-65% of the Virex. Again the samples with the samples with 5 charge equivalents of aluminum tended to perform better than the samples with 3 charge equivalents of aluminum.

[0054] Overall, the results show that the compositions containing aluminum cations rejected quaternary ammonium salts much better than the compositions without aluminum cations. In both the circumstances with and without aluminum cations a higher proportion of the pure quaternary ammonium salts (BAC and DDAC) were rejected than observed with quaternary ammonium salts from Virex.

EXAMPLE 6

CE Test Method For Analyzing Quaternary ammonium Salts in Solution

[0055] 1. Scope

[0056] This method is applicable to the determination of alkylbenzyldimethyl ammonium chlorides in reagent water and to aqueous client matrices after recovery confirmation via sample spiking. Alkyl groups ranging from n-$C_{12}H_{25}$ to n-$C_{16}H_{33}$ have been shown in the literature to be separated by this method. The present application is limited to n-$C_{12}H_{25}$ and n-$C_{14}H_{29}$ alkyl substituents as these are the ones present in BAC. It is based on the work of Ya-Hui, et al. adapted for the Agilent G1600A Capillary Electrophoresis System.

Analyte	Range (μg/mL)
C12-BAC	1.0-30
C14-BAC	1.0-30

[0057] 2.0 Summary of Method

[0058] In capillary electrophoresis, solutes are separated in an electrolyte-filled fused silica capillary due to differences in their electrophoretic mobilities. Useful features of CE include: the ability to determine anions, cations, and neutral species using the various modes of separation, short analysis times, high efficiency separations, selective or universal detection modes (using a photodiode array detector), the ability to analysis complex matrices with little sample preparation, and the use of simple commercially-available buffers and inexpensive capillary columns. The Agilent CE system has an autosampler carousel which provides for unattended operation. Each

analytical method provides a recommended technique for dilution, and occasionally, derivatization of the samples to be analyzed. Before the prepared sample is introduced into the CE, a procedure for standardization must be followed to determine the recovery and the limits of detection for the analytes of interest. Following sample introduction into the CE, analysis proceeds with a comparison of sample values with standard values. Qualitative identification is by means of migration time (MT) and quantitative analysis is achieved through integration of peak area which is normalized by migration time.

[0059] The present application uses a simple phosphate buffer modified with acetonitrile. This modification disrupts BAC micelle formation and adsorption of BAC to the capillary wall. For this method, the buffer is 40 mM sodium phosphate (pH 4.0) in 40% acetonitrile. At pH 4.0, the BAC is protonated and migrates toward the detector where they are detected by direct absorbance at 200 nm. Caution is warranted regarding BAC levels higher than 50 μg/mL. Preliminary work using higher concentrations fouled the capillary to the point of no migration being seen within a reasonable time. Replacing the capillary column was required.

[0060] 3.0 Interferences

[0061] 3.1 No interferences were noted. The samples are prepared at a dilution of at least 20 to 1, due to expected levels being higher than the calibrated range. The initial samples are likely to be sufficiently clean as to not present an interfering matrix.

[0062] 3.2 Fresh buffer and column conditions typically provide a stable baseline near the analyte migration times. As the buffer is used over the course of a series of

runs, spurious responses will be seen both early and late in the separation. As the baseline stabilizes and migration times don't shift, this is generally of little concern. Initial analyses indicate buffer stability for up to 13 runs. After buffer vial replacement, migration times become stable after an initial standard run.

[0063] 3.3 Changes in migration times and resolution are symptoms of buffer deterioration or may be caused by the buildup of contaminants on the inner capillary wall. Refer to the manufacturer's guidelines for instructions on cleaning the column. If the above procedures do not restore the retention times, replace the column.

[0064] 3.4 The presence of air bubbles or particulants in the column may cause baseline fluctuations, low current readings, or peak variability. All samples require filtration to 0.45 μm. Commercial buffer systems are already filtered. The use of degassed water for dilution may help to minimize the introduction of air. Freshly prepared buffer must be degassed ultrasonically during filtration.

[0065] 4.0 Amount of Sample Required

[0066] A sample of 40 mL is preferred. The amount of diluted sample required depends on vial type used. It is recommended that glass vials be used. They require 500 μL. The actual criterion is the sample vials need to be filled to a level 1.4 cm from the base. This is a requirement of the CE injection system. Always using the same vial volume supports injection reproducibility. Samples have required two dilutions: a 1 to 25 dilution for BAC when it is known present; and a 1 to 5 dilution for a good detection limit for others. Hence, the actual minimum volume requirement has been determined by filtration needs and is likely to be on the order of 1 mL.

[0067] 5.0 Sampling, Sample Handling, and Preservation

[0068] Samples have been stored in plastic bottles without apparent deleterious effect. The sample should be stored at 4° C. (39° F.) and returned to the lab for analysis as soon as possible. There is no known holding time for BAC solutions. Commercially available aqueous solutions are stable at a 50% concentration when refrigerated. Material Safety Data Sheets for various BAC mixtures also state these are stable compounds.

[0069] 6.0 Equipment Required

[0070] 6.1 Capillary Electrophoresis System

[0071] The Agilent G1600A Capillary Electrophoresis System contains in one cabinent an autosampling carosel, a thermostatted capillary column cassette, A Diode Array Detector (DAD) operating in the UV-Visible range, an integral high voltage power supply capable of both positive and negative inlet electrode voltages, and a buffer solution replenishment system (if needed). The ChemStation data acquisition and analysis system is supported by a PC running Windows XP Professional SP 2.

[0072] 6.2 Capillary Column

[0073] The capillary column used for this application is the Agilent P/N G1600-61232. It is a bare fused silica capillary with a 50 μm internal diameter, a length of 56 cm, and an extended light path bubble cell. The bubble cell is an internal bubble blown into the detector region of the column. As it widens the inner channel, it produces an extended path for absorbance detection. An attribute of laminar flow in CE keeps the

analyte zone from mixing in the larger volume and thus maintains the concentration within the zone.

[0074] 6.3 Detector

[0075] The DAD is used with a signal wavelength of 200 nm and bandwith of 20 nm. The reference wavelength is 425 nm (50 nm). The detection method uses the direct scheme in which a UV absorbing analyte creates an absorbance signal. The reference wavelength helps compensate for minor shifts in the buffer background.

[0076] 6.4 Data Acquisition System

[0077] The Agilent G1600A Capillary Electrophoresis System includes a version of ChemStation software configured for use with CE. In one PC environment are combined instrument control, raw data acquisition and reduction, and report generation. All aspects are included in a single method file.

[0078] 6.5 Glassware/Plasticware

[0079] If one is preparing a CE buffer system from individual components, it is generally recommended to use polypropylene volumetric flasks dedicated to each aqueous buffer. This avoids trace contamination from the glass surface which could affect migration time stability and cleanliness of the electropherogram baseline. This method uses an operator-prepared buffer system.

[0080] 6.5.19-mL borosilicate glass culture tube, VWR, 47729-572.

[0081] 6.5.2 14-mL borosilicate glass culture tube, VWR, 47729-576.

[0082] 6.5.3 Polyethylene Cap for 14-mL Tube, Becton Dickinson, Falcon 352030.

[0083] 6.5.4 2-mL (3 mL) Norm-Ject disposable syringe with Luer adapter.

[0084] 6.5.5 GHP Acrodisc 25 mm 0.45 micron syringe filter,

[0085] 6.5.6 2-mL clear (glass) wide opening crimp vial, Agilent 5181-3375.

[0086] 6.5.7 Snap caps, polyurethane for 2-mL vials, Agilent 5181-1512.

[0087] 6.5.8 Microduster III, CleanTex, inert gas for glassware dust purging.

[0088] To avoid particulate contamination, it is a good idea to purge test tubes and vials with a quick burst of inert Microduster III gas just prior to use. Calibration standards and samples are prepared in disposable glass ware. The final dilutions of standards and samples are filtered using disposable filter cartridges and dispensed into disposable glass sample vials. Volumetric pipettes should be used to measure stock solutions. The pipettes may be either fixed or variable volume and preferably those with disposable tips in order to reduce contamination.

[0089] 7.0 Reagents and Materials

[0090] 7.1 Buffer System

[0091] The buffer is based on a 66.7 mM $NaH_2PO_4 \cdot H_2O$ solution adjusted to pH 4.0 using phosphoric acid. It is then mixed with actonitrile to a final concentration of 40 mM.

[0092] 7.1.1 Sodium Phosphate, Monobasic, monohydrate ($NaH_2PO_4 \cdot H_2O$), 100.7%, JTBACer 3818-01/Lot Y10145. Formula weight is 137.99 g/mol. [0093] 7.1.2 Phosphoric acid, 85.2%, JT BACer 0260-05/Lot N08803. Formula weight is 98.0 g/mol.

[0094] 7.1.3 Acetonitrile (ACN), B&J, Biosyn Grade, BB017-4 Lot CM370.

[0095] 7.1.4 Distilled deionized water, use the distilled water available from

SLM 212S-5. It has been demonstrated as clean for CE work. If used immediately as a water blank, it requires filtration.

[0096] To make a buffer stock solution place 1.058 gm $NaH_2PO_4 \cdot H_2O$ in a 100 mL polypropylene volumetric flask and add ca. 90 mL of distilled deionized water. Swirl until dissolved, then carefully dispense into a 100 mL plastic beaker and add a small Teflon-coated stir bar. Use a pH meter calibrated for measurement between pH 4 and 7 to measure the initial pH. It should read about pH 4.3. Take a disposable glass pipet and just wet it with conc. phosphoric acid. A quick dip into the buffer should lower its pH significantly. Less than a drop of acid is required to adjust the pH to 4.0. Use dilute NaOH solution to raise the pH, if needed. Once adjusted, redispense the buffer into the 100 mL volumetric, fill to volume, shake well, then pour into a 4 oz. plastic bottle.

[0097] The run buffer is composed as 40:60 ACN:Phosphate. A convenient volume is composed by placing 2400 µL ACN into a 14 mL tube with 3600 µL pH 4.0 phosphate buffer, capping, then mixing well by inversion. This volume is immediately vacuum filtered through a 0.45 µm filter with ultrasonic degassing for about a minute. Significant degassing is seen initially. This filtered buffer is immediately dispensed into the glass CE sample vials as determined by the method run table. Currently, there is need for 4 buffer vials. Fill them to 1.0 ml and cap them with polyurethane caps.

[0098] 7.2 Standard Solutions

[0099] The stock standard solution is best prepared as needed within the week of its use. The working standard is a dilution which is completely used to make the calibration standards. The calibration standards are prepared in sufficient volume for a

single filtration and use. It may be best to consider these solutions as replaceable after one week. Store the solutions at 4° C in freshly-capped CE sample vials.

[0100] 7.2.1 Benzalkonium Chloride (BAC), 100%, Alpha Easar 41339 (current lot: E22R060). Label states a range only for alkylation, but analysis has demonstrated this is 60% dodecyl (C12) form and 40% is tetradecyl (C14) form. As this is a mixture, there is no single formula weight. The calibration is performed in units of µg/ml.

[0101] 7.2.3 Distilled water, use the distilled water available from SLM 212S-5. It has been demonstrated as clean for CE work. If used immediately as a water blank, it requires filtration.

[0102] Methanol, B&J, Purge and Trap Grade, 232-1 (current lot: CN637).

[0103] 7.2.4 70:30 Methanol:Water. A convenient volume is prepared by adding 3.0 mL of Distilled water to 7.0 mL P&T methanol. This is the CE sample diluent and further protects the BAC from micelle formation.

[0104] The BAC stock standard is prepared 70:30 methanol:water. Place 8.0 mg BAC in a 4 mL screw cap vial and add 4.0 ml using a pipet for a concentration of 2000 µg/mL. A working 500 µg/mL standard is prepared using 250 µl of this stock in 1000 mL total volume of 70:30 MeOH:H_2O. A final volume of 1 mL is likely stable to evaporation for the short period it is needed to make the calibration standards.

[0105] The six calibration standards currently defined in the method are then prepared using aliquots of the 500 µg/mL (or 10 µg/mL) working standard added to separate 9-mL borosilicate glass culture tubes for final dilution to 1000 or 3000 µL in 70:30 MeOH:H_2O according to the following table.

	Standard #					
	#1	#2	#3	#4	#5	#6
Final Conc, µg/mL	1	5	10	15	20	30
Final Volume, µL	1000	1000	3000	1000	1000	1000
Stock Conc, µg/mL	10	10	500	500	500	500
Volume Stock, µL	100	500	60	30	40	60
C12-BAC, µg/mL	0.60	3.0	6.0	9.0	12	18
C14-BAC, µg/mL	0.40	2.0	4.0	6.0	8.0	12

[0106] After all additions have been made, the tube is briefly hand shaken or vortexed then the contents immediately drawn into 3-mL disposable syringe. A 0.45 µm filter is added and 0.5 mL filtered directly into the CE autosampler vial.

[0107] 7.3 Sample Containers

[0108] Samples have been provided for analysis in polyethylene sample bottles with no apparent deleterious effects. The best CE operability has been found using the 2-mL glass vials sealed with the polyurethane snap caps. Proper sealing is essential as the system uses pressure for sample injection and monitors system pressure for failure.

[0109] While the preferred embodiment of the invention has been illustrated and described, it will be appreciated that various changes can be made therein without departing from the spirit and scope of the invention.

5.3 – Claims

1. A product comprising cellulosic fiber in sheet form, 0.0001 to 0.03 moles of one or more water soluble metal salts per 100 grams of cellulosic fiber, on the basis of oven-dried weight of cellulosic fiber, water and a quantity of quaternary ammonium salts to provide 100 to 3000 ppm of quaternary ammonium salts in solution.

2. The product of claim 1 wherein the metal salts are present in an amount of 0.001 to 0.02 moles of metal salts used per 100 grams of cellulosic fiber, on the basis of oven-dried weight of the cellulosic fiber.

3. The product of claim 1 wherein the metal salts are present in the amount of 0.0001 to 0.03 moles of each metal salt per 100 grams of cellulosic fiber, on the basis of oven-dried weight of cellulosic fiber.

4. The product of claim 1 wherein the metal salts are present in the amount of 0.001 to 0.02 moles of each metal salt per 100 grams of cellulosic fiber, on the basis of oven-dried weight of cellulosic fiber.

5. The product of claim 1 wherein the metal salts are selected from water soluble salts of alkali metals, alkali earth metals, first row (period 4) transition metals, aluminum, or tin.

6. The product of claim 1 wherein the quaternary ammonium salts are selected from n-alkyl benzyl dimethyl ammonium chlorides; di-n-alkyl dimethyl ammonium chlorides; and n-alkyl dimethyl ethylbenzyl ammonium chlorides.

7. The product of claim 1 wherein the cellulosic fibers are wood pulp fibers.

8. The product of claim 6 wherein the wood pulp fibers include a debonder, cationic polymer, clay, or a mixture thereof.

9. The product of claim 1 further comprising synthetic fibers.

10. The method of making a cellulosic product comprising combining cellulosic fiber, 0.0001 to 0.03 moles of one or more water soluble metal salts per 100 grams of cellulosic fiber, on the basis of oven-dried weight of the cellulosic fiber, water and one or more quaternary ammonium salts, the quaternary ammonium salts being present in an amount to provide 100 to 3000 ppm of quaternary ammonium salts in solution.

11. The method of claim 10 wherein the cellulosic fiber and metal salts are combined prior to combining with quaternary ammonium salts.

12. The method of claim 10 wherein the cellulosic fiber, the metal salts and the quaternary ammonium salts are combined at the same time.

13. The method of claim 10 wherein the quaternary ammonium salts and metal salts are combined first and the mixture is combined with the cellulosic fiber.

14. The method of claim 10 wherein the cellulosic fiber is in the form of a sheet.

15. The method of claim 10 wherein the metal salts are present in an amount of 0.0001 to 0.03 moles of each metal salt used per 100 grams of cellulose fiber, based on oven-dried weight of the cellulose fiber.

16. The method of claim 15 wherein the metal salts are present in an amount of 0.001 to 0.02 moles of each metal salt used per 100 grams of cellulosic fiber, based on oven-dried weight of the cellulosic fiber.

17. The method of claim 10 wherein the metal salts are selected from water soluble salts of alkali metals, alkali earth metals, first row (period 4) transition metals, aluminum or tin.

18. The method of claim 10 wherein the quaternary ammonium salts are selected from n-alkyl benzyl dimethyl ammonium chlorides; di-n-alkyl dimethyl ammonium chlorides; and n-alkyl dimethyl ethylbenzyl ammonium chlorides.

19. The method of claim 10 wherein the cellulosic fibers are wood pulp fibers.

20. The method of claim 19 wherein the wood pulp fibers include a debonder, cationic polymer, clay or a mixture thereof.

* * * * *

Chapter 6: Conclusions and Future Directions

6.1 Conclusions

Conjugated polymer semiconductors capable of ambipolar (both n-type and p-type) charge transport are of great interest for application in photovoltaic cells and ambipolar thin film transistors. Towards the achievement of all-polymer ambipolar field-effect transistors, we investigated two classes of polymer semiconductor systems: (i) conjugated donor–acceptor copolymers; and (ii) p-type/n-type polymer/polymer heterojunctions. Conjugated polymer semiconductors with donor–acceptor architectures by virtue of intramolecular charge transfer between the donor and acceptor moieties can have electronic structures that facilitate conduction of both holes and electrons. Few examples of ambipolar organic field-effect transistors, but one that has been studied extensively is the use of heterojunctions of conjugated organic small molecules of p- and n-type materials. Previously, no one had attempted this method with polymer systems, but we have achieved ambipolar charge transport in FETs fabricated from bilayer heterojunctions of p- and n-type polymers: poly(3-hexylthiophene) (P3HT)/poly (benzobisimidazobenzophenanthroline (BBL).

Thiophene-quinoxaline donor-acceptor conjugated copolymers were synthesized and explored for use as active materials in organic thin film transistors. The copolymers PTHQx, PTDDQx, and P2TDDQx were demonstrated as being promising p-channel field-effect transistors. OFETs fabricated from PTHQx thin films had the maximum saturation hole mobility of 8.3×10^{-3} $cm^2/(Vs)$ with an on/off current ratio of 10^6. The

polymers PTDDQx and P2TDDQx, with longer alkyl side-chains, allowed for the use of high-boiling-point solvents, which were shown to enhance FET performance to saturation hole mobilities of 1-2 x 10^{-3} $cm^2/(Vs)$ and on/off current ratios of 5 x 10^5 to 5 x 10^6. Spin-coated PTHQx thin films were found to have a densely packed polycrystalline grain morphology using atomic force microscopy, whereas the PTDDQx and P2TDDQx had networks of copolymer aggregates. Although the studied thiophene-quinoxaline copolymers displayed electrochemical reduction indicating such copolymer systems have potential as n-type and ambipolar field-effect transistors, no electron mobility was found in devices fabricated with low work-function metal electrodes. The temperature dependence of PTHQx FET performance was explored, which showed a unique termination of hole conduction above 410 K. This unusual phenomenon is likely the result of a crystallographic phase transition within the copolymer that, thereby, inhibits the conduction of holes. Research confirming whether this is occurring will be done in the future.

Donor-acceptor conjugated copolymers with alternating thiophene and pyridopyrazine monomers were studied for use in organic field-effect transistors. Pyridopyrazine was explored in addition to the previously studied quinoxaline due to it being a better acceptor or electron-withdrawing group. This was of interest because it was forecast that the stronger intermolecular charge transfer would result and as a consequence of this the copolymer would have a smaller band gap, which is crucial for an organic material to be ambipolar. The thiophene-pyridopyrazine copolymers, PTHPPz and PTDPPz, did exhibit reduction and have greater LUMO energy levels,

than the thiophene-quinoxaline copolymers, as found through electrochemical analysis, which would imply a higher likelihood of they demonstrating n-channel FET performance, and thereby ambipolar performance, but none was observed. The thiophene-pyridopyrazine copolymers did demonstrate promising p-channel performance as semiconductors in field-effect transistors. OFETs fabricated from PTDPPz thin films cast from the high-boiling-point solvent TCB had a maximum saturation hole mobility of 4.4 x 10^{-3} $cm^2/(Vs)$ with an on/off current ratio of 10^6. Spin-coated PTHPPz thin films were found to have an isolated aggregate grain morphology within an amorphous copolymer thin film, whereas PTDPPz had networks of copolymer aggregates.

Thieno[3,4-*b*]pyrazine-based conjugated donor-acceptor polymer semiconductors with moderate to high molecular weights studied for their use as active materials in field-effect transistors. The strength of intramolecular charge transfer interaction and thus the electronic and optical properties of the thieno[3,4-*b*]pyrazine-based copolymers were systematically varied by incorporating dioctylfluorene, bis(decyloxy)phenylene, or thiophene moieties along with 5,7-bis-(3-dodecyl-thiophen-2-yl)-thieno[3,4-*b*]pyrazine and, thus, affected the FET properties and performance. The copolymers had small band gaps in the range of 1.1 to 1.6 eV and ambipolar redox properties with rather low ionization potentials (4.6-5.04 eV), which, as it increased, facilitated hole injection gold electrodes and good hole transport in thin film field-effect transistors. The field effect mobility of holes varied from 4.2 $\times$ 10^{-4} $cm^2/(Vs)$ for the poorly soluble BTTP-T to 1.6 $\times$ 10^{-3} $cm^2/(Vs)$ with an on/off ratio of 3 $\times$ 10^4 in the

high molecular weight BTTP-F. These results demonstrate that thieno[3,4-*b*]pyrazine-based conjugated donor-acceptor copolymers combine fairly high charge carrier mobility with their broad visible-to-near infrared absorption making them of interest for photovoltaic cells and other device applications.

Ambipolar field-effect transistors were fabricated utilizing a bilayer of BBL and P3HT. These devices have reasonably good mobility for semiconductor polymers with relatively balanced charge transport with electron and hole mobilities of 9.3×10^{-4} and 4.2×10^{-4} $cm^2/(Vs)$, respectively. They represent a considerable improvement on our previous ambipolar polymer/polymer performance using a single device as well as being the first to employ at polymer heterostructure for the transport of both holes and electrons in FETs. These results provide promise for the future of both polymer photovoltaic cells and integrated circuits using CMOS-type inverters.

6.2 Future Directions

Alternating donor-acceptor (D-A) moieties in conjugated oligomers and copolymers was first established as reducing the band-gaps of said materials first in 1992.[1] It has been shown by those within our group that synthesized copolymers with alternating thiophene (D) with electron-accepting groups (A), including quinoxaline, pyridopyrazine, and thienopyrazine, have demonstrated relatively narrow band gaps (1.1-2.2 eV). Additional copolymers of quinoxaline, pyridopyrazine, and thienopyrazine are already being worked on by synthesists within the group.

There are additionally a large number of low band gap oligomers and polymers have been discovered without sufficient study into the charge transport capabilities. Figure 6.1 displays some potential low band gap polymers for study as charge transport materials in FETs. Similar to the copolymers researched within the Jenekhe group, thiophene (D) copolymers with thienopyrazine (**1**),[2] thienothiadiazole (**2**),[3] and thiadiazolothienopyrazine (**3**)[4] have demonstrated band gaps as low as 0.50 eV and may make attractive polymers for FET studies. Furthermore, substituting 3,4-ethylenedioxythiophene (EDOT) for thiophene as an electron-donating group (D) for thienopyrazine copolymers (**4**) has been demonstrated to reduce the band gap to a very low 0.36 eV.[5] The importance of the ratio of D:A group in the resulting band gap is shown in (**5**) where a shift from 1:1 to 2:1 shifts the band gap from 0.36 to 1.10 eV.[6] Also, measures taken to improve processibility, as well as molecular weight, which both are known to improve FET performance, such as substitution of a dodecyl alkyl chain (**6**) may also shift the band gap.[6]

Notes to Chapter 6

(1) Havinga, E. E.; ten Hoeve, W.; Wynberg, H. *Polym. Bull.* **1992**, *29*, 119.

(2) Kitamura, C.; Tanaka, S.; Yamashita, Y. *J. Chem. Soc., Chem. Commun.* **1994**, 1585.

(3) Tanaka, S.; Yamashita, Y. *Synth. Met.* **1993**, *55–57*, 1251.

(4) Karikomi, M.; Kitamura, C.; Tanaka, S.; Yamashita, Y. *J. Am. Chem. Soc.* **1995**, *117*, 6791.

(5) Akoudad, S.; Roncali, J. *Chem. Commun.* **1998**, 2081.

(6) Casado, J.; Ortiz, R. P.; Ruiz Delgado, M. C.; Herandez, V.; Lopez-Navarette, J. T.; Raimundo, P. J. M.; Blanchard, P.; Allain, M.; Roncali, J. *J. Phys. Chem. B* **2005**, *109*, 16616.

(7) (a) Meijer, E. J.; de Leeuw, D. M.; Setayesh, S.; Van Veenendaal, E. ; Huisaman, B.-H.; Blom, P. W. M.; Hummelen, J. C.; Scherf, U.; Klapwijk, T. M. *Nat. Mater.* **2003**, *2*, 678. (b) Anthopoulos, T. D.; Tanase, C.; Setayesh, S.; Meijer, E. J.; Hummelen, J. C.; Blom, P. W. M.; de Leeuw, D. M. *Adv. Mater.* **2004**, *16*, 2174. (c) Anthopoulos, Thomas D.; de Leeuw, Dago M.; Cantatore, Eugenio; Setayesh, Sepas; Meijer, Eduard J.; Tanase, C.; Hummelen, J. C.; Blom, P. W. M. *Appl. Phys. Lett.* **2004**, *85*, 4205.

(8) (a) Sandberg, H. G. O.; Baecklund, T. G.; Oesterbacka, R.; Stubb, H. *Adv. Mater.* **2004**, *16*, 1112. (b) Kawase, T.; Sirringhaus, H.; Friend, R. H.; Shimoda, T. *Adv. Mater.* **2001**, *13*, 1601. (c) Sirringhaus, H.; Kawase, T.; Friend, R. H.; Shimoda, T.; Inbasekaran, M.; Wu, W.; Woo, E. P. *Science* **2000**, *290*, 2123.

Bibliography

(1) (a) Shirakawa, H.; Louis, E. J.; MacDiarmid, A. G.; Chiang, C. K.; Heeger, A. J. *Chem. Commun.* **1977**, 578. (b) Shirakawa, H. *Angew. Chem., Int. Ed.* **2001**, *40*, 2574. (c) MacDiarmid, A. G. *Angew. Chem., Int. Ed.* **2001**, *40*, 2581. (d) Heeger, A. J. *Angew. Chem., Int. Ed.* **2001**, *40*, 2591. (e) Nalwa, H.S. *Handbook of Organic Conductive Molecules and Polymers, Vol.1-4*; John Wiley & Sons Ltd.: Chichester, U.K., 1997. (f) Skotheim, T.A.; Elsenbaumer, R.L.; Reynolds J.R. *Handbook of Conducting Polymers*; Marcel Dekker, Inc.: New York, 1998.

(2) (a) Tang, C. W.; VanSlyke, S. A. *Appl. Phys. Lett.* **1987**, *51*, 913. (b) Tang, C. W.; VanSlyke, S. A.; Chen, C. H. *J. Appl. Phys.* **1989**, *65*, 3610. (c) Burroughes, J. H.; Bradley, D. D. C.; Brown, A. R.; Marks, R. N.; Mackay, K.; Friend, R. H.; Burns, P. L.; Holmes, A. B. *Nature* **1990**, *347*, 539. (d) Braun, D.; Heeger, A. J. *Appl. Phys. Lett.* **1991**, *58*, 1982. (e) Kraft, A.; Grimsdale, A. C.; Holmes, A. B. *Angew. Chem., Int. Ed.* **1998**, *37*, 402.

(3) (a) Scherf, U.; Riechel, S.; Lemmer, U.; Mahrt, R. F. *Curr. Opin. Solid State Mater. Sci.* **2001**, *5*, 143. (b) Hide, F.; Diaz-Garcia. M. A.; Schwartz, B. J.; Andersson. M. R.; Pei, Q.; Heeger, A. J. *Science* **1996**, *273*, 1833.

(4) (a) Chamberlain, G. A. *Solar Cells* **1983**, *8*, 47. (b) Wöhrle, D.; Meissner, D. *Adv. Mater.* **1991**, *3*, 129. (c) Brabec, C. J.; Sariciftci, N. S.; Hummelen, J. C. *Adv. Funct. Mater.* **2001**, *11*, 15. (d) Peumans, P.; Yakimov, A.; Forrest, S.R. *J. Appl. Phys.* **2003**, *93*, 3693. (e) Brabec, C. J.; Dyakonov, V.; Parisi, J.; Sariciftci, N. S. *Organic Photovoltaics: Concepts and Realization*, *Vol. 60*, Springer: Berlin, Germany, 2003.

(5) (a) Garnier, F.; Horowitz, G.; Fichou, D.; Yassar, A. *Synth. Met.* **1996**, *81*, 163-171. (b) Katz, H. E. *J. Mater. Chem.* **1997**, *7*, 369. (c) Brown, A. R.; Jarrett, C. P.; d. Leeuw, D. M.; Matters, M. *Synth. Met* **1997**, *88*, 37. (d) Horowitz, G. *Adv. Mater.* **1998**, *10*, 365. (e) Katz, H. E.; Bao, Z. *J. Phys. Chem. B* **2000**, *104*, 671. (f) Katz, H. E.; Bao, Z.; Gilat, S. L. *Acc. Chem. Res.* **2001**, *34*, 359. (g) Dimitrakopoulos, C. D.; Malenfant, P. R. L. *Adv. Mater.* **2002**, *14*, 99. (h) Horowitz, G. *J. Mater. Chem.* **2004**, *19*, 1946. (i) Newman, C. R.; Frisbie, C. D.; da Silva Filho, D. A.; Bredas, J.-L.; Ewbank, P. C.; Mann K. R. *Chem. Mater.* **2004**, *16*, 4436.

(6) (a) Anthopoulos, Thomas D.; de Leeuw, Dago M.; Cantatore, Eugenio; Setayesh, Sepas; Meijer, Eduard J.; Tanase, C.; Hummelen, J. C.; Blom, P. W. M. *Appl. Phys. Lett.* **2004**, *85*, 4205.

(7) (a) Sandberg, H. G. O.; Baecklund, T. G.; Oesterbacka, R.; Stubb, H. *Adv. Mater.* **2004**, *16*, 1112. (b) Kawase, T.; Sirringhaus, H.; Friend, R. H.; Shimoda, T. *Adv. Mater.* **2001**, *13*, 1601. (c) Sirringhaus, H.; Kawase, T.; Friend, R. H.; Shimoda, T.; Inbasekaran, M.; Wu, W.; Woo, E. P. *Science* **2000**, *290*, 2123.

(8) (a) Taur, Y.; Ning, T. H. *Fundamentals of Modern VLSI Devices*; Cambridge University Press: Cambridge, 1998, p. 11. (b) Sze, S. M. *Physics of Semiconducting Devices*; Wiley: New York, 1981.

(9) Lin, Y.-Y.; Gundlach, D. J.; Jackson, T. N. *Mater. Res. Soc. Symp. Proc.* **1996**, *413*, 413.

(10) (a) Borsenberger, P. M.; Weis, D. S. *Organic Photoreceptors for Xerography;* Marcel Dekker: New York, 1998. (b) Pope, M.; Swenberg, C. E. *Electronic Processes in Organic Crystals and Polymers*; Oxford University Press: Oxford, 1999, pp. 337.

(11) Nelson, S. F.; Lin, Y. –Y; Gundlach, D. J.; Jackson. T. N. *Appl. Phys. Lett.* **1998**, *72*, 1854.

(12) Warta, W.; Stehle, R.; Karl, N. *Appl. Phys. A* **1985**, *36*, 163. (b) Karl, N.; Marktanner, J.; Stehle, R.; Warta, W. *Synth. Met.* **1991**, *41-43*, 2473.

(13) (a) Burland, D. M. *Phys. Rev. Lett.* **1974**, *33*, 833. (b) Burland, D. M.; Konzelmann, U. *J. Chem. Phys.* **1977**, *67*, 319.

(14) (a) Jenekhe, S. A. *Polym. Mater. Sci. Eng.* **1989**, *60*, 419. (b) Arnold, F. E.; Van Deusen, R. L. *Macromolecules* **1969**, *2*, 497. (c) Kim, O.–K. *Mol. Cryst. Liq. Cryst.* **1984**, *105*, 161. (d) Hong, S. Y.; Kertesz, M.; Lee, Y. S.; Kim, O. K. *Macromolecules* **1992**, *25*, 5424. (e) Scherf, U. *J. Mater. Chem.* **1999**, *9*, 1853.

(15) (a) Horowitz, G.; Fichou, D.; Peng, X. Z.; Xu, Z. G.; Garnier, F. *Solid State Commun.* **1989**, *72*, 381. (b) Akimichi, H.; Waragai, K.; Hotta, S.; Kano, H.; Sakati, H. *Appl. Phys. Lett.* **1991**, *58*, 1500. (c) Garnier, F.; Yassar, A.; Hajlaoui, R.; Horowitz, G.; Deloffre, F.; Servet, B.; Ries, S.; Alnot, P. *J. Am. Chem. Soc.* **1993**, *115*, 8716. (d) Servet, B.; Horowitz, G.; Ries, S.; Lagorsse, O.; Alnot, P.; Yassar, A.; Deloffre, F.; Srivastava, P.; Hajlaoui, R.; Lang, P.; Garnier, F. *Chem. Mater.* **1994**, *6*, 1809.

(16) (a) Katz, H. E.; Torsi, L.; Dodabalapur, A. *Chem. Mater.* **1995**, *7*, 2235. (b) Hajlaoui, R.; Fichou, D.; Horowitz, G.; Nessakh, B.; Constant, M.; Garnier, F. *Adv. Mater.* **1997**, *9*, 557. (c) Hajlaoui, R.; Horowitz, G.; Garnier, F.; Arce-Brouchet, A.; Laigre, L.; Elkassmi, A.; Demanze, F.; Kouki, F. *Adv. Mater.* **1997**, *9*, 389.

(17) (a) Dodabalapur, A.; Torsi, L.; Katz, H. E. *Science* **1995**, *268*, 270. (b) Torsi, L.; Dodabalapur, A.; Lovinger, A. J.; Katz, H. E.; Ruel, R.; Davis, D. D.; Baldwin, K. W. *Chem. Mater.* **1995**, *7*, 2247. (c) Katz, H. E.; Dodabalapur, A.; Torsi, L.; Elder, D. *Chem. Mater.* **1995**, *7*, 2238. (d) Katz, H. E.; Lovinger, A. J.; Laquindanum, J. G.; *Chem. Mater.* **1998**, *10*, 457.

(18) (a) Horowitz, G.; Peng, X. Z.; Fichou, D. ; Garnier, F. *J. Mol. Electron.* **1991**, *7*, 85. (b) Dimitrakopoulos, C. D.; Brown, A. R.; Pomp, A. *J. Appl. Phys.* **1996** *80*, 2501. (c) Gundlach, D. J.; Lin, Y. Y.; Jackson, T. N.; Nelson, S. F.; Schlom, D. G. *IEEE Electron. Device Lett.* **1997**, *18*, 87. (d) Klauk, H.; Halik, M.; Zschieschang, U.; Schmid, G.; Radlik, W.; Weber, W. *J. Appl. Phys.* **2002**, *92*, 5259. (e) Kelley, T. W.; Boardman, L. D.; Dunbar, T. D.; Muyres, D. V.; Pellerite, M. J.; Smith, T. P. *J. Phys. Chem. B*. **2003**, *107*, 5877. (f) Kelley, T. W.; Muyres, D. V.; Baude, P. F.; Smith, T. P.; Jones, T. D. *Mater. Res. Soc. Symp. Proc.* **2003**, *771*, L6.5.

(19) (a) Brown, A. R.; Pomp, A.; de Leeuw, D. M.; Klaassen, D. B. M.; Havinga, E. E.; Herwig, P. T.; Müllen, K. *J. Appl. Phys.* **1996**, *79*, 2136. (b) Herwig, P. T.; Müllen, K. *Adv. Mater.* **1999**, *11*, 480. (c) Brown, A. R.; Pomp, A.; Hart, C. M.; Deleeuw, D. M. *Science* **1995**, *270*, 972. (d) Afzali, A.; Dimitrakopoulos, C. D.; Breen, T. L. *J. Am. Chem. Soc.* **2002**, *124*, 8812.

(20) (a) Eley, D. D. *Nature* **1948**, *162*, 819. (b) Eley, D. D.; Parfitt, G. D.; Perry, M. J.; Taysum, D. H. *Trans. Faraday Soc.* **1953**, *49*, 79. (c) Hoshino, S.; Kamata, T.; Yase, K. *J. Appl. Phys.* **2002**, *92*, 6028. (d) Xiao, K.; Liu, Y.; Yu, G.; Zhu, D. *Appl. Phys A*, **2003**, *77*, 367. (e) Bao, Z.; Lovinger, A. J.; Dodabalapur, A. *Appl. Phys. Lett.* **1996**, *69*, 3066.

(21) Gundlach, D. J.; Lin, Y.–Y; Jackson, T. N.; Schlom, D. G. *Appl. Phys. Lett.* **1997**, *71*, 3853.

(22) Sirringhaus, H.; Friend, R. H.; Li, X. C.; Moratti, S. C.; Holmes, A. B.; Feeder, N. *Appl. Phys. Lett.* **1997**, *71*, 3871.

(23) (a) Katz, H. E.; Li, W.; Lovinger, A. J.; Laquindanum, J. G. *Synth. Met.* **1999** *102*, 897. (b) Laquindanum, J. G.; Katz, H. E.; Lovinger, A. J. *J. Am. Chem. Soc.* **1998**, *120*, 664.

(24) Burroughes, J. H.; Jones, C. A.; Friend, R. H. *Nature* **1988**, *335*, 137.

(25) (a) Tsumura, A.; Koezuka, H.; Ando, T. *Appl. Phys. Lett.* **1986,** *49,* 1210-1212. (b) Koezuka, H.; Tsumura, A.; Ando, T. *Synth. Met.* **1987**, *18*, 699-704. (c) Assadi, A.; Svensson, C.; Willander, M.; Inganas, O. *Appl. Phys. Lett.* **1988**, *53*, 195.

(26) Fuchigami, H.; Tsumura, A.; Koezuka, H. *Appl. Phys. Lett.* **1993**, *63*, 1372.

(27) (a) Pichler, K.; Jarrett, C. P.; Friend, R. H.; Ratier, B.; Moliton, A. *J. Appl. Phys.* **1995**, *7*, 3523. (b) Roichman, Y.; Tessler, N. *Appl. Phys. Lett.* **2002**, *80*, 151.

(28) Tsumura, A.; Koezuka, H.; Tsunoda, S.; Ando, T. *Chem. Lett.* **1986**, *15*, 863.

(29) Kuo, C.-T.; Chen, S.-A. Hwang, G.-W.; Kuo, H.-H. *Synth. Met.* **1998**, *93*, 155.

(30) (a) Paloheimo, J.; Kuicalainen, P.; Stubb, H.; Vuorimaa, E.; Yli-Lahti, P. *Appl. Phys. Lett.* **1990**, *56*, 1157. (b) Paloheimo, J.; Stubb, H.; Yli-Lahti, P.; Dyrekelev, P.; Inganas, O. *Thin Solid Films* **1992**, *210-211*, 283.

(31) Dyrekelev, P.; Gustafsson, G.; Inganas, O.; Stubb, H. *Sol. State. Comm.* **1992**, *82*, 317.

(32) Cacialli, F.; Daik, R.; Dounis, P.; Feast, W. J.; Friend, R. H.; Haylett, N. D.; Jarrett, C. P.; Schoenenberger, C.; Stephens, J. A.; Widawski, G. *Philos. Trans. R. Soc. London Ser A* **1997**, *355*, 707.

(33) Pichler, K.; Friend, R. H.; Murray, K. A.; Holmes, A. B.; Moratti, S. C. *Mol. Cryst. Liq. Cryst.* **1994**, *256,* 671.

(34) (a) Bao, Z.; Dodabalapur, A.; Lovinger, A. J. *Appl. Phys. Lett.* **1996**, *69*, 4108. (b) Sirringhaus, H.; Brown, P. J.; Friend, R. H.; Nielsen, M. M.; Bechgaard, K.; Langeveld, V., B. M. W.; Spiering, A. J. H.; Janssen, R. A. J.; Meijer, E. W.; Herwig, P.; de Leeuw, D. M. *Nature* **1999**, *401*, 685. (c) Chang, J. F.; Sun, B. Q.; Breiby, D. W.; Nielsen, M. M.; Solling, T. I.; Giles, M.; McCulloch, I.; Sirringhaus, H. *Chem. Mater.* **2004**, *16*, 4772. (d) Kline, R. J.; McGhee, M. D.; Kadnikova, E. N.; Liu, J.; Frechet, J. M. J.; Toney, M. F. *Macromolecules* **2005**, *38*, 3312. (e) Zen, A.; Pflaum, J.; Hirschmann, S.; Zhuang, W.; Jaiser, F.; Asawapirom, U.; Rabe, J. P.; Scherf, U.; Neher, D. *Adv. Funct. Mater.* **2004**, *14*, 757. (f) Wang, G. M.; Moses, D.; Heeger, A. J.; Zhang, H. M.; Narasimhan, M.; Demaray, R. E. *J. Appl. Phys.* **2004**, *95*, 316-322. (g) Ullmann, A.; Ficker, J.; Fix, W.; Rost, H.; Clemens, W.; McCulloch, I.; Giles, M. *Mat. Res. Soc. Symp. Proc.* **2001**, *665*, C 7.5.

(35) Ong, B. S.; Wu, Y.; Liu, P.; Gardner, S. *J. Amer. Chem. Soc.* **2004**, *126*, 3378.

(36) (a) Ong, B.; Wu, Y. L.; Jiang, L.; P. L.; Muck, T. *Synth. Met.* **2004**, *142*, 49. (b) Kim, Y. H.; Park, S. K.; Moon, D. G.; Kim, W. K.; Han, J. I. *Jpn. J. Appl. Phys.* **2004**,

43, 3605. (c) Heeney, M.; Bailey, C.; Genevicius, K.; Shkunov, M.; Sparrowe, D.; Tierney, S.; McCulloch, I. *J. Am. Chem. Soc.* **2005**, *127*, 1078.

(37) (a) Sirringhaus, H.; Wilson, R. J.; Friend, R. H.; Inbasekaran, M.; Wu, W.; Woo, E. P.; Grell, M.; Bradley, D. D. C. *Appl. Phys. Lett.* **2000**, *77*, 406. (b) Morin, J.-F.; Drolet, N.; Tao, Y.; Leclerc, M. *Chem. Mater.* **2004**, *16*, 4619. (c) Champion, R. D.; Cheng, K.-F. ; Pai, C.-L. ; Chen, W.-C. *Macromol. Rapid Commun.* **2005**, *26*, 1835. (d) Lee, B. L.; Yamamoto, T. *Macromolecules* **1999**, *32*, 1375. (e) Zhu, Y.; Babel, A.; Jenekhe, S. A.; *Macromolecules*, **2005**, *38*, 7983.

(38) Heeney, M.; Bailey, C.; Giles, M.; Shkunov, M.; Sparrowe, D.; Tierney, S.; Zhang, W.; McCulloch, I. *Macromol.* **2004**, *37*, 5250.

(39) (a) McCulloch, I.; Heeney, M.; Bailey, C.; Genevicius, K.; MacDonald, I.; Shkunov, M.; Sparrowe, D.; Tierney, S.; Wagner, R.; Zhang, W.; Chabinyc, M. L.; Kline, R. J.; McGehee, M. D.; Toney, M. F. *Nat. Mater.* **2006**, *5*, 328. (b) Pan, H.; Li, Y.; Wu, Y.; Liu, P.; Ong, B. S.; Zhu, S.; Xu, G. *Chem. Mater.* **2006**, *18*, 3237. (c) Li, Y.; Wu, Y.; Liu, P.; Birau, M.; Pan, H.; Ong, B. S. *Adv. Mater.* **2006**, *18*, 3029.

(40) (a) Horowitz, G.; Kouki, F.; Spearman, P.; Fichou, D.; Nogues, C.; Pan, X.; Garnier, F. *Adv. Mater.* **1996**, *8*, 242. (b) Ostrick, J. R.; Dodabalapur, A.; Torsi, L. Lovinger, A. J.; Kwock, E. W.; Miller, T. M.; Galvin, M.; Berggren, M.; Katz, H. E. *J. Appl. Phys.* **1997**, *81*, 6804. (c) Malenfant, P. R. L.; Dimitrakopoulos, C. D.; Gelorme, J. D.; Kosbar, L. L.; Graham, T. O.; Curioni, A.; Andreoni, W. *Appl. Phys. Lett.* **2002**, *80*, 2517.

(41) (a) Laquindanum, J. G.; Katz, H. E.; Dodabalapur, A.; Lovinger, A. J. *J. Am. Chem. Soc.* **1996**, *118*, 11331. (b) Katz, H. E. ; Johnson, J.; Lovinger, A. J.; Li, W. *J. Am. Chem. Soc.* **2000**, *122*, 7787. (c) Katz, H. E.; Lovinger, A. J.; Johnson, J.; Kloc, C.; Siergrist, T.; Li, W.; Lin, Y.-Y.; Dodabalpur, A. *Nature*, **2000**, *404*, 478.

(42) (a) Haddon, R. C.; Perel, A. S.; Morris, R. C.; Palstra, T. T. M.; Hebard, A. F.; Fleming, R. M. *Appl. Phys. Lett.* **1995**, *67*, 121. (b) Jarret, C. P.; Pichler, K.; Newbould, R.; Friend, R. H. *Synth. Met.* **1996**, *77*, 35. (c) Kobayashi, S.; Takenobu, T.; Mori, S.; Fujiwara, A.; Iwasa, Y. *Appl. Phys. Lett.* **2003**, *82*, 4581. (d) Haddon, R. C. *J. Am. Chem. Soc.* **1996**, *118*, 3041. (e) Waldauf, C.; Schilinsky, P.; Perisutti, M.; Hauch, J.; Brabec, C. *J. Adv. Mater.* **2003**, *15*, 2084.

(43) (a) Babel, A.; Jenkhe, S. A. *Adv. Mater.* **2003**, *14*, 371. (b) Babel, A.; Jenekhe, S. A. *J. Am. Chem. Soc.* **2003**, *125*, 13656. (c) Babel, A.; Jenekhe, S. A. *J. Phys. Chem. B* **2002**, *106*, 6129.

(44) Yamamoto, T.; Yasuda, T.; Sakai, Y.; Aramaki, S. *Macromol. Rapid Commun.* **2005**, *26*, 1214.

(45) Babel, A.; Wind, J. D.; Jenekhe, S. A. *Adv. Funct. Mater.* 2004, *14*, 891.

(46) Babel, A.; Zhu, Y.; Cheng, K.-F.; Chen, W.-C.; Jenekhe, S. A. *Adv. Funct. Mater.* **2007**, *17*, 2542.

(47) (a) Dodabalapur, A.; Katz, H. E.; Torsi, L.; Haddon, R. C. *Science* **1995**, *269*, 1560. (b) Wang, H.; Wang, J.; Yan, X.; Shi, J.; Tian, H.; Geng, Y.; Yan, D. *Appl. Phys. Lett.* **2006**, *88*, 133508. (c) Torres, W.; Fox, M. A. *Chem. Mater.* **1990**, *2*, 306. (d) Wojda, A.; Maksymiuk, K. *Electroanal.* **1998**, *10*, 1269.

(48) (a) Cheng, K.-F.; Liu, C.-L.; Chen, W.-C. *J. Poly. Sci., Part A: Poly. Chem.* **2007**, *45*, 5872. (b) Lee, W.-Y.; Cheng, K.-F.; Wang, T.-F.; Chueh, C.-C.; Chen, W.-C.; Tuan, C.-S.; Lin, J.-L. *Macromol. Chem. Phys.* **2007**, *208*, 1919. (c) Zaumseil, J.; Sirringhaus, H. *Chem. Rev.* **2007**, *107*, 1296. (d) Yasuda, T.; Sakai, Y.; Aramaki, S.; Yamamoto, T. *Chem. Mater.* **2005**, *17*, 6060. (e) Yamamoto, T.; Kokubo, H.; Kobashi, M.; Sakai, Y. *Chem. Mater.* **2004**, *16*, 4616. (f) Yamamoto, T.; Zhou, Z.-h.; Kanbara, T.; Shimura, M.; Kizu, K.; Maruyama, T.; Nakamura, Y.; Fukuda, T.; Lee, B.-L.; Ooba, N.; Tomaru, S.; Kurihara, T.; Kaino, T.; Kubota, K.; Sasaki, S. *J. Amer. Chem. Soc.* **1996**, *118*, 10389.

(49) Reisch, H.; Wiesler, U.; Scherf, U.; Tuytuylkov, N. *Macromol.* **1996**, *29*, 8204.
(50) (a) Agrawal, A. K.; Jenekhe, S. A. *Macromolecules* **1993**, *26*, 895. (b) Karikomi, M.; Kitamura, C.; Tanaka, S.; Yamashita, Y. *J. Am. Chem. Soc.* **1995**, *117*, 6791. (c) Kanbara, T.; Miyazaki, Y.; Yamamoto, T. *J. Polym. Sci. A: Polym. Chem.* **1995**, *33*, 999. (d) Jenekhe, S. A.; Lu, L.; Alam, M. M. *Macromolecules* **2001**, *34*, 7315.

(51) (a) Zhang, X.; Jenekhe, S. A.; *Macromolecules* **2000**, *33*, 2069. (b) Ego, C.; Marsitzky, D.; Becker, S.; Zhang, J.; Grimsdale, A. C.; Müllen, K.; MacKenzie, J. D.; Silva, C.; Friend, R. H.; *J. Am. Chem. Soc.* **2003**, *125*, 437. (c) Thompson, B. C.; Madrigal, L. G.; Pinto, M. R.; Kang, T.-S.; Schanze, K. S.; Reynolds, J. R. *J. Polym. Sci. A: Polym. Chem.* **2005**, *43*, 1417. (d) Kulkarni, A. P.; Zhu, Y.; Jenekhe, S. A.; *Macromolecules* **2005**, *38*, 1553.

(52) (a) Yoon, M.-H.; DiBenedetto, S. A.; Facchetti, A.; Marks, T. J. *J. Am. Chem. Soc.* **2005**, *127*, 1348. (b) Ando, S.; Nishida, J.-I.; Tada, H.; Inoue, Y.; Tokito, S.; Yamashita, Y. *J. Am. Chem. Soc.* **2005**, *127*, 5336. (c) Kunugi, Y.; Takimiya, K.; Negishi, N.; Otsubo, T.; Aso, Y. *J. Mater. Chem.* **2004**, *14*, 2840. (d) Chua, L.-L.; Zaumseil, J.; Chang, J.-F.; Ou, E. C.-W.; Ho, P. K.-H.; Sirringhaus, H.; Friend, R. H. *Nature* **2005**, *434*, 194.

(53) (a) Yu, G.; Gao, J.; Hummelen, J. C.; Wudl, F.; Heeger, A. J. *Science* **1995**, *270*, 1789. (b) Jenekhe, S. A.; Yi, S. *Appl. Phys. Lett.* **2000**, *77*, 2635. (c) Alam, M. M.; Jenekhe, S. A. *J. Phys. Chem. B* **2001**, *105*, 2479. (d) Alam, M. M.; Jenekhe, S. A. *Chem. Mater.* **2004**, *16*, 4647.

(54) (a) Yasuda, T.; Imase, T.; Sasaki, S.; Yamamoto, T. *Macromolecules* **2005**, 38, 1500. (b) Tsai, F.-C.; Chang, C.-C.; Liu, C.-L.; Chen, W.-C.; Jenekhe, S. A. *Macromolecules* **2005**, *38*, 1958. (c) Liu, C.-L.; Tsai, F.-C.; Chang, C.-C.; Hsieh, K.-H.; Lin, J.-L.; Chen, W.-C. *Polymer* **2005**, *46*, 4950.

(55) (a) Horowitz, G.; Hajlaoui, R.; Delannoy, P. *J. Phys. III* **1995**, *5*, 355. (b) Knipp, D.; Street, R. A.; Völkel, A. R. *Appl. Phys. Lett.* **2003**, *82*, 3907.

(56) Agrawal, A. K.; Jenekhe, S. A.; *Chem. Mater.* **1996**, *8*, 579.

(57) Lee, D. H.; Kim, D.; Oh, T.; Cho, K. *Langmuir* **2004**, *20*, 8124.

(58) Babel, A.; Jenekhe, S. A. *J. Phys. Chem. B* **2003**, *107*, 1749.

(59) Knipp, D.; Street, R. A.; Völkel, A.; Ho, J. *J. Appl. Phys.* **2003**, *93*, 347.

(60) Katz, H.E. *Chem. Mater.* **2004,** *16,* 4748;

(61) Salleo, A.; Chabinyc, M. L.; Yang, M. S.; Street, R. A. *Appl. Phys. Lett.* **2002**, *81*, 4383.

(62) Vissenberg, M. C. J. M.; Matters, M. *Phys. Rev. B: Condens. Matter* **1998**, *57*, 12964.

(63) Meijer, E. J.; Tanase, C.; Blom, P. W. M.; van Veenendaal, E.; Huisman, B.-H.; de Leeuw, D. M.; Klapwijk, T. M.; *Appl. Phys. Lett.* **2002**, *80*, 3838.

(64) (a) Chesterfield, R. J.; McKeen, J. C.; Newman, C. R.; Frisbie, C. D.; Ewbank, P. C.; Mann, K. R.; Miller, L. L. *J. Appl. Phys.* **2004**, *95*, 6396. (b) Horowitz, G.; Hajlaoui, M. E.; Hajlaoui, R. *J. Appl. Phys.* **2000**, *87*, 4456. (c) Dimitrakopoulos, C. D.; Purushothaman, S. ; Kymissis, J. ; Callegari, A.; Shaw, J. M.; *Science* **1999**, *283*, 822. (d) Le Comber, P. G.; Spear, W. *Phys. Rev. Lett.* **1970,** *25*, 509.

(65) (a) Baranovskii, S. D.; Faber, T.; Hensel, F.; Thomas, P. *J. Phys.: Condens. Matter* **1997**, *9*, 2699. (b) Monroe, D. *Phys. Rev. Lett.* **1985**, *54*, 146.

(66) Salleo, A.; Chen, T. W.; Volkel, A. R.; Wu, Y.; Liu, P.; Ong, B. S.; Street, R. A.; *Phys. Rev. B* **2004**, *70*, 115311.

(114) (a) *Organic Electronics*; Klauck, H., Ed.; VCH: Weinheim, Germany, 2007. (b) *Organic Field-Effect Transistors*; Bao, Z., Locklin, J., Eds.; CRC Press: Boca Raton, FL, 2007.

(115) Hancock, J. M.; Gifford, A. P.; Champion, R. D.; Jenekhe, S. A. *Macromolecules* **2008**, *41*, 3588.

(116) Babel, A. "Molecular Engineering of Polymer Thin Film Transistors" Ph.D. Dissertation, University of Washington, Seattle, WA, U.S.A., 2006.

Vita

Richard David Champion was born in Medford, Oregon on November 12, 1979, which was where the closest hospital was to his parents' home in Central Point, Oregon. His father and mother are Guy Wilfred Champion and Belinda Sue Champion, née Slape (now Wellner). Soon after the birth of his younger brother Corbin, his family, including three brothers and one sister from an earlier marriage of his father, one brother from an earlier marriage of his mother, Robert, and Corbin moved to Pendleton, Oregon. At the age of two, his parents separated and soon divorced, his mother with he and Robert and Corbin moved to her hometown of Longview, Washington. Soon afterward his mother remarried a great husband and father figure in Mark Martin Wellner.

The family moved from low middle class to middle class eventually becoming homeowners in adjacent Kelso, Washington when Richard was in fourth grade. Richard always participated in sports year-round with baseball, wrestling, soccer and swimming in grade school before settling on football, wrestling and track & field in junior and high school. He worked hard at both athletics and academics becoming a captain of both the football and wrestling teams his senior year, while at the same time achieving National Merit Scholar – Commended Status and AP Scholar with Honor.

After graduating from Kelso High School in 1998, Richard spent a year at both Linfield College and Lower Columbia College, before transferring to Easter Oregon University in the hopes of playing collegiate football as he had done at Linfield College. Unfortunately, soon after practices begun, he severely injured his shoulder and

subsequently injured the same shoulder multiple more times that season. After a year of rehab and strengthening, he had hoped to revive his football career only to injure the same shoulder on the second day of practice. After this, he quit football, focused on his studies, and discovered a passion for scientific research. Under the guidance of his undergraduate research advisor, Professor Ronald B. Kelley, his work on isolated bioactive chemicals from natural products was published in one paper and presented at two national ACS meetings. Richard graduated with a Bachelor of Sciences, Magna cum Laude, in Chemistry with minors in Mathematics and Biology in June 2003.

In the summer before Richard Champion received his undergraduate degree, he worked at the Pacific Northwest National Laboratories (PNNL) in Richland, Washington under R. Shane Addleman, PhD, an Eastern Oregon University alum. There worked on the synthesis of sorbents and sensors for metals, radionuclides and nerve agents. After graduating from Eastern Oregon University, Richard returned to PNNL for another year on the same topic.

After a year at PNNL, Richard Champion began his graduate studies in Chemical Engineering at the University of Washington. For his Masters work, he conducted research on novel organic and polymeric field-effect transistors under his advisor, Professor Samson A. Jenekhe. His work on transistors produced several publications and was even the featured cover article in Macromolecular Rapid Communications. After his Masters defense in 2006, Richard did post-Masters work with Professor Guozhong Cao at the University of Washington, where he again published a number of academic research papers. In 2009, he began his work at

Weyerhaeuser, under the advisement of Professor G. Graham Allan at the University of Washington and James H. Wiley at Weyerhaeuser, on his doctoral research studying organic-inorganic and organic-organic ion-exchange in cellulosic materials. Previous to Richard's work, no studies on the ion-exchange of organic species with cellulosic material, i.e. wood pulp. To date his work has resulted in one published patent with more academic papers in the offing.

Richard enjoys sports – both playing and watching – and is a die-hard fan of the Washington Huskies, Kelso Hilanders, Cleveland Browns, Los Angeles Dodgers, and Arsenal Football Club. He also enjoys reading classical literature and fervent reader of the news. In addition, Richard has become active politics recently and holds a few positions with the Democratic Party at a local level.